OPTIMAL SHUNT CAPACITORS' PLACEMENT AND SIZING IN RADIAL DISTRIBUTION SYSTEMS USING MULTI-VERSE OPTIMIZER, MODIFIED LOSS SENSITIVITY FACTORS AND MATLAB MATRIX REDUCTION TECHNIQUES

THOMSON PRECIOUS MALUMBO MTONGA

MASTER OF SCIENCE

(Electrical Engineering)

JOMO KENYATTA UNIVERSITY

OF

AGRICULTURE AND TECHNOLOGY

2023

Optimal Shunt Capacitors' Placement and Sizing in Radial Distribution Systems using Multi-Verse Optimizer, Modified Loss Sensitivity Factors and Matlab Matrix Reduction Techniques

Thomson Precious Malumbo Mtonga

A Thesis Submitted in Partial Fulfilment of the Requirements for the Degree of Master of Science in Electrical Engineering of the Jomo Kenyatta University of Agriculture and Technology

2023

DECLARATION

This thesis is my original work and has not been presented for a degree in any other University

Signature …….……. Date …….……...

Thomson Precious Malumbo Mtonga

This thesis has been submitted for examination with our approval as the University Supervisors

Signature …….……. Date ….……...

Dr. Keren K. Kaberere, PhD.

JKUAT, Kenya

Signature ….……. Date …….……...

Dr. George K. Irungu, PhD.

JKUAT, Kenya

DEDICATION

This work is dedicated to my parents, spouse, children and siblings.

ACKNOWLEDGEMENT

First and foremost, I hereby extend my heartfelt gratitude to Almighty Jehovah, the Most High God for constantly shining His gracious light on my paths and enabling me to reach this far in my studies.

Secondly, I am so grateful for the guidance my supervisors, Dr. Keren K. Kaberere, PhD. and Dr. George K. Irungu, PhD., provided during the entire time the research was being undertaken. The invaluable criticisms, suggestions, recommendations and motivation they offered eased my entire research journey while at the same time nurturing in me the ability to look at things critically.

I also wish to thank the Malawian Government through the Department of Human Resource Management and Development (DHRMD) for according me the opportunity to further my studies. However, the journey would not have been a success without having Jomo Kenyatta University of Agriculture and Technology (JKUAT) as my host university, it is in this regard that I also extend my gratitude to the university's entire management and staff.

Last but not least, I give special thanks to my beloved family and friends for the invaluable support they rendered in many different ways. A special thanks also goes to my friend from our undergraduate days, Lucius Chimwemwe Mawanga; a friend whom I ended up sharing a house and ideas with during my stay in Kenya.

TABLE OF CONTENTS

LIST OF TABLES

LIST OF FIGURES

LIST OF APPENDICES

LIST OF ABBREVIATIONS

ABC	Artificial Bee Colony
BSI	Bus Sensitivity Index
CSO	Chicken Swarm Optimization
CrSA	Crow Search Algorithm
CSA	Cuckoo Search Algorithm
CA	Cultural Algorithm
DA	Dragonfly Algorithm
DE	Differential Evolution
DFO	Dragonfly Optimizer
DG	Distributed Generator
FL	Fuzzy Logic
FPA	Flower Pollination Algorithm
GA	Genetic Algorithm
GSA	Gravitational Search Algorithm
GWO	Grey Wolf Optimizer
ICrSA	Improved Crow Search Algorithm
kVAr	Kilo Volt-Ampere Reactive
kVA	Kilo Volt-Ampere
kW	Kilowatt
kWh	Kilowatt hour
LSF	Loss Sensitivity Factors
MATLAB	Matrix Laboratory
MCA	Modified Cultural Algorithm
MFO	Moth-Flame Optimizer
MLSF	Modified Loss Sensitivity Factors
MVO	Multi-Verse Optimizer
NI	Normalized Inflation
O&M	Operation and Maintenance
PFCC	Power Factor Correction Capacitor

PLI	Power Loss Index
PSO	Particle Swarm Optimization
TDR	Travelling Distance Rate
TTC	Total Transfer Capability
VSI	Voltage Stability Index
WEP	Worm hole Existence Probability

LIST OF NOMENCLATURES

C_{ci}	Shunt capacitors installation cost per location
C_{co}	Shunt capacitors O&M cost per location per year
C_{cp}	Shunt capacitor purchase cost
$Q_{cs}(j)$	Size of the shunt capacitor installed at bus *j*
C_e	Average electrical energy cost
I	Current
I_S	The sending end current
nb	Total number of branches within an electrical network
$ncap$	The total number of buses with shunt capacitors installed
P_s	Sending end real power
P_R	Receiving end real power
P_L	Real power load demand
$P_{La}(i)$	The electric power loss in branch *i*
Q_s	Sending end reactive power
Q_R	Receiving end reactive power
Q_L	Reactive power load demand
Q_C	Reactive power being supplied by shunt capacitors
R	Resistance
S_s	Sending end apparent power
T_i	Duration of the load level under consideration
V_R	Receiving end voltage
V_s	Sending end voltage
X_c	Capacitive reactance
X_L	Inductive reactance
Z	Impedance

ABSTRACT

The installation of shunt capacitors in radial distribution systems results in the reduction of branch power flows, currents, power losses and voltage drop. Consequently, this further results in improved voltage profiles and voltage stability margins. However, for efficient attainment of the aforementioned benefits, the installation of shunt capacitors needs to be carried out in an optimal manner, that is, optimally sized shunt capacitors need to be installed at the global optimum buses within a given electrical network. Identification of the global optimum buses at which to install shunt capacitors in radial distribution systems is one critical task that greatly affects the overall cost of total real power losses, shunt capacitors' purchase, installation, operation, and maintenance (O&M). If an existing approach ably identifies the global optimum buses, then the overall cost of total real power losses, shunt capacitors' purchase, installation, and O&M would be minimized to the least value possible. However, if an approach only identifies sub-optimal buses, then the minimization of the aforementioned overall cost would only be partial. There are two general approaches that are used to identify optimal buses on which to install shunt capacitors. These are: *approaches for searching of optimal buses from unreduced search spaces* and *approaches for searching of optimal buses from reduced search spaces.* The exhaustive search-based approach, which belongs to the former approach, gives the global optimum buses and consequently the global optimum overall cost of total real power losses, shunt capacitors' purchase, installation, and O&M. However, its major shortfall is its high computation time. This is mainly so because under this approach, the search for the global optimum buses is carried out in unreduced search spaces. On the other hand, for approaches in which the search for optimal buses is carried out in reduced search spaces, the computation time is also reduced. However, this reduction in the search space, hence the computation time, results in reduced accuracy levels for the attained solutions. Consequently, in an attempt to counter shortfalls of existing approaches, i.e. high solutions' accuracy at the expense of computation time; and shorter computation time at the expense of solutions accuracy, in this thesis a new optimal shunt capacitors' placement and sizing approach has been developed, evaluated, and validated. The approach is based on Modified Loss Sensitivity Factors (MLSF), the Multi-Verse Optimizer (MVO) and MATLAB matrix or search space reduction techniques. In the developed approach, the MLSF and MATLAB's matrix reduction techniques have been used to reduce the search space of optimal buses that require the provision of reactive power through the installation of shunt capacitors. Thereafter, MVO is used to do a concurrent search of the global optimum bus(es) from the reduced search spaces and the corresponding optimum shunt capacitor sizes to be installed. The developed approach was tested on the IEEE 10- and 33-bus radial distribution systems with the aim of minimizing the overall cost of total real power losses, shunt capacitors' purchase, installation, and O&M while assuming fixed and variable system loading. Despite disregarding some bus combinations, the developed approach was still able to attain the same overall costs, real power losses, reactive power losses and bus voltages as the exhaustive search based algorithm. Additionally, the developed approach was able to attain the least overall cost than those obtained using

approaches based on Artificial Bee Colony (ABC), Crow Search Algorithm (CrSA), Cuckoo Search Algorithm (CSA), Differential Evolution (DE), Dragonfly Optimizer (DFO), Genetic Algorithm (GA), Gravitational Search Algorithm (GSA), Grey Wolf Optimizer (GWO), Improved Crow Search Algorithm (ICrSA), Modified Cultural Algorithm (MCA), Moth Flame Optimizer (MFO) and Particle Swarm Optimization (PSO) algorithm. Consequently, because the search space becomes reduced after disregarding some bus combinations, the developed approach attains the global optimum results with relatively shorter computation times than the exhaustive search. In summary, the developed algorithm stands out as a potentially reliable tool for power system planners to adopt and use when solving the radial distribution systems' optimal shunt capacitors' placement and sizing problem for either minimization of the overall cost of total real power losses and shunt capacitors' purchase or minimization of the overall cost of total real power losses, shunt capacitors' purchase, installation, and O&M. This is so because, unlike available optimal shunt capacitors' placement and sizing algorithms, the developed algorithm exactly matches the accuracy of the exhaustive search algorithm.

CHAPTER ONE

INTRODUCTION

1.1. Background Information

The optimal placement and sizing of shunt capacitors in radial distribution systems is one of the most important activities that electric power utility companies carry out with the aim of reducing current flow, improving power factor and consequently reducing radial distribution systems' power losses and voltage drops. Additionally, there is a resulting optimal improvement in an electrical network's Total Transfer Capability (TTC) whenever shunt capacitors are optimally placed and sized within a network under consideration (Gonen, 2014; Weedy et al., 2012). This improvement in TTC enables existing electrical networks to transmit and distribute greater amounts of real power over the same existing electrical infrastructure than before. This then lowers the overall cost of electric power transmission and distribution as it leads to the probable cancellation or postponement of expensive electrical network infrastructure expansion activities.

Most studies that focus on solving the radial distribution system's optimal shunt capacitors placement and sizing problem disregard the slack bus as a potential candidate bus on which shunt capacitors may be installed. This is so because the installation of shunt capacitors at the slack bus would not change the flow of reactive power in the branches beyond it. Consequently, when considering a radial distribution system with m buses, shunt capacitors may only be installed at any of the $m - 1$ buses within the system (Sedighizadeh & Bakhtiary, 2015).

Furthermore, it should also be noted that for any bus system, the total possible bus combination(s) for shunt capacitor placement can be generated exhaustively using the combinations (nCr) command (Bigdeli et al., 2012; Magadum & Kulkarni, 2019). In using the combinations command, n represents the total number of buses at which shunt capacitors may be installed while r represents the desired total number of buses to be compensated.

Consequently, for instances where shunt capacitors have to be installed at r bus(es) within a radial distribution system having m buses, the total number of possible bus combinations (or the search space for the buses) can be generated using (1.1).

$$\text{Total possible bus combinations} = nCr = \frac{n!}{r!(n-r)!} = \frac{(m-1)!}{r!(m-1-r)!} \quad (1.1)$$

With reference to (1.1), when m is an even number and is kept constant while r is increased from 1 up to $\left(\frac{m}{2}-1\right)$, then the total number of possible bus combinations also increases. The total number of possible bus combinations for cases where r is equal to $\left(\frac{m}{2}-1\right)$ is the same as that for cases where r is equal to $\left(\frac{m}{2}\right)$. However, for all values of r greater than $\left(\frac{m}{2}\right)$, the total number of possible bus combinations starts to decrease until it becomes equal to one. On the other hand, when m is an odd number and is kept constant while r is increased from 1 up to $\left(\frac{m}{2}\right)$, then the total number of possible bus combinations also increase. However, for all values of r greater than $\left(\frac{m}{2}\right)$, the total number of possible bus combinations starts to decrease until it becomes equal to one. On the other hand, when r is kept constant while m is increased, the total number of possible bus combinations also increase.

The increase in the list of total possible bus combinations, as discussed above, makes the exercise of determining the global optimum bus combination from the list burdensome. This is so because when searching for the global optimum bus combination, the optimization algorithm is executed a number of times equal to the total number of possible combinations (Bigdeli et al., 2012). Therefore, in an attempt to reduce the computational burden (when determining the global optimum bus combination from the list of total possible bus combinations) researchers have proposed and developed a number of different approaches. The proposed approaches tend to reduce the search space, i.e., the considered total number of possible bus combinations, hence the computation time (Bilal et al., 2021).

Among many different search space reduction approaches, research on optimized shunt capacitors placement and sizing has adopted and used Fuzzy Logic (FL) (Das, 2008; Murthy et al., 2010; Shetty & Ankaliki, 2016), Voltage Stability Index (VSI)

(Devabalaji et al., 2018; Sukraj et al., 2018), Bus Sensitivity Index (BSI) (Arcanjo et al., 2012), Power Loss Index (PLI) (El-Fergany & Abdelaziz, 2014a; Abdelaziz et al., 2016a), and Loss Sensitivity Factors (LSF) (El-Fergany & Abdelaziz, 2014b; Dixit et al., 2016) to identify and rank candidate buses for shunt capacitors placement. Depending on the method used, the ranking is in either an ascending or descending order. Further, in determining the global optimum bus(es) for capacitor placement, some researchers just choose from the list of ranked candidate buses based on either a higher or lower index value (Das, 2008; Murthy et al., 2010; Shetty & Ankaliki, 2016; Dixit et al., 2016; Chege et al., 2018). Some researchers however use an optimization algorithm to search for the optimal bus(es) from the list of ranked candidate buses (El-Fergany & Abdelaziz, 2014a; El-Fergany & Abdelaziz, 2014b; Abdelaziz et al., 2016; Elsheikh et al., 2016; Diab & Rezk, 2018). The approach in which an optimization algorithm is used to search for the global optimum bus(es) from the list of ranked candidate buses tend to give better results than the one in which researchers just choose the highly ranked bus(es) as optimal locations for capacitor placement. However, the latter approach takes relatively high computation time to converge to the global optimum solution.

Furthermore, despite being of great help in reducing the computation time, the use of the available indices or search space reduction techniques leads to a compromise in solutions accuracy. This is so because the solutions they give out tend to be inferior as compared to those obtained when a search is carried out in unreduced search spaces (Gnanasekaran et al., 2016; George et al., 2018; Idris & Zaid, 2016; Askarzadeh, 2016; Haldar & Chakravorty, 2015). Despite giving solutions of the best quality, the greatest drawback in searching for global optimum solutions from unreduced search spaces is that it takes more computation time (due to the required high number of iterations and search agents) for the optimization algorithms to converge to the global optimum solutions (Kumar & Rudramoorthy, 2021). Thus, due to existing shortfalls in these two approaches, the essence of developing an approach that counters their respective weaknesses was manifested, hence formulation of this thesis.

1.2. Problem Statement

Identification of the optimal buses on which to install shunt capacitors within radial distribution systems is one critical task that greatly affects the overall cost of total real power losses, shunt capacitors' purchase, installation, and O&M. Currently, the existing challenge when solving the radial distribution system's optimal shunt capacitors' placement and sizing problem lies in the identification of the global optimum bus(es) within short computation times. In this study, a new approach based on the Modified Loss Sensitivity Factors (MLSF), the Multi-Verse Optimizer (MVO) and MATLAB matrix reduction techniques has been used to address the challenge.

1.3. Justification

The benefits yielding from the minimization of electric power system losses include the consequential increase in an electric circuits' ability to transfer power as well as an improvement in its voltage profile (Weedy et al., 2012). Installation of shunt capacitors is one way by which the power system losses may be minimized, and when carried out properly, the exercise may result in the attainment of the aforementioned benefits. However, both electric power system losses and shunt capacitors placement have financial costs attached to them. As such, this raises the need to have them both optimized so that the benefits may be attained while incurring the most minimal overall cost.

1.4. Research Objectives

1.4.1. Main Objective

To develop an algorithm using MVO, MLSF and MATLAB matrix reduction methods for optimal shunt capacitors' placement and sizing in radial distribution systems for overall cost minimization.

1.4.2. Specific Objectives

(a) To formulate the shunt capacitors placement and sizing optimization problem through the adoption of an appropriate objective function, constraints and capacitors' data as found in published literature.

(b) To develop a MLSF, MVO and MATLAB matrix reduction methods based optimal shunt capacitors placement and sizing algorithm.

(c) To evaluate the performance of the developed algorithm using the IEEE 10- and 33-bus radial distribution systems.

(d) To validate the results obtained using the developed approach with those that were obtained using the exhaustive search, the exhaustive search and MVO, and other selected typical approaches reported in literature.

1.5. Scope of the Study

This study solely focused on developing an approach for solving the optimal shunt capacitors' placement and sizing problem in radial distribution systems. As a result, only radial distribution systems (the IEEE 10- and 33-bus radial distribution systems) were used in evaluating the effectiveness of the developed approach. The two test systems were considered, firstly, because of being relatively small, hence being feasible to use the exhaustive search algorithm on them. Secondly, the two test systems were considered because of the availability of results which would be used to validate the results obtained in this study.

1.6. Contribution of the Thesis

The following are the three ultimate deliverables of this research: -

(i) A new effective technique for reducing the search space of buses for the optimal installation of shunt capacitor(s). The technique is based on MLSF and MATLAB's matrix reduction techniques. Unlike existing search space reduction techniques, the new technique reduces the search space but still end up having the global optimum bus(es) in the reduced search space.

(ii) A new optimal shunt capacitors' placement and sizing algorithm that is based on MLSF, MATLAB's matrix reduction techniques and MVO. The new algorithm exactly matches the accuracy of the exhaustive search algorithm.

(iii) Results of the absolute optimal buses and shunt capacitor sizes that gives the least overall cost of operating the IEEE 10- and 33- bus radial distribution systems.

These have been obtained using the exhaustive search. The results did not exist prior to this research and their availability will greatly help with the benchmarking of new optimization algorithms.

1.7. Thesis Outline

This thesis has been divided into five chapters with Chapter 1 serving to introduce the work by giving the background information, statement of the problem, justification, study objectives, and then the scope of the research work. Afterwards, Chapter 2 gives a review of the essential literature relating to the current research problem. Thereafter, Chapter 3 discusses the methodology adopted for this research and then Chapter 4 presents and analytically discusses the results. Further, in consideration of the obtained results and the set scope for this study, Chapter 5 gives the conclusion as well as recommendations for further studies.

CHAPTER TWO

LITERATURE REVIEW

2.1. Highlights

This chapter discusses the theory behind electric power system losses and then goes further to discuss the theory behind their minimization through the installation of shunt capacitors. Afterwards, the chapter present reviews of the LSF as well as the approaches that have been used to identify optimal buses on which shunt capacitors may be installed. Later, a review of the theory behind the MVO is presented. This is followed by a presentation of the comparative analysis of the approaches that are used to identify optimal buses on which shunt capacitors may be installed. The comparison which is based on results from published literature aims at highlighting shortfalls in available search space reduction techniques.

2.2. Electrical Power System Losses

Electricity is a result of current flow through a conductor. However, this flow does not happen unopposed because electric current always encounters an opposing force whenever it flows through conductors. This opposition, whose unit of measure is the ohm, is termed resistance (R) for purely resistive circuits, inductive reactance (X_L) for purely inductive circuits, capacitive reactance (X_C) for purely capacitive circuits, and impedance (Z) for circuits containing both resistance and reactance. Consequently, due to this opposition, considerable voltage drop exists between a conductor's sending and receiving end terminals (Bird, 2003) and if the conductor length is either increased or decreased then there is a corresponding increase or decrease in the voltage drop (Bird, 2003; Gill, 2008; Robbins & Miller, 2000). For certain cases the voltage drop is overly insignificant such that with approximation, the sending and receiving end voltages tend to be the same. For some cases however, the voltage drop is so significant such that it results into having the receiving end voltage being noticeably lower than the sending end voltage. Equation (2.1) gives the relationship between the per phase sending and receiving end voltages as electric power flows through the radial feeder given in Figure 2.1 (Weedy et al., 2012).

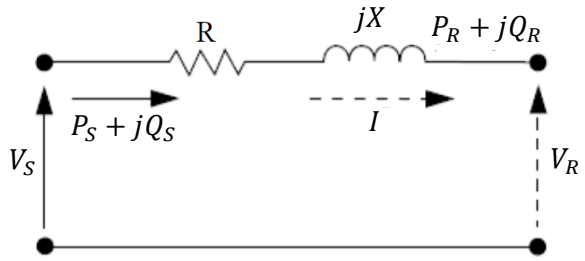

Figure 2.1: Power flow in a two-busbar system

$$V_R = V_S - (R + jX)I \tag{2.1}$$

where

V_R is the receiving end voltage per phase

V_S is the sending end voltage per phase

R is the resistance of the line between the two buses per phase

X is the reactance of the line between the two buses per phase

I is the phase current flowing between the two buses

P_S is the per phase sending end real power

Q_s is the per phase sending end reactive power

P_R is the per phase receiving end real power

Q_R is the per phase receiving end reactive power

Converting elements of (2.1) from voltage to complex power by multiplying both sides by I^* (since complex power, $S = VI^*$), expression (2.1) becomes

$$V_R I^* = V_S I^* - ((R + jX)I \times I^*) \tag{2.2}$$

where I^* is the complex conjugate of I.

From (2.2), the apparent power loss, S_{loss}, is given as:

$$S_{loss} = I^2 R + jI^2 X \tag{2.3}$$

and then

$$P_{loss} = I^2R \tag{2.4}$$

$$Q_{loss} = jI^2X \tag{2.5}$$

With reference to (2.4) and (2.5) it must be noted that both the active (P_{loss}) and reactive (Q_{loss}) power losses can be controlled by manipulating the current flow. Additionally, changes in resistance and reactance also brings forth changes in the total electric power losses. This change in resistance and reactance may be a result of changes in an electrical network's conductors. Furthermore, the switching in and out of series capacitor banks or reactors also brings forth changes in the overall conductor impedance and consequently the total electric power losses.

For the radial system given in Figure 2.1, the sending end complex power is given as

$$S_S = V_S I_S^* = P_S + jQ_S \tag{2.6}$$

where I_s is the sending end branch current which is also the same as the receiving end current.

Rearranging (2.6) gives

$$I_S^* = \frac{P_S + jQ_S}{V_S} \tag{2.7}$$

$$I_S = \left(\frac{P_S + jQ_S}{V_S}\right)^* = \left(\frac{P_S - jQ_S}{V_S^*}\right) \tag{2.8}$$

And multiplying (2.7) and (2.8) yields (2.9) as follows

$$I_S^2 = \left(\frac{P_S + jQ_S}{V_S}\right) \left(\frac{P_S - jQ_S}{V_S^*}\right) = \left(\frac{P_S^2 + Q_S^2}{|V_S|^2}\right) \tag{2.9}$$

And then the substitution of I_s^2 from (2.9) into (2.4) and (2.5) yields

$$P_{loss} = \left(\frac{P_S^2 + Q_S^2}{|V_S|^2}\right) \times R \tag{2.10}$$

$$Q_{loss} = \left(\frac{P_S^2 + Q_S^2}{|V_S|^2}\right) \times jX \tag{2.11}$$

Equations (2.10) and (2.11) shows that by either changing the sending end voltage, the sending end real power and the sending end reactive power, the value of current

can also be changed. Consequently, this also results in a change in the electrical power losses. A critical look at these equations also leads to a revelation as to why transmission of electric power at high voltage helps in lowering the electric power system losses. Ultimately, this leads to an improvement in the electrical power system's efficiency.

Another factor that helps in lowering the electric power system losses is the installation of localized electric power generation sources. With reference to Figure 2.1, the installation of a localized electric power generation source at the receiving end busbar would help in lowering the amount of power coming from the sending end busbar. This would then lead to a reduction in power flow through the line, thus reducing the current flowing and consequently the total losses. If the localized electric power generation source is a Type 3 Distributed Generator (DG) i.e. one that injects both active and reactive power (Hung et al., 2010), then (2.7) and (2.8) changes to

$$I_S^* = \frac{(P_S - \Delta P_{loss} - P_{DG}) + j(Q_S - \Delta Q_{loss} - Q_{DG})}{(V_S + \Delta V_S)} \tag{2.12}$$

and

$$I_S = \frac{(P_S - \Delta P_{loss} - P_{DG}) - j(Q_S - \Delta Q_{loss} - Q_{DG})}{(V_S + \Delta V_S)^*} \tag{2.13}$$

where

P_s is the per phase sending end real power before installation of the DG

Q_S is the per phase sending end reactive power before installation of the DG

P_{DG} is the per phase real power being supplied by the DG unit

Q_{DG} is the per phase reactive power being supplied by the DG unit

V_S is the per phase sending end voltage before installation of the DG

ΔP_{loss} is the per phase change in real power losses between the sending and receiving end buses after installation of the DG

ΔQ_{loss} is the per phase change in reactive power losses between the sending and receiving end buses after installation of the DG

ΔV_s is the change in the sending end voltage after installation of the DG

And then multiplying (2.12) and (2.13) yields (2.14) as follows

$$I_S^2 = \frac{(P_S - \Delta P_{loss} - P_{DG})^2 + (Q_S - \Delta Q_{loss} - Q_{DG})^2}{(|V_s + \Delta V_s|)^2} \tag{2.14}$$

Thereafter, S_{loss} would be given as,

$$S_{loss} = (R + jX)\left(\frac{(P_S - \Delta P_{loss} - P_{DG})^2 + (Q_S - \Delta Q_{loss} - Q_{DG})^2}{(|V_s + \Delta V_s|)^2}\right) \tag{2.15}$$

With the real power losses, P_{loss}, being given as

$$P_{loss} = R \times \left(\frac{(P_S - \Delta P_{loss} - P_{DG})^2 + (Q_S - \Delta Q_{loss} - Q_{DG})^2}{(|V_s + \Delta V_s|)^2}\right) \tag{2.16}$$

And the reactive power losses, Q_{loss}, being given as

$$Q_{loss} = jX \times \left(\frac{(P_S - \Delta P_{loss} - P_{DG})^2 + (Q_S - \Delta Q_{loss} - Q_{DG})^2}{(|V_s + \Delta V_s|)^2}\right) \tag{2.17}$$

On the other hand, when the localized electric power generation source is a Type 2 DG i.e. one that injects reactive power only (Hung et al., 2010), then (2.7) and (2.8) changes to

$$I_S^* = \frac{(P_s - \Delta P_{loss}) + j(Q_S - \Delta Q_{loss} - Q_{DG})}{(V_s + \Delta V_s)} \tag{2.18}$$

and

$$I_s = \frac{(P_s - \Delta P_{loss}) - j(Q_S - \Delta Q_{loss} - Q_{DG})}{(V_s + \Delta V_s)^*} \tag{2.19}$$

And then multiplying (2.18) and (2.19) yields (2.20) as follows

$$I_S^2 = \frac{(P_S - \Delta P_{loss})^2 + (Q_S - \Delta Q_{loss} - Q_{DG})^2}{(|V_s + \Delta V_s|)^2} \tag{2.20}$$

Thereafter, S_{loss} would be given as,

$$S_{loss} = (R + jX)\left(\frac{(P_S - \Delta P_{loss})^2 + (Q_S - \Delta Q_{loss} - Q_{DG})^2}{(|V_s + \Delta V_s|)^2}\right) \quad (2.21)$$

With the real power losses being given as

$$P_{loss} = R \times \left(\frac{(P_S - \Delta P_{loss})^2 + (Q_S - \Delta Q_{loss} - Q_{DG})^2}{(|V_s + \Delta V_s|)^2}\right) \quad (2.22)$$

And the reactive power losses being given as

$$Q_{loss} = jX \times \left(\frac{(P_S - \Delta P_{loss})^2 + (Q_S - \Delta Q_{loss} - Q_{DG})^2}{(|V_s + \Delta V_s|)^2}\right) \quad (2.23)$$

2.3. Loss Minimization through the Installation of Shunt Capacitors

Proper shunt capacitors placement and sizing helps in reducing the current flowing between two buses. Consequently, this results in reductions in power system losses, improvements in the voltage profiles and improvements in the system's voltage stability margin (Seifi & Sepasian, 2011). However, as put forth by Kothari and Nagrath (2003), the effectiveness of the installed shunt capacitors is so much dependent on the proper selection of their size, ratings and installation buses. The following discussion highlights the impact of shunt capacitors on both active and reactive power losses.

2.3.1. Base Case: Operation without Shunt Capacitors

Figure 2.2 gives a schematic representation of a radial feeder spanning between two areas. Bus-1 is at the feeder's sending end while Bus-2 is at the receiving end.

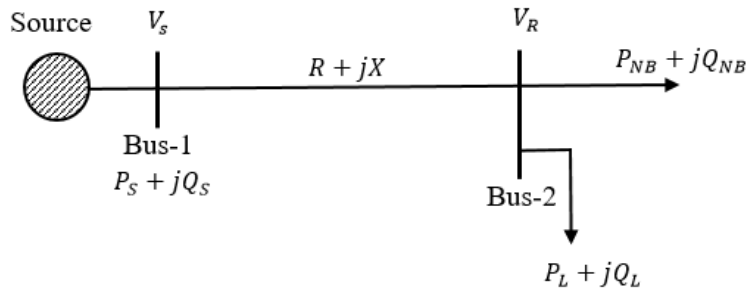

Figure 2.2: Operation without shunt capacitors

With reference to Figure 2.2, the line or feeder's real and reactive power losses, P_{loss} and Q_{loss} respectively, are given as

$$P_{loss} = R \times \left(\frac{P_S^2 + Q_S^2}{|V_S|^2}\right) = R \times \left(\frac{(P_L+P_{NB})^2 + (Q_L+Q_{NB})^2}{|V_R|^2}\right) \quad (2.24)$$

$$Q_{loss} = X \times \left(\frac{P_S^2 + Q_S^2}{|V_S|^2}\right) = X \times \left(\frac{(P_L+P_{NB})^2 + (Q_L+Q_{NB})^2}{|V_R|^2}\right) \quad (2.25)$$

where

P_S is the per phase sending end real power

Q_S is the per phase sending end reactive power

$|V_S|$ is the per phase magnitude of the sending end bus voltage

P_L is the per phase real power load at the receiving end bus (Bus-2)

Q_L is the per phase reactive power load at the receiving end bus (Bus-2)

P_{NB} is the summation of the per phase real power loads and losses beyond Bus-2

Q_{NB} is the summation of the per phase reactive power loads and losses beyond Bus-2

$|V_R|$ is the per phase magnitude of the receiving end bus voltage

R and X are the distribution lines resistance and reactance per phase

For this case, all the demanded active and reactive power is taken from the source.

2.3.2. Operation with Shunt Capacitors at Source Side

Figure 2.3 replicates Figure 2.2 and illustrates the operation with a shunt capacitor installed at the source side.

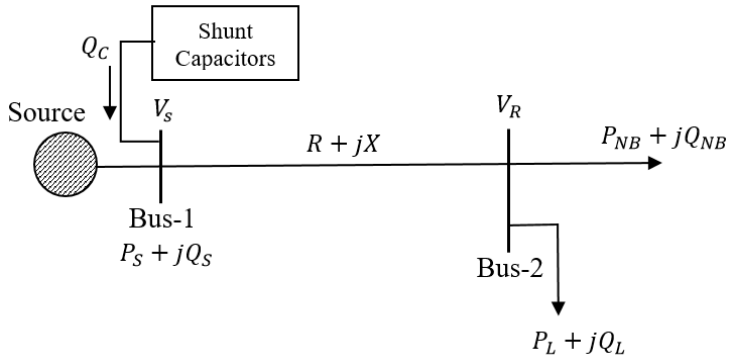

Figure 2.3: Operation with shunt capacitors at the source side

For this case, the active and reactive power losses are the same as those given in (2.24) and (2.25), that is, the installation of shunt capacitors at the source side does not help in reducing the electric power system losses occurring between Bus-1 and Bus-2. This is so because the amount of reactive power flowing between Bus-1 and Bus-2 is the same as given for case one. However, for this case

$$P_S + jQ_S = P_S + j(Q'_S + Q_C) \tag{2.26}$$

where

Q_C is the reactive power being supplied by the shunt capacitors; and

Q'_S is the reduced amount of reactive power that the source still supplies.

Despite the resulting inability to reduce the radial feeder's electric power losses, the installation of shunt capacitors at the source helps in the reduction of thermal overloads on the source, be it a transformer or a generator (Natarajan, 2005). This is so because the installation of shunt capacitors at the source helps in reducing the amount of reactive power that the source gives out. This reduction then leads to a consequent reduction in current (which lead to thermal overloads when at high levels) injection from the source. Furthermore, a reduction in the current that the source injects into a feeder can also lead to the release of the source's kVA capability (Natarajan, 2005; Gonen, 2014).

2.3.3. Operation with Shunt Capacitors at the Load Side

Figure 2.4 illustrates the same system but then with inclusion of the shunt capacitors at the load side.

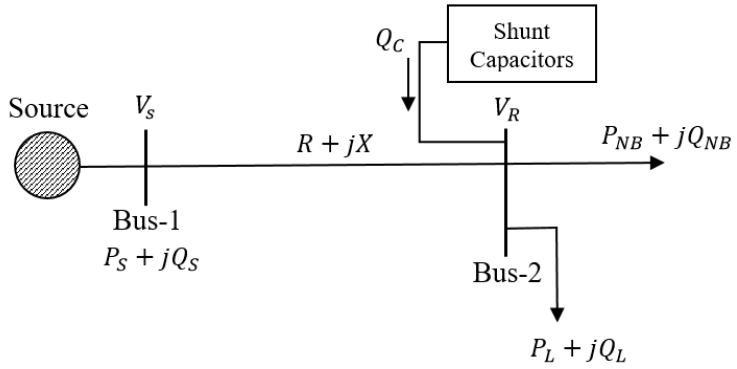

Figure 2.4: Operation with shunt capacitors at the load side

For this case the active and reactive power losses are given as

$$P_{loss} = R \times \frac{(P_S - \Delta P_{loss})^2 + (Q_S - \Delta Q_{loss} - Q_C)^2}{(|V_S + \Delta V_S|)^2} = R \times \left(\frac{(P_L + P_{NB})^2 + (Q_L + Q_{NB} - Q_C)^2}{|V_R|^2}\right) \quad (2.27)$$

$$Q_{loss} = X \times \left(\frac{(P_S - \Delta P_{loss})^2 + (Q_S - \Delta Q_{loss} - Q_C)^2}{(|V_S + \Delta V_S|)^2}\right) = X \times \left(\frac{(P_L + P_{NB})^2 + (Q_L + Q_{NB} - Q_C)^2}{|V_R|^2}\right) \quad (2.28)$$

where

P_s is the per phase sending end real power before installation of the shunt capacitor.

Q_S is the per phase sending end reactive power before installation of the shunt capacitor.

V_S is the per phase sending end voltage before installation of the shunt capacitor.

ΔP_{loss} is the per phase change in real power losses between the sending and receiving end buses after installation of the shunt capacitor.

ΔQ_{loss} is the per phase change in reactive power losses between the sending and receiving end buses after installation of the shunt capacitor.

ΔV_s is the per phase change in the sending end voltage after installation of the shunt capacitor.

From (2.27) and (2.28), it can be noted that the introduction of the shunt capacitor (Q_C) at the load side helps in giving a resulting reduction in the net reactive power loading (i.e. ($Q_L + Q_{NB} - Q_C$)) hence a reduction in the amount of reactive power flowing between buses 1 and 2. Additionally, since the reduction in the amount of reactive power flowing between buses 1 and 2 also result in a reduction in current flow; therefore, the active and reactive power losses for this case also becomes less than those for the base case and for the case where the power system is operated with the shunt capacitor installed at the source side.

It is advisable to provide reactive power compensation (e.g. through the installation of shunt capacitors) closer to the point of use as practically as possible. This is done in order to avoid the need to have to distribute reactive power which leads to higher electric currents flowing between buses and consequently, increased electric power system losses (EuropeAid, 2016). In (EuropeAid, 2016), it is further stated that the placement of reactive power compensation devices is primarily determined by the reason for compensation. For example, as stated under case two, by locating the shunt capacitors at Bus-1 (i.e. the source side), the source's real power generation capability would be improved. However, the electric power losses would remain the same. So if the reason for reactive power compensation is loss minimization, the best location for capacitor placement is the load side. On the other hand, if the reason for reactive power compensation is to reduce thermal overloads on the source or to release the source's kVA capability, then the best location for capacitor placement is the source side.

2.4. Loss Sensitivity Factors (LSF)

Use of LSF in solving the optimized shunt capacitors placement and sizing problem within radial distribution systems was pioneered by Prakash and Sydulu (2007). These factors give a measure of how responsive the real power losses in a given

branch are to changes in the reactive power flow between its two ends. The LSF are calculated from a base case load flow according to (2.29).

$$\text{LSF} = \frac{\partial P_{loss_k}}{\partial Q_{pq}} = \frac{2Q_{pq}}{V_p^2} R_{pq} \tag{2.29}$$

where with reference to Figure 2.5, Q_{pq} is the total reactive power (VArs) leaving bus *p* and flowing towards bus *q*, R_{pq} is the resistance of the k[th] branch (ohms) and V_p is the voltage at node or bus *p* (volts).

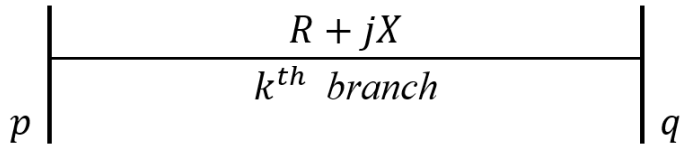

Figure 2.5: A distribution branch between buses *p* and *q*

According to Prakash and Sydulu (2007), identification of the optimal buses on which to install shunt capacitors using LSF is carried out as follows:

(a) Compute the LSF values using (2.29);

(b) Arrange the LSF values in descending order;

(c) Compute the normalized voltages for all receiving end buses $(V_q/0.95)$. The division of V_q by 0.95 significantly helps in reducing the search space and consequently the computation time;

(d) Select receiving end buses with $(V_q/0.95) < 1.01$ as optimal candidate buses for the installation of shunt capacitors.

Thereafter, the sequence for compensation is given by the LSF values in such a way that buses with higher LSF values are compensated first before the ones with lower LSF values.

2.5. Optimal Shunt Capacitors' Placement Techniques

There are several different approaches that are used to identify optimal buses on which to install shunt capacitors. This section presents a general description of these

approaches by looking at two of their broad categories which are differentiated based on restrictions posed during the search. The author (of this thesis) categorize these approaches as: *(a) Approaches for searching of optimal buses from unreduced search spaces* and *(b) Approaches for searching of optimal buses from reduced search spaces*. A discussion of these approaches follows.

2.5.1. Approaches for searching of optimal buses from unreduced search spaces

For this approach, if an electrical system has m buses, then shunt capacitors may be installed at any of the $m-1$ buses or at any combination of the $m-1$ buses. The slack bus is the only bus which is completely discarded as a potential candidate bus on which shunt capacitors may be installed (Sedighizadeh & Bakhtiary, 2015). This approach may further be subdivided into two other approaches which are *exhaustive search based* and *metaheuristic search-based approaches.*

A. Exhaustive search-based approach

This is a very basic approach. Under this approach, in an attempt to determine the global best, each and every possible solution within the search space is evaluated. Since the search process is exhaustive, there is a guarantee that the global or absolute optima will be attained. However, this approach becomes ineffective when the number of candidate solutions being dealt with is large. This is due to its accompanying overall high computation time (Hitzeroth, 1995; Anilkumar et al., 2017; Baghzouz, 1991).

For this approach, the search space for buses is generated using the following command (which is a representation of (1.1) under MATLAB software programming language):

$$B = nchoosek(A,r) \tag{2.30}$$

where A is a $(1 \times n)$ matrix made up of all the buses of a given radial distribution system (except the slack bus) and r represents the desired total number of buses to be compensated.

On the other hand, since capacitors of the same size can be installed at different buses of a combination, the permutation with repetition command is used in generating the search space for available shunt capacitor sizes (Ghosh & Sinha, 2017; Askarzadeh, 2016). The resulting search space size, D, for the capacitors is given by (2.31).

$$D = E^r \times r \tag{2.31}$$

where E is the total number of available shunt capacitor sizes and r is the desired total number of buses to be compensated.

A flowchart for optimizing the placement and sizing of shunt capacitors using this approach is given in Figure 2.6.

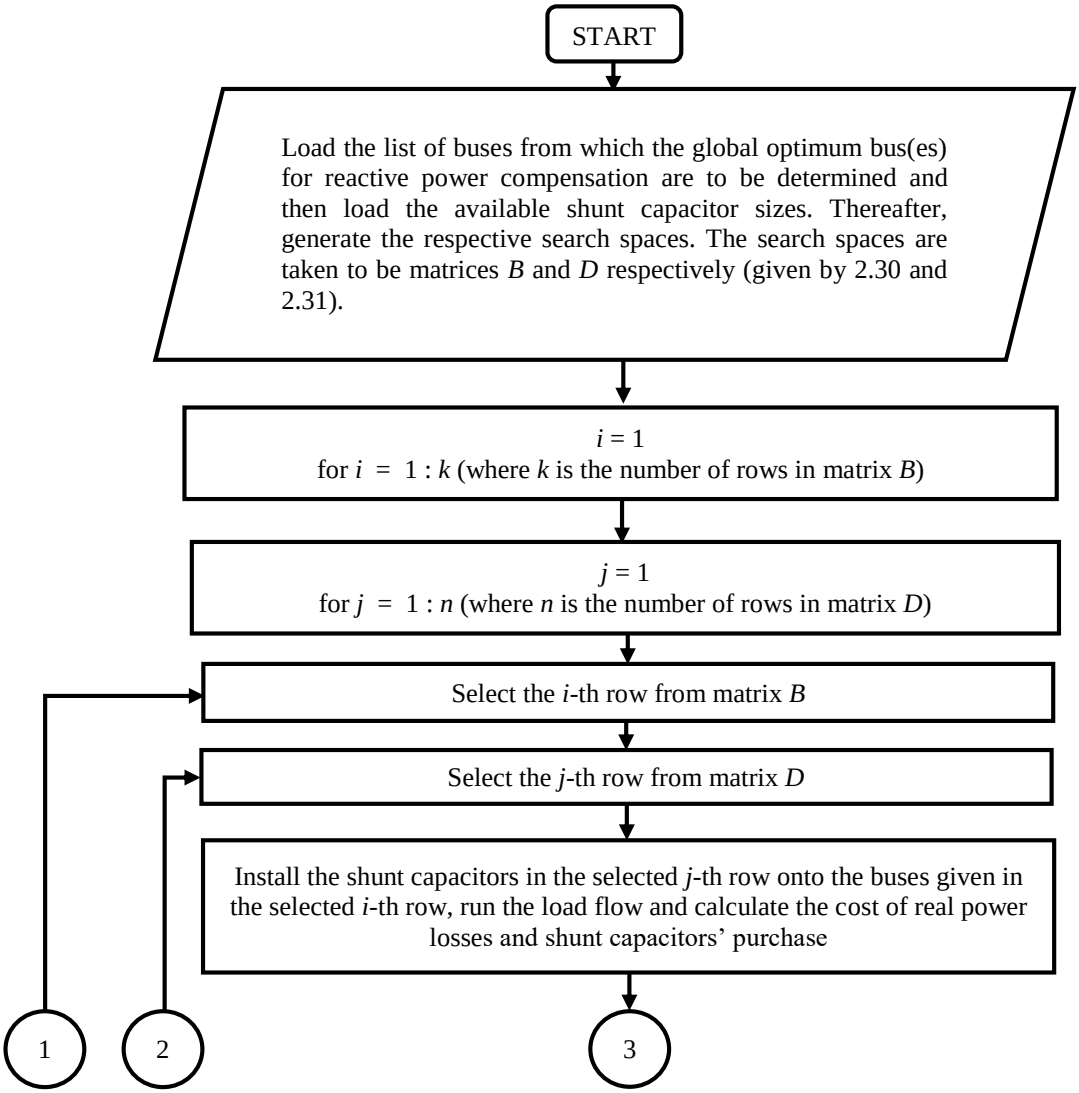

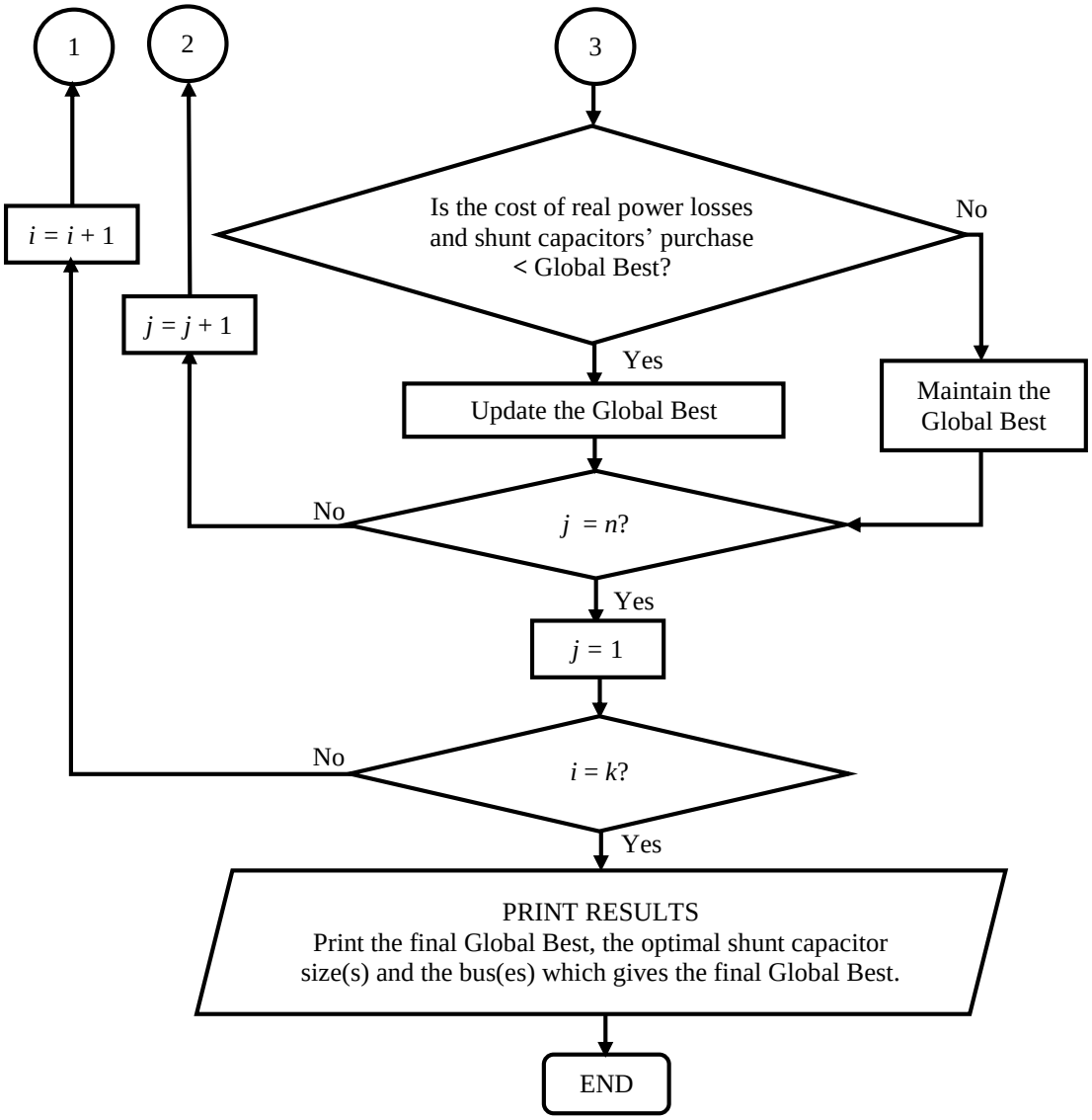

Figure 2.6: Flowchart for optimal shunt capacitors placement and sizing using the exhaustive search

B. Metaheuristic search-based approach

Metaheuristic search-based approaches for optimal shunt capacitors placement and sizing are formulated so as to reduce the high computation times which result from the use of exhaustive search-based approaches. Despite being computationally efficient, these approaches do not guarantee the attainment of the absolute optimal solution (Nesmachnow, 2014). In a manner similar to the exhaustive search, for this approach all the buses except the slack bus also qualify as candidate buses on which

shunt capacitors may be installed. However, for this approach, only a limited number of candidate solutions are evaluated. This limitation is brought forth by the defined number of search agents or population size, the maximum number of iterations and the algorithm's exploration and exploitation mechanisms (Piotrowski et al., 2020; Kavaliauskas & Sakalauskas, 2019; Mirjalili et al., 2016). Under this approach, the search for optimal buses is conducted intelligently in such a way that the search agents learn to avoid non-promising regions and focus their search for the global best in promising regions. Their learning capability is what enable metaheuristic search based approaches identify the absolute optimum or near optimum solution quickly than exhaustive search-based approaches (Yang, 2012).

Figure 2.7 gives a general flowchart of the search process in metaheuristic-based search algorithms.

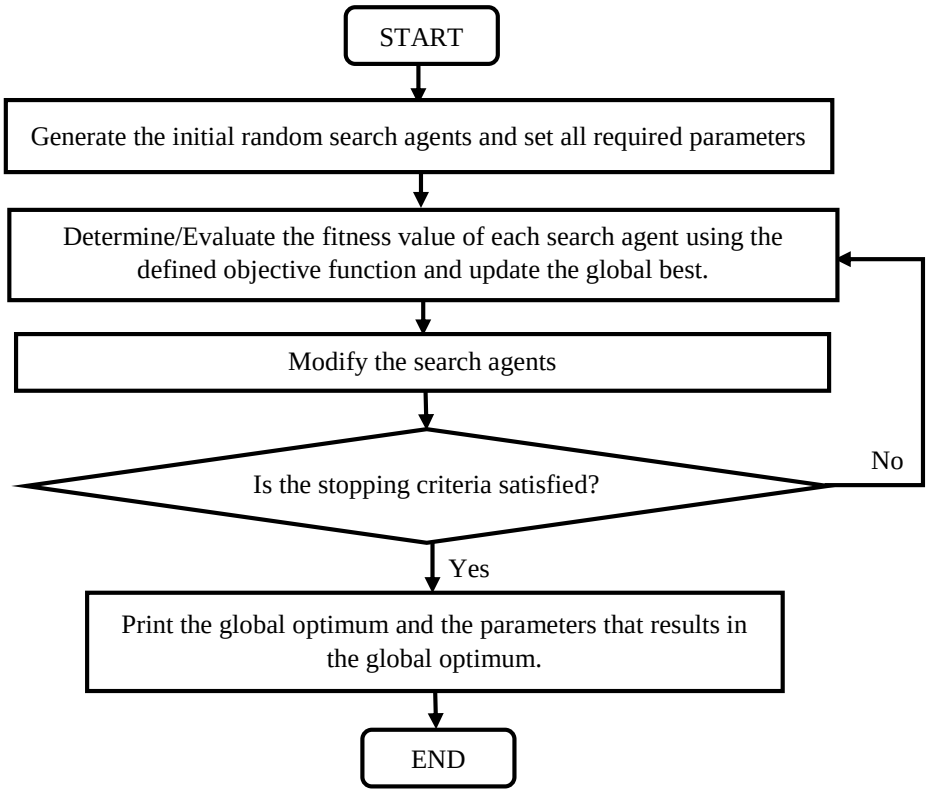

Figure 2.7: General flowchart of metaheuristic search-based algorithms

Literature has several metaheuristic search-based optimal shunt capacitors' placement and sizing algorithms that were implemented in unreduced search spaces

as is discussed in the preceding paragraphs. Some of these, whose results have been compared against the ones obtained in this study are based on CrSA (Askarzadeh, 2016), Cuckoo Search Algorithm (CSA) (Idris & Zaid, 2016), Genetic Algorithm (GA) (Askarzadeh, 2016), Improved Crow Search Algorithm (ICrSA) (Diaz et al., 2018), Modified Cultural Algorithm (Haldar & Chakravorty, 2015) and PSO (Idris & Zaid, 2016).

2.5.2. Approaches for searching of optimal buses from reduced search spaces

Under this approach, in determining the optimal bus(es) on which to install shunt capacitors, the buses of a given radial distribution system are firstly ranked and then classified into two groups using different ranking and classification techniques (e.g. LSF, PLI). One group is made up of buses that qualify for the installation of shunt capacitors, and the other one is made up of buses that do not qualify. Thereafter, optimally sized shunt capacitors are then installed at either a single bus or multiple buses which is/are selected from the class made up of buses that qualify for the installation of shunt capacitors (Prakash and Sydulu, 2007; Prakash and Sydulu, 2012; Tolba et al., 2017; Abou El-Ela et al., 2016; Youssef et al., 2018).

In selecting the global optimum bus(es) for the installation of shunt capacitors some researchers just choose the top most *n* bus(es) (from the list of ranked candidate buses that qualify for the installation of shunt capacitors) as being the optimal bus(es) (Das, 2008; Murthy et al., 2010; Shetty & Ankaliki, 2016; Dixit et al., 2016). Some researchers however use an optimization algorithm to search for the optimal bus(es) from the list of ranked candidate buses (El-Fergany & Abdelaziz, 2014a; El-Fergany & Abdelaziz, 2014b; Abdelaziz et al., 2016a; Abdelaziz et al., 2016b; Elsheikh et al., 2016; Diab & Rezk, 2018). The approach in which an optimization algorithm is used to search for the global optimum bus(es) from the list of ranked candidate buses tend to give better results than the one in which researchers just choose the highly ranked bus(es) as optimal bus(es) for capacitor placement. However, the latter approach takes relatively high computation time to converge to the global optimum solution.

As is the case for the approaches discussed in section 2.5.1 (B), literature also has several metaheuristic search-based optimal shunt capacitors' placement and sizing

algorithms that were implemented in reduced search spaces in a manner as discussed above. Some of these, whose results have been compared against the ones obtained in this study are based on Artificial Bee Colony (ABC) algorithm (Diaz et al., 2018), Differential Evolution (DE) (Diaz et al., 2018), Dragon-Fly Optimizer (DFO) (Diab & Rezk, 2018), Gravitational Search Algorithm (GSA) (Diaz et al.,), Grey Wolf Optimizer (GWO) (Diab & Rezk, 2018), ICrSA (Diaz et al., 2018), and Moth-Flame Optimizer (MFO) (Diab & Rezk, 2018).

2.6. The Multi-Verse Optimization (MVO) Algorithm

In their preliminary studies building up to this thesis, Mtonga et al. (2020) demonstrated the superiority of the MVO against Chicken Swarm Optimization (CSO) algorithm, Cultural Algorithm (CA), Flower Pollination Algorithm (FPA), GSA and Particle Swarm Optimization (PSO) algorithm. This comparison served as a supplement to the already existing literature, given in (Sulaiman et al., 2016; Chopra & Sharma, 2016; Trivedi et al., 2016; Bentouati et al., 2016; Zhao et al., 2016; Singh et al., 2016; Kumar & Suhag, 2017a; Kumar & Suhag, 2017b; Fathy & Rezk, 2017; Guha et al., 2017; Priyanto & Robith, 2017), on power system optimization using MVO. Due to its proved effectiveness in optimal shunt capacitors' sizing (as shown in Mtonga et al., 2020), this study therefore used it in identifying the discrete optimal shunt capacitor sizes to be installed in the IEEE 10- and 33-bus radial distribution systems.

MVO, which belong to a family of nature inspired metaheuristic optimization algorithms, was developed by Mirjalili et al. (2016). The algorithm is based on the concepts of the black hole, the white hole and the worm hole. In the MVO, a candidate solution is termed universe and its fitness function value is termed inflation rate. For minimization problems, universes with lower inflation rates are considered to have a higher probability of having white holes while universes with higher inflation rates are considered to have higher probability of having black holes and the opposite is true for maximization problems. Now in an attempt to determine the desired inflation rate, universes with lower inflation rates tend to send objects (decision variables) to universes with high inflation rates through white holes. On the

other hand, universes with high inflation rates tend to receive objects through black holes. The black/white hole mechanism is responsible for the search space exploration and its formula is given by equation (2.32).

$$x_i^j = \begin{cases} x_k^j & r1 < NI(U_i) \\ x_i^j & r1 \geq NI(U_i) \end{cases} \tag{2.32}$$

where x_i^j indicates the *j*-th parameter of the *i*-th universe, U_i shows the *i*-th universe, $NI(U_i)$ is the normalized inflation rate of the *i*-th universe, $r1$ is a random number (between 0 and 1) generated using MATLAB's *rand* command, and x_k^j indicates the *j*-th parameter of *k*-th universe selected by a roulette wheel selection mechanism (Mirjalili et al., 2016).

Contrary to the foregoing, the exploitation phase of the MVO is not influenced by the universes' inflation rates. However, at a given iteration, each universe undergoes the exploitation phase through the worm hole computational mechanism given by equation (2.33).

$$x_i^j = \begin{cases} \begin{cases} X_j + \text{TDR} \times \left(\left(ub_j - lb_j \right) \times r4 + lb_j \right) & r3 < 0.5 \\ X_j - \text{TDR} \times \left(\left(ub_j - lb_j \right) \times r4 + lb_j \right) & r3 \geq 0.5 \end{cases} & r2 < \text{WEP} \\ x_i^j & r2 \geq \text{WEP} \end{cases} \tag{2.33}$$

where X_j indicates the *j*-th parameter of the best universe formed; Travelling Distance Rate (TDR) and Wormhole Existence Probability (WEP) are coefficients; lb_j and ub_j denote the lower and upper bounds of the *j*-th variable; x_i^j indicates the *j*-th parameter of *i*-th universe while $r2$, $r3$, $r4$ are random numbers (between 0 and 1) generated using MATLAB's *rand* command. WEP is adaptive and decreases over the iterations. Its formula is given by equation (2.34) (Mirjalili et al., 2016).

$$\text{WEP} = \min + l \times \left(\frac{\max - \min}{L} \right) \tag{2.34}$$

In equation (2.34), min and max denote minimum and maximum values respectively. Just as in (Mirjalili et al., 2016), the values of min and max that this study has used

are 0.2 and 1 respectively. Lastly, l and L correspondingly denote the present and maximum iterations. On the other hand, TDR which defines the distance rate (variation) by which an object can be teleported around the best universe obtained so far is given by equation (2.35) (Mirjalili et al., 2016):

$$\text{TDR} = 1 - \frac{l^{1/p}}{L^{1/p}} \tag{2.35}$$

where p defines the exploitation accuracy over the iterations. In this study its value was set to 6 (Mirjalili et al., 2016). Further, in order to have more precise exploitation/local search around the best universe obtained, TDR is increased over the iterations. Figure 2.8 gives the general flowchart for the MVO (Mtonga et al., 2020).

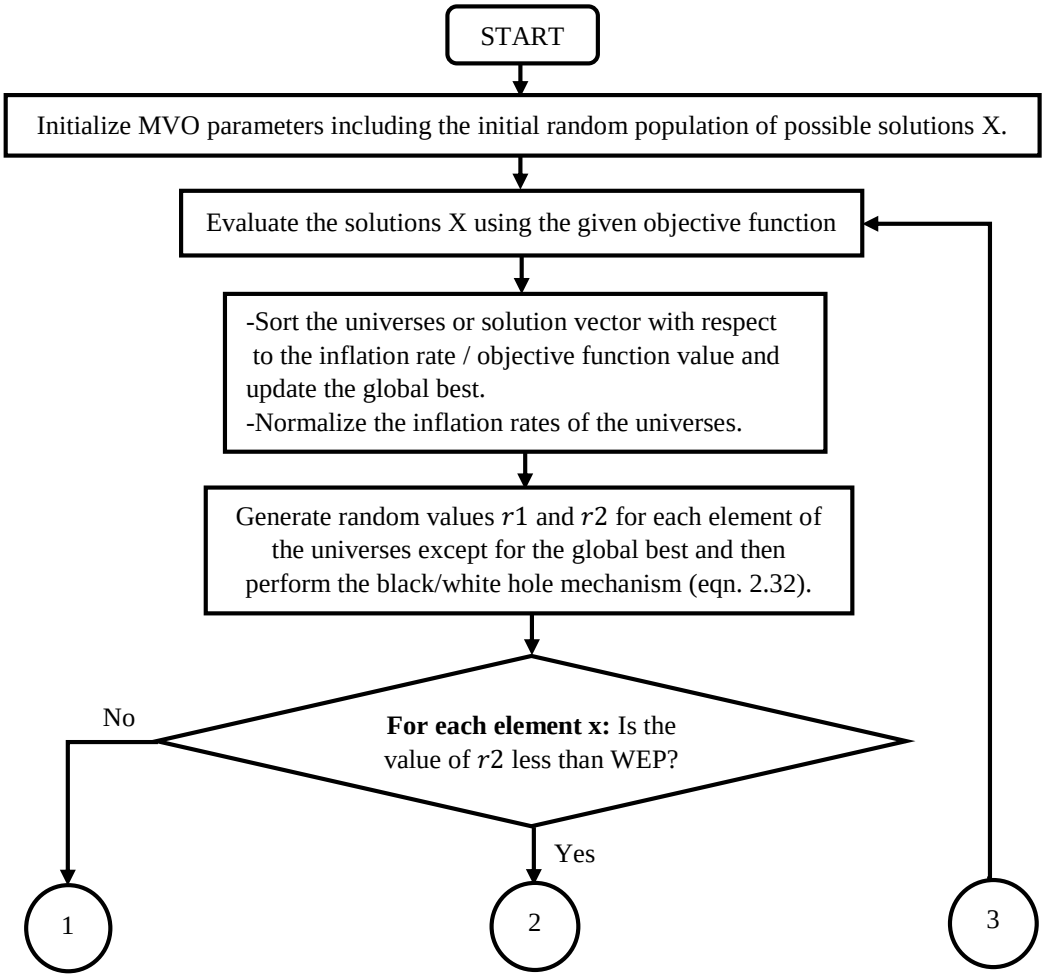

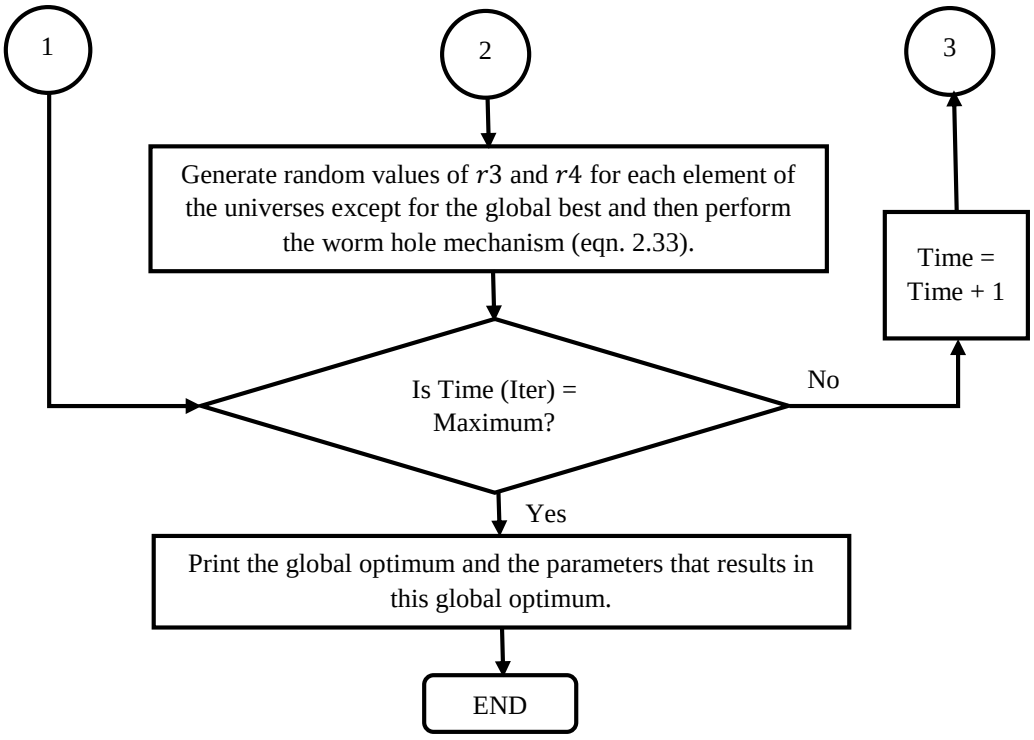

Figure 2.8: Flowchart of the general steps involved in the MVO algorithm

2.7. Comparative Analysis of the Shunt Capacitors Placement Techniques

Sections 2.5.1 and 2.5.2 gave a review of two general approaches that are used in identifying optimal bus(es) on which to install shunt capacitors. This section advances that review by carrying out a comparative analysis of the approaches based on results reported in literature. The analysis will only consider the LSF and the IEEE 33-bus radial distribution system. This is due to the fact that in the conducted literature survey it was found that the approaches discussed in Sections 2.5.1 and 2.5.2 have both been applied to the IEEE 33-bus radial distribution system using the LSF while also using the same optimization algorithms (i.e. PSO and FPA). Consequently, this formed a fair basis for comparing the approaches.

Upon applying the LSF approach to the IEEE 33-bus radial distribution system, the following bus rank vector results, {6, 3, 28, 29, 5, 4, 30, 24, 9, 13, 10, 8, 27, 31, 2, 26, 23, 25, 20, 14, 7, 12, 17, 16, 15, 11, 32, 18, 21, 19, 22, 33}. In this vector, bus numbers 6 and 33 have the highest and lowest LSF values respectively. However, when only buses with normalized voltages below 1.01 are considered, the 32-element bus rank vector reduces to the following 21 element bus rank vector: {6, 28, 29, 30,

9, 13, 10, 8, 27, 31, 26, 14, 7, 12, 17, 16, 15, 11, 32, 18, 33} (Diab & Rezk, 2018).

In their studies for a case of the IEEE 33-bus radial distribution system, Idris and Zaid (2016); and Diab and Rezk (2018) used the approaches discussed in Section 2.4.1 (B) and Section 2.4.2 respectively. In all instances, the authors used PSO to search for the global optimum buses on which to install shunt capacitors. However, Idris and Zaid (2016), used PSO to search for the optimum buses from the unreduced search space of buses. As such, for capacitor placement at three buses, PSO was free to search for the global optimum bus combination from the existing 4960 (i.e. $nCr = 32C3$) possible combinations. On the other hand, Diab and Rezk (2018), used PSO to search for the optimum buses from eight (8) highly ranked buses of the search space that was firstly reduced through the use of LSF. For capacitor placement at three buses, the search space was reduced from (4960×3) to (56×3) (i.e. $nCr = 8C3$). In the end, PSO searched for the global optimum bus combination from the existing 56 possible combinations, and not the original 4960 combinations. Table 2.1 gives the base case status for the IEEE 33-bus radial distribution system while Table 2.2 compares the different approaches as applied to the distribution system under consideration. Equations (2.36) and (2.37) have been used in calculating the results presented in Tables 2.1 and 2.2.

$$Total\ Cost = \{Total\ Cost\ of\ Real\ Power\ Losses + Cost\ of\ Shunt\ Capacitors\ Purchase\}$$

$$= \left\{ C_e \sum_{i=1}^{nb} P_{La}(i) T_i + \sum_{j=1}^{ncap} C_{cp} Q_{cs}(j) \right\} \quad (2.36)$$

$$Net\ Savings = \{Initial\ Cost\ of\ Total\ Real\ Power\ Losses - Overall\ Cost\} \quad (2.37)$$

where:

C_e is the average electrical energy cost

$P_{La}(i)$ is the kW electric power loss in branch i

nb is the total number of branches within a given electrical network

T_i is the duration of the load level under consideration (in years)

C_{cp} is the purchase cost of capacitor per kVAr

$Q_{cs}(j)$ is the size (kVAr) of the shunt capacitor installed at bus j

$ncap$ is the total number of buses with shunt capacitors installed

NB: All constants were taken from Tamilselvan et al. (2018).

Table 2.1: Base Case Status for the IEEE 33-bus radial distribution system

Parameters	
Total cost/year ($)	34,049.95
Real power losses/hour (kW)	202.68
Reactive power loss/hour (kVAr)	135.1559
V_{min} (p.u.)	0.9131
V_{max} (p.u.)	1.0000

Table 2.2: Comparison of Optimal Shunt Capacitors Placement Techniques

Parameters	**Unreduced Search Space**				**LSF Reduced Search Space**	
			Particle Swarm Optimization (PSO) Algorithm			
	Exhaustive Search Based Approach		**Metaheuristic Search Based Approach (Idris & Zaid, 2016)**		**Searching for three optimum bus combination (Diab & Rezk, 2018)**	
Total cost/year ($)	22,700.79		22,798.44		22,920.75	
Cost reduction/year (%)	33.33		33.04		32.68	
Net savings/year ($)	11,349.16		11,251.51		11,129.20	
Real power losses/hour (kW/hr)	132.68		133.08		134.15	
Loss reduction/hour (%)	34.54		34.34		33.81	
Reactive power losses/hour (kVAr/hr)	88.63		89.12		89.54	
Loss reduction/hour (%)	34.43		34.06		33.75	
Optimal buses and capacitor size (kVAr)	12	450	14	300	8	450
	24	600	24	600	13	300
	30	900	30	1200	30	900

Parameters	Unreduced Search Space		LSF Reduced Search Space
		Particle Swarm Optimization (PSO) Algorithm	
	Exhaustive Search Based Approach	Metaheuristic Search Based Approach (Idris & Zaid, 2016)	Searching for three optimum bus combination (Diab & Rezk, 2018)
Total kVAr installed	1950	2100	1650
V_{min}	0.9355	0.9381	0.9395
V_{max}	1.0000	1.0000	1.0000
Search space dimension	(4960×3)	(4960×3)	(56×3)
Population size	-	20	20
Maximum iterations	-	200	20
No of objective function evaluations	97627680	4000	400

With reference to Tables 2.1 and 2.2, it can be noted that in searching for the optimal bus combination from the eight (8) highly ranked buses of the reduced search space (which is made up of 21 buses), when PSO is put to use, the total real power losses are reduced from 202.68 to 134.15 kW. The reduction in total real power losses result in a corresponding reduction in the total cost from $34,049.95 to $22,920.75. On the other hand, when a search for the required three optimal buses is carried out in an unreduced search space, when PSO is put to use, the total real power losses are further reduced to 133.08 kW. The reduction in the total real power losses also reduces the total cost to $22,798.44. It would be appreciated from the results computed by the latter approach that instead of using PSO to search for the optimal buses from the reduced search space; the application of PSO to search for the optimal buses from the unreduced search space brings forth better results. The results are even much better when the search for optimal buses is carried out using the exhaustive search-based approach. Application of the exhaustive search-based approach results in the attainment of the global optimal solution while the other approaches only give sub-optimal solutions. For this approach, the total real power losses are reduced to 132.68 kW while the corresponding total cost is reduced to

$22,700.79.

Table 2.3 gives results of a comparison of the different approaches when FPA and the exhaustive search based approach were put to use.

Table 2.3: Comparison of Optimal Shunt Capacitors Placement Techniques

Parameters	Unreduced Search Space		LSF Reduced Search Space	
		Flower Pollination Algorithm (FPA)		
	Exhaustive Search Based Approach	Metaheuristic Search Based Approach (Tamilselvan et al., 2018)	Searching for three optimum buses (Abdelaziz et al., 2016b)	
Total cost/year ($)	22,700.79	22,733.04	23,094.63	
Cost reduction/year (%)	33.33	33.24	32.17	
Net savings/year ($)	11,349.16	11,316.91	10,955.32	
Real power losses/hour (kW/hr)	132.68	132.98	135.31	
Loss reduction/hour (%)	34.54	34.39	33.24	
Reactive power losses/hour (kVAr/hr)	88.63	88.7615	90.33	
Loss reduction/hour (%)	34.43	34.33	33.17	
Optimal buses and capacitor size (kVAr)	12 450 24 600 30 900	13 450 24 450 30 900	6 250 9 400 30 950	
Total kVAr installed	1950	1800	1600	
V_{min}	0.9355	0.9387	0.9333	
V_{max}	1.0000	1.0000	1.0000	
Search space dimension	(4960×3)	(4960×3)	(1330×3)	
Population size	-	20	25	
Maximum iterations	-	200	100	
No of objective function evaluations	97627680	4000	2500	

With reference to Table 2.3, it can also be noted that in searching for the optimal bus combination from the reduced search space (which is made up of 21 buses), when

FPA is put to use, the total real power losses are reduced from 202.68 to 135.31 kW. The reduction in the total real power losses result in a corresponding reduction in the total cost from $34,049.95 to $23,094.63. On the other hand, when a search for the required three optimal buses is carried out in an unreduced search space, when FPA is put to use, the total real power losses are further reduced to 132.98 kW. The reduction in total real power losses also reduces the total cost to $22,733.04. It would be appreciated from the results computed by the latter approach that instead of using FPA to search for the optimal buses from the reduced search space; the application of FPA to search for the optimal buses from the unreduced search space brings forth better results. The results are even much better when the search for optimal buses is carried out using an exhaustive search-based approach. Application of the exhaustive search-based approach results in the attainment of the global optimal solution while the other approaches only give sub-optimal solutions. For this approach, the total real power losses are reduced to 132.68 kW while the corresponding total cost is reduced to $22,700.79.

2.8. Summary of the Literature Review

From the presented literature, particularly section 2.7, it has been shown by the results in Tables 2.2 and 2.3, that a search for optimal buses for shunt capacitor placement from unreduced search spaces brings forth better results than for a case where the search is carried out in reduced search spaces. Furthermore, between the two approaches (i.e. the exhaustive and metaheuristic search-based approaches) which search for the optimal buses from unreduced search spaces, the exhaustive search-based approach stands out as the best approach since it guarantees the attainment of the absolute optimum solution. However, the main drawback of this approach is its high computation time which result from having the search carried out in a relatively large solutions space. Researchers have introduced different approaches (e.g. LSF, PLI, the metaheuristic search-based approach, etc.) that reduce the search space and consequently, the computation time. Despite their advantage with regards to the reduction in computation time, these approaches tend to give compromised solutions. Hence in considering the shortfalls in either of these approaches, there is a need to come up with approaches that strikes a balance

between these two approaches i.e. approaches that reduce the search space prior to searching for the optimal solution and the ones in which the search for the optimal solution is carried out in unreduced search spaces. This research endeavored to bridge that gap by introducing a search space reduction technique that is based on the MLSF and MATLAB's matrix reduction techniques. After reducing the search space, MVO was then used to identify the optimal buses on which to install shunt capacitors as well as the corresponding optimal shunt capacitor sizes.

2.9. Research Gaps

This work has addressed research gaps that included:

(i) The absence of effective search space reduction techniques. Existing search space reduction techniques are ineffective because, for the different compensation options, some buses that make up the global optimum bus combinations are not found in the final reduced search space(s). To address this gap, a new effective technique for reducing the search space of buses for the optimal installation of shunt capacitor(s) has been developed. The technique is based on MLSF and MATLAB's matrix reduction techniques. Unlike existing search space reduction techniques, the new technique reduces the search space but still end up having the global optimum bus(es) in the reduced search space.

(ii) The absence of optimal shunt capacitors' placement and sizing algorithms that exactly match the accuracy of the exhaustive search algorithm. To address this gap, a new optimal shunt capacitors' placement and sizing algorithm that is based on MLSF, MATLAB's matrix reduction techniques and MVO has been developed. The new algorithm exactly matches the accuracy of the exhaustive search algorithm.

(iii) The absence of results obtained using the exhaustive search algorithm about the optimum buses and the corresponding optimum shunt capacitor sizes to be installed in the IEEE 10- and 33-bus radial distribution systems in order to minimize the overall cost of total real power losses, shunt capacitors' purchase, installation, and O&M. The current practice is based on the benchmarking of the performance of metaheuristic optimization algorithms against each other, and not the exhaustive search algorithm. To address this gap, in this thesis results of the absolute optimal

buses and shunt capacitor sizes that gives the least overall cost of operating the IEEE 10- and 33- bus radial distribution systems have been obtained and reported. These have been obtained using the exhaustive search. The results did not exist prior to this research and their availability will greatly help with the benchmarking of new optimization algorithms.

CHAPTER THREE

METHODOLOGY

3.1. Highlights

A literature survey on optimal shunt capacitors' placement and sizing showed the LSF as a commonly used approach in reducing the search space and identifying the optimal buses on which to install shunt capacitors. Furthermore, works reported in (Murthy et al., 2010; Abdelaziz et al., 2016c; Essallah et al., 2017) have shown that this approach is superior to other existing approaches. Consequently, this work initially opted to use the LSF. However, preliminary simulations revealed a weakness in the use of the conventional LSF for cases where shunt capacitors had to be installed at a single bus within the IEEE 10- and 33-bus radial distribution systems as well as other systems with similar characteristics. This notable weakness necessitated modification of the conventional LSF.

This chapter starts off with a discussion about the formulation of the optimal shunt capacitors' placement and sizing problem. Thereafter, discussions about the MLSF, MATLAB's matrix reduction techniques, the developed search space reduction technique and the flowchart of the developed optimal shunt capacitors' placement and sizing algorithm are presented. What follows further are discussions about the adopted evaluation criteria and the considered test cases, i.e. the IEEE 10- and 33-bus radial distribution systems. In summing up the chapter, a discussion about the procedure that was used to validate the performance of the developed will be presented.

3.2. Tools and Methods

To meet the study's main objective, the MVO was used to search for the global optimum buses on which to install shunt capacitors and determine the corresponding shunt capacitor sizes to be installed in the IEEE 10- and 33-bus radial distribution systems. However, before using the MVO, the search space was firstly reduced through the partial use of the MLSF (i.e. by only considering the bus with the highest MLSF value and then using it to reduce the search space) and MATLAB's matrix

reduction techniques. MATPOWER, a free, open-source MATLAB-language M-files for solving steady-state power system simulation and optimization problems (Zimmerman et al., 2011), was used in running power flows. In this work, the Newton Raphson power flow method was used. The simulations were carried out on a personal computer with a 2GHz Intel® Core™ i3-5005U processor and a 4GB RAM.

3.3. Formulation of the Optimal Shunt Capacitors' Placement and Sizing Problem

The optimal shunt capacitors' placement and sizing problem was formulated through the adoption and modification of objective functions and constraints given in (El-Fergany & Abdelaziz, 2014b) and (Das, 2008). The objective functions were formulated in such a way that the annual overall cost of total real power losses, shunt capacitors' purchase, installation, and O&M was minimized while constrained by voltage and reactive power injection limits. The objective functions for fixed and variable system loading conditions are given in (3.1) and (3.2) respectively.

Minimize{Total Cost of Real Power / Energy Losses + Shunt Capacitors' Purchase Cost + Shunt Capacitors' Installation Cost + Shunt Capacitors' O&M Cost}

$$minimize\left\{C_e \sum_{i=1}^{nb} P_{La}(i) + \sum_{j=1}^{ncap} C_{cp} Q_{cs}(j) + ncap\frac{C_{ci}}{T} + ncapC_{co}\right\} \quad (3.1)$$

$$minimize\left\{C_e \sum_{k=1}^{L} P(k)T_d(k) + \sum_{j=1}^{ncap} C_{cp} Q_{cs}(j) + ncap\frac{C_{ci}}{T} + ncapC_{co}\right\} \quad (3.2)$$

where:

C_e is the average electrical energy cost. For fixed system loading, C_e was taken to be equal to 168$/kW-Year while for variable system loading (i.e. light, medium and full system loading) it was taken to be equal to 0.06$/kWh.

$P_{La}(i)$ is the kW electric power loss in branch i.

$P(k)$ is the total kW electric power loss for any load level k.

nb is the total number of branches in a given electrical network.

T is the planning period (in years) under consideration (i.e. 10 years). It also represent the assumed useful lifespan of the shunt capacitors.

$T_d(k)$ is the duration of any load level k.

C_{cp} is the size dependent, purchase cost of capacitors per $kVAr$.

$Q_{cs}(j)$ is the size ($kVAr$) of the shunt capacitor installed at bus j. For variable system load condition, $Q_{cs}(j)$ is the size of the largest shunt capacitor installed at bus j.

$ncap$ is the total number of buses with shunt capacitors installed.

C_{ci} is the shunt capacitors' installation cost per location ($1,600). This cost was equally spread over the 10-year planning period, T. So, the cost per location per year was then taken as $160 after dividing C_{ci} by T.

C_{co} is the shunt capacitors O&M cost per year per location ($300).

L is the total number of considered load levels. In this study, L was equal to 3 representing light, medium and full load levels.

NB: The average electrical energy cost that has been used for the assumed fixed system loading was adopted from (Rao et al., 2011). On the other hand, the rest of the constants were adopted from (El-Fergany & Abdelaziz, 2014a).

The optimization of (3.1) and (3.2) was subjected to the following operational constraints:

(i) Voltage magnitude at each bus must be maintained within its lower ($V_{n,min}$) and upper ($V_{n,max}$) limits. $V_{n,min}$ and $V_{n,max}$ were taken to be equal to 0.9 and 1.1 p.u. respectively (Standard EN 50160, 2010).

$$V_{n,min} \leq |V_n| \leq V_{n,max} \tag{3.3}$$

(ii) The total reactive power injection at each candidate bus is governed by the assumed available minimum ($Q_{cn,min}$) and maximum ($Q_{cn,max}$) shunt capacitor bank sizes. For fixed system loading and for variable system loading operation at full

(100%) load, $Q_{cn,min}$ and $Q_{cn,max}$ were taken to be equal to 150 and 4050 $kVAr$ respectively (Rao et al., 2011). For variable system operation at light (50%) and medium (75%) load conditions, $Q_{cn,min}$ and $Q_{cn,max}$ were taken to be equal to 0 and 4050 $kVAr$ respectively.

$$Q_{cn,min} \leq Q_{cn} \leq Q_{cn,max} \tag{3.4}$$

For all instances, the considered maximum number of iterations and population size were empirically set to 50 and 30 respectively. The MVO parameters such as WEP_Max, WEP_Min and p were set to 1, 0.2 and 6 respectively (Mirjalili et al., 2016).

Shunt capacitor costs per kVAr

Details about the cost of shunt capacitor units as well as the annual costs per $kVAr$ for each given unit were taken from (Rao et al., 2011). Tables 3.1 and 3.2 give these respective costs.

Table 3.1: Available three-phase capacitor sizes and costs

Size ($kVAr$)	150	300	450	600	900	1200
Cost ($)	750	975	1140	1320	1650	2040

Various combinations of the shunt capacitor sizes given in Table 3.1 were used to generate other shunt capacitor sizes as shown in Table 3.2.

Table 3.2: Possible choice of capacitor sizes and cost/$kVAr$

j	1	2	3	4	5	6	7	8	9
Q_j^c	150	300	450	600	750	900	1050	1200	1350
$\$/kVAr$	0.500	0.350	0.253	0.220	0.276	0.183	0.228	0.170	0.207
j	10	11	12	13	14	15	16	17	18
Q_j^c	1500	1650	1800	1950	2100	2250	2400	2550	2700
$\$/kVAr$	0.201	0.193	0.187	0.211	0.176	0.197	0.170	0.189	0.187
j	19	20	21	22	23	24	25	26	27
Q_j^c	2850	3000	3150	3300	3450	3600	3750	3900	4050
$\$/kVAr$	0.183	0.180	0.195	0.174	0.188	0.170	0.183	0.182	0.179

For example, the 4050 $kVAr$ capacitor is made up of three 1200 $kVAr$ and one 450 $kVAr$ capacitors. In calculating the annual cost/$kVAr$, the overall cost of each unit or the sum of the respective costs is divided by the product of the resulting capacitor size and 10, where 10 represents the assumed useful lifespan (in years) of the capacitors. The overall cost of each shunt capacitor unit is divided by 10 years so as to equally spread the overall cost over the 10-year planning period. This is done in line with the principles of depreciation computation using the straight-line method (Wood & Horner, 2010). As an example, the annual cost/$kVAr$ for the 4050 $kVAr$ capacitor is given as (2040×3+1140) / (4050×10) = 0.179 (Rao et al., 2011).

3.4. MATLAB's Matrix Reduction Techniques

In this thesis, the combined usage of MATLAB's *any* and *ismember* commands has been used to reduce the search space or matrix of buses for the installation of shunt capacitors. The following paragraphs highlight the workings of the *any* and *ismember* commands.

Lia = *ismember*(*A*, *B*) returns an array containing 1 (true) where the data in *A* is also found in *B* and elsewhere it returns 0 (false) (Tutorials Point, 2014). For example, when given matrices, *A* and *B* (shown in (3.5) and (3.6) respectively)

$$A = \begin{bmatrix} 2 & 3 & 4 & 5 \\ 4 & 6 & 7 & 9 \\ 2 & 1 & 7 & 8 \\ 5 & 3 & 8 & 7 \end{bmatrix} \tag{3.5}$$

$$B = [5] \tag{3.6}$$

Executing the command, Lia =*ismember*(*A*, *B*) results in (3.7)

$$\text{Lia} = \begin{bmatrix} 0 & 0 & 0 & 1 \\ 0 & 0 & 0 & 0 \\ 0 & 0 & 0 & 0 \\ 1 & 0 & 0 & 0 \end{bmatrix} \tag{3.7}$$

From (3.7) it can be noted that the last element in the first row and the first element in the last row are ones while the rest are zeros. That is, there is a one for each location at which there was a five while there are zeros for all other locations that did not contain the number five. This trait of the *ismember* command greatly helped in

the development of the search space reduction technique that was used in this research to reduce the search space of possible optimal buses for shunt capacitors placement.

Further, Tutorials Point (2014) states that the *any* command determines if any array elements are non-zeros such that if A is a vector, then $B = any(A)$ returns logical 1 (true) if any of the elements of A is a non-zero number or logical 1, and returns logical 0 (false) if all the elements are zero. For example, for matrix A (as shown in (3.8))

$$A = \begin{bmatrix} 6 & 8 & 1 & 2 \\ 3 & 9 & 5 & 4 \end{bmatrix} \tag{3.8}$$

Executing the command, $B = any(A)$ results in (3.9)

$$B = any(\mathrm{A}) = [1 \quad 1 \quad 1 \quad 1] \tag{3.9}$$

In (3.9), the *any* command checks every column of matrix A and since none of the columns is made up of all zeros, the command $any(A)$ returns a (1×4) row matrix made up of all ones.

On the other hand, executing the command, $C = any(A,2)$ results in (3.10)

$$C = any(A,2) = \begin{bmatrix} 1 \\ 1 \end{bmatrix} \tag{3.10}$$

In (3.10), the *any* command checks every row of matrix A and since none of the rows is made up of all zeros, the command $any(A,2)$ returns a (2×1) column matrix made up of all ones.

Furthermore, for matrix D (as shown in (3.11))

$$D = \begin{bmatrix} 1 & 9 & 11 \\ 0 & 0 & 0 \\ 18 & 8 & 3 \end{bmatrix} \tag{3.11}$$

Executing the command, $E = any(D)$ results in (3.12)

$$E = any(D) = [1 \quad 1 \quad 1] \tag{3.12}$$

In (3.12), the *any* command checks every column of matrix D and since none of the columns is made up of all zeros, the command *any*(D) returns a (1×3) row matrix made up of all ones.

On the other hand, executing the command, F = *any*(D,2) results in (3.13)

$$F = any(D,2) = \begin{bmatrix} 1 \\ 0 \\ 1 \end{bmatrix} \tag{3.13}$$

In (3.13), the *any* command checks every row of matrix A and since row number 2 is made up of all zeros, the command *any*(D,2) returns a (3×1) column matrix whose rows, except the second, are made up of ones.

Looking at another matrix A (given in (3.14)

$$A = \begin{bmatrix} 5 & 9 \\ 0 & 0 \\ 7 & 3 \end{bmatrix} \tag{3.14}$$

For this matrix, executing the command B=A(any(A,2),:) results in (3.15)

$$B = A(any(A,2),:) = \begin{bmatrix} 5 & 9 \\ 7 & 3 \end{bmatrix} \tag{3.15}$$

That is, the command deletes the rows in (3.14) that are made up of all zeros. Additionally, the command C = A(~*any*(A,2),:) results in (3.16)

$$C = A(\sim any(A,2),:) = [0 \quad 0] \tag{3.16}$$

That is, the command prints out the rows in (3.14) that are made up of all zeros.

3.5. Modified Loss Sensitivity Factors

The conventional LSF approach discussed in Section 2.4 demonstrates a notable weakness when shunt capacitors have to be installed at a single bus within the IEEE 10- and 33-bus radial distribution systems as well as other systems with similar characteristics. For these systems, the LSF do not give a realistic representation of the actual change in real power losses with respect to the change in reactive power flow. This is so because the placement and sizing of shunt capacitors at a bus whose preceding branch has a higher LSF value does not result in the global optimum real

power losses. However, the resulting optimal real power loss level (unlike the LSF value) is to a greater extent influenced by the connected reactive power load at each given bus. The MLSF counters the weakness of the conventional LSF because it considers both the sensitivity of real power losses to reactive power flow (i.e. kW change in real power losses per $kVAr$ change in reactive power flow) as well as the amount of reactive load connected at each respective bus. These factors are calculated using (3.17).

$$\text{MLSF} = \frac{\partial P_{loss_k}}{\partial Q_{pq}} \times Q_{Lq} = \frac{2Q_{pq}}{V_p} \times R_{pq} \times Q_{Lq} \tag{3.17}$$

where with reference to Figure 2.5, Q_{Lq} is the reactive load connected at bus q. MLSF is computed for each load connected in the system. If a load is purely active, the MLSF is equal to zero.

3.6. The Developed Search Space Reduction Technique

The developed search space reduction technique is based on the MLSF and MATLAB's *ismember* and *any* commands. The use of the MLSF is partial such that in the developed approach, consideration is only given to the highly ranked bus in the MLSF bus rank vector. The highly ranked bus is taken to be the critical bus and consequently, it has been used in reducing the search space. The step-by-step outline of the developed search space reduction technique is as follows, and the IEEE 10-bus system is used for illustration.

STEP 1: Load the bus and branch data for the test system under consideration in MATLAB and then calculate the MLSF.

STEP 2: Enter the total number of buses at which one intends to have shunt capacitors installed. It is assumed that the desired total number of buses is 2.

STEP 3: Using MATLAB's *nchoosek(A,r)* command presented in sub-section 2.4.1., generate the search space from which to search for the 2 global optimum buses on which to install shunt capacitors. For the 10-bus test system, $A = [2,3,4,5,6,7,8,9,10]$. Bus 1 is not considered as a candidate location for capacitor installation because as illustrated in Section 2.3.2, the installation of shunt capacitors

at this bus would not change the flow of reactive power in the branches. Consequently, the branch power losses would remain the same. Further, as per assumption made in step 2, $r = 2$. Therefore, the search space is then given as (3.18).

B = [2 3; 2 4; 2 5; 2 6; 2 7; 2 8; 2 9; 2 10; 3 4; 3 5; 3 6; 3 7; 3 8; 3 9; 3 10; 4 5; 4 6; 4 7; 4 8; 4 9; 4 10; 5 6; 5 7; 5 8; 5 9; 5 10; 6 7; 6 8; 6 9; 6 10; 7 8; 7 9; 7 10; 8 9; 8 10; 9 10]

(3.18)

which is a (36×2) matrix.

STEP 4: Select the highly ranked bus in the MLSF bus rank vector and make it a sole element of matrix C. For example, if bus 5 is the highly ranked bus in the 10-bus radial distribution system's MLSF bus rank vector, C is given as (3.19)

$$C = [5] \tag{3.19}$$

STEP 5: Use the *ismember* command to check for the rows in matrix B which contain the sole element of matrix C, i.e. 5. Executing the command, D = *ismember*(B,C) results in (3.20)

D = [0 0; 0 0; 0 1; 0 0; 0 0; 0 0; 0 0; 0 0; 0 0; 0 1; 0 0; 0 0; 0 0; 0 0; 0 0; 0 1; 0 0; 0 0; 0 0; 0 0; 0 0; 1 0; 1 0; 1 0; 1 0; 1 0; 0 0; 0 0; 0 0; 0 0; 0 0; 0 0; 0 0; 0 0; 0 0; 0 0]

(3.20)

From (3.20) it can be noted that there is a one for each location at which there was a five while there are zeros for all other locations that did not contain the number five.

STEP 6: Create an all zeros matrix of the same dimension as the search space (i.e. matrix B (3.18) in this case). Label this matrix as E (3.21).

E = [0 0; 0 0; 0 0; 0 0; 0 0; 0 0; 0 0; 0 0; 0 0; 0 0; 0 0; 0 0; 0 0; 0 0; 0 0; 0 0; 0 0; 0 0; 0 0; 0 0; 0 0; 0 0; 0 0; 0 0; 0 0; 0 0; 0 0; 0 0; 0 0; 0 0; 0 0; 0 0; 0 0; 0 0; 0 0; 0 0]

(3.21)

STEP 7: Initialize i; where i represents the total number of rows in the search space (i.e. the total number of rows in matrix B for this case). For the considered example, i

ranges from 1 to 36 (as given in (3.18)).

STEP 8: for i = 1 : 36

(a) Select the i-th row from matrix B (3.18);

(b) Select the i-th row from matrix D (3.20);

(c) Determine the maximum value for the selected i-th row from matrix D by executing the MATLAB command $max(D(i,:)$);

(d) **If** $max\big(D(i,:)\big) == 1$, replace the elements in the i-th row of matrix E by the elements in the i-th row of matrix B **else** maintain the zeros in the i-th row of matrix E and **end**;

STEP 9: Print out the results from step 8. For this case the result is matrix E which is given in (3.22)

$$E = [0\ 0;\ 0\ 0;\ 2\ 5;\ 0\ 0;\ 0\ 0;\ 0\ 0;\ 0\ 0;\ 0\ 0;\ 0\ 0;\ 3\ 5;\ 0\ 0;\ 0\ 0;\ 0\ 0;\ 0\ 0;\ 0\ 0;\ 4\ 5;\ 0\ 0;\ 0\ 0;\ 0\ 0;\ 0\ 0;\ 0\ 0;\ 5\ 6;\ 5\ 7;\ 5\ 8;\ 5\ 9;\ 5\ 10;\ 0\ 0;\ 0\ 0;\ 0\ 0;\ 0\ 0;\ 0\ 0;\ 0\ 0;\ 0\ 0;\ 0\ 0;\ 0\ 0;\ 0\ 0] \quad (3.22)$$

From (3.22) it can be noted that all other rows, except the ones which have the element 5, are made up of zeros.

STEP 10: Use the *any* command given in (3.15) to only print out the non-all-zero rows of matrix *E*. Executing the command, $E(any(E,2),:)$, results in (3.23)

$$Reduced\ Search\ Space = E(any(E,2),:) = \begin{bmatrix} 2 & 5 \\ 3 & 5 \\ 4 & 5 \\ 5 & 6 \\ 5 & 7 \\ 5 & 8 \\ 5 & 9 \\ 5 & 10 \end{bmatrix} \quad (3.23)$$

From (3.23) it can be noted that it is only the rows which contain the *critical bus* (i.e. bus number 5) that have been printed hence reducing the search space dimension from (36×2) to (8×2). Figure 3.1 gives a flowchart of the preceding steps.

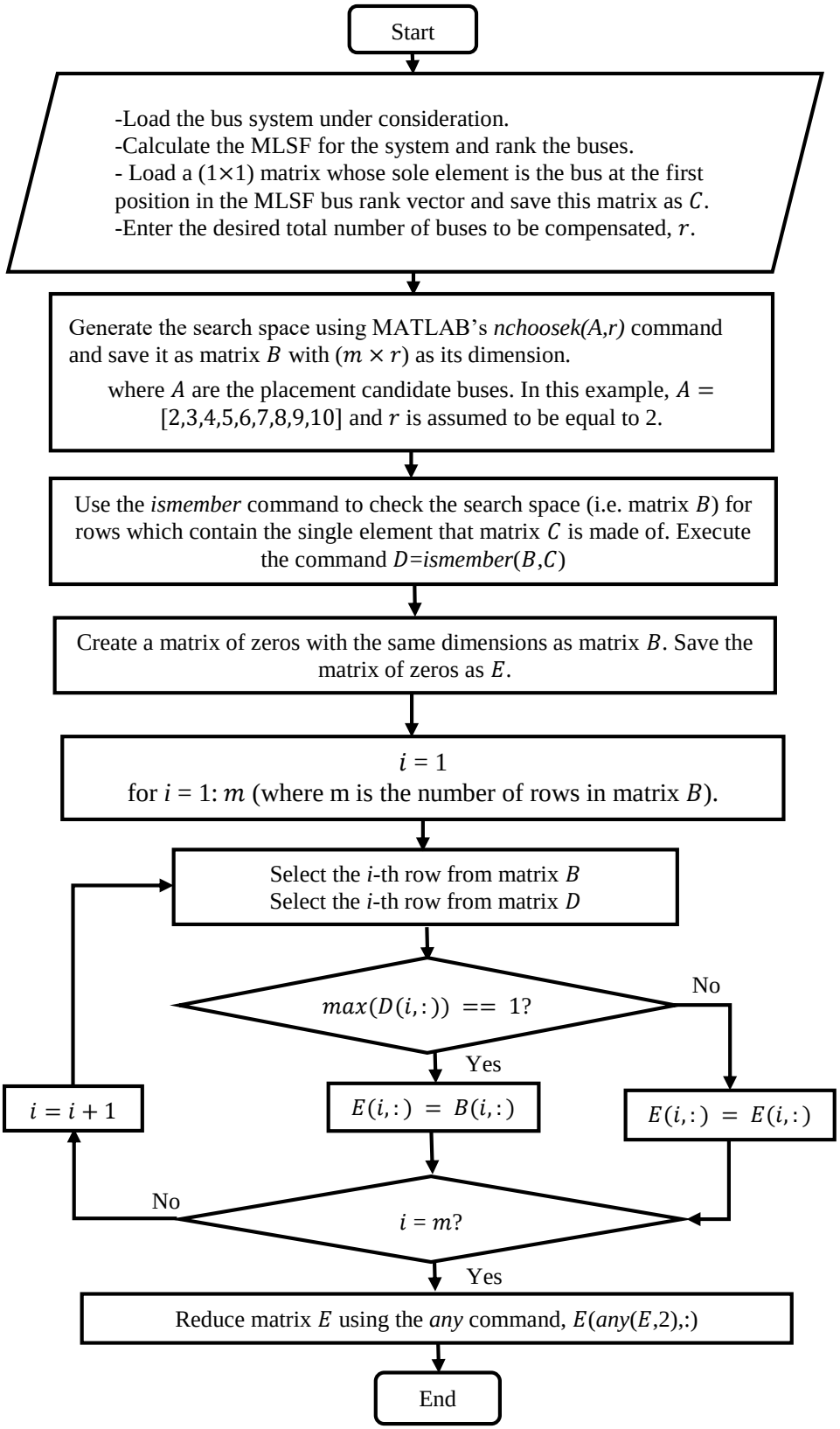

Figure 3.1: Flowchart for the developed search space reduction technique

3.7. Flowchart for the Developed Optimal Shunt Capacitors' Placement and Sizing algorithm

Figures 3.2 gives a flowchart for the developed MLSF, MVO and MATLAB matrix reduction methods based optimal shunt capacitors placement and sizing approach.

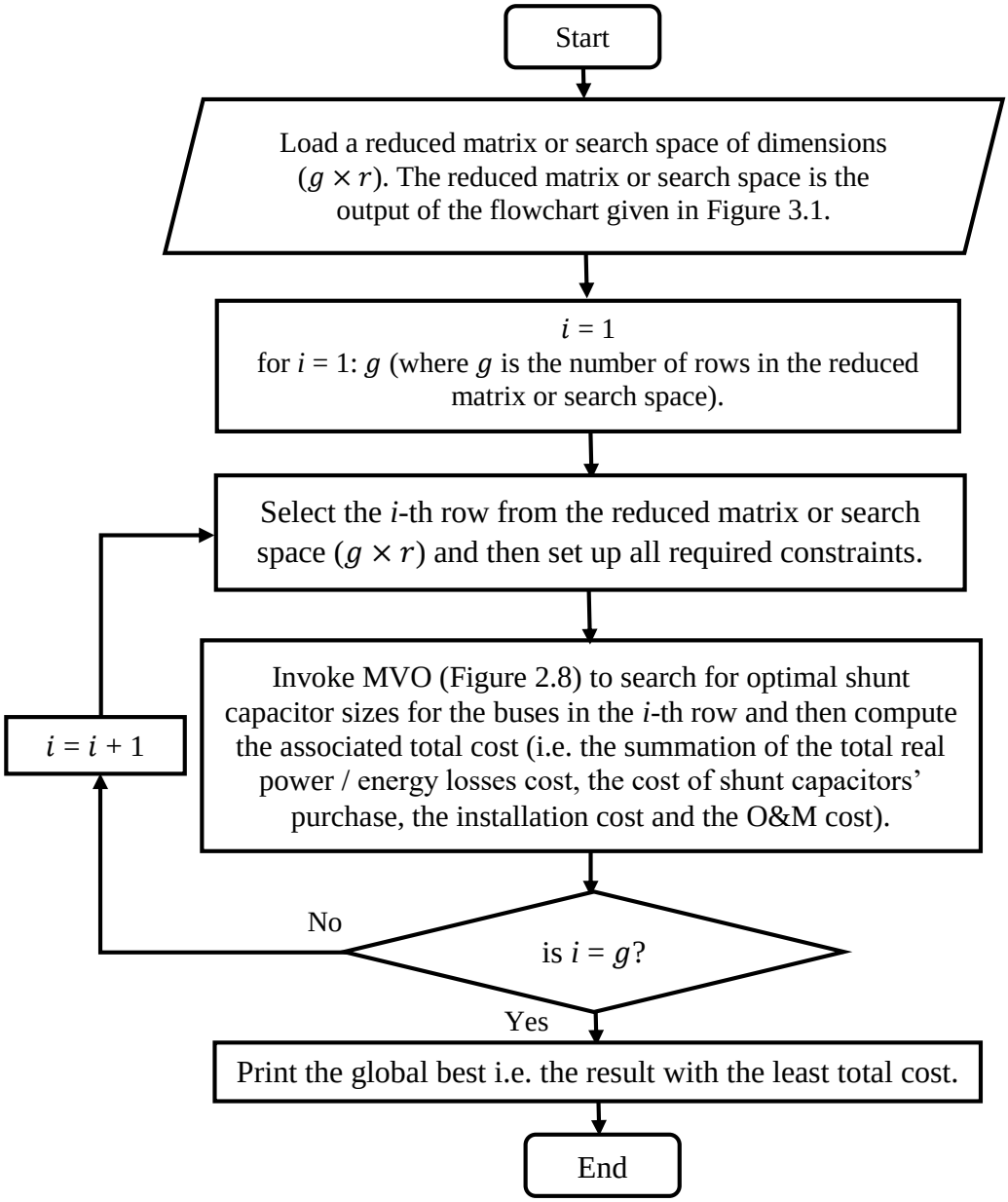

Figure 3.2: Flowchart of developed MLSF and MVO based optimal shunt capacitors placement and sizing algorithm for radial distribution networks

Due to the stochastic nature of metaheuristics, the developed optimal shunt capacitors placement and sizing algorithm was run 100 times for capacitor placement at 1 to 9 buses in the IEEE 10-bus radial distribution system. For the IEEE 33-bus radial distribution system, the developed optimal shunt capacitors placement and sizing algorithm was run 100 times when shunt capacitors had to be installed at a single bus; 10 times when the shunt capacitors had to be installed at 2 buses; 5 times when the shunt capacitors had to be installed at 3 buses, and finally, 2 times when the shunt capacitors had to be installed at 4 buses. Thereafter, the minimum, maximum, and average computation times were recorded. Determination of the number of runs to be implemented depended on the search space size. In the interest of time, as the search space size grew, the number of runs were reduced. The decision to settle for a given total number of runs was randomly done and not based on any procedure.

3.8. Evaluation Criteria

The effectiveness of the developed approach has been assessed through its application in solving the optimized shunt capacitors placement and sizing problem in two systems – the IEEE 10- and 33-bus radial distribution systems. The attractiveness of the computed solution has been assessed while assuming a 10-year planning period. This period was chosen based on the assumption that the shunt capacitors output would not be degraded for the first 10 years after installation. The assumption was considered valid because according to WEG Electric Corporation, Power Factor Correction Capacitors (PFCC) are typically designed to last for about 20 years when operating within their design parameters (WEG Electric Corporation, 2012).

3.9. Test Cases: The IEEE 10- and 33-Bus Radial Distribution Systems

A. The IEEE 10-bus radial distribution system

The system is made up of 10 buses and 9 branches with no laterals. The rated line voltage is 23 kV and the total active and reactive power loads are 12,368 kW and 4,186 kVAr respectively. Figure 3.3 gives the single-line diagram whereas Table 3.3 gives the system data (Rao et al., 2011).

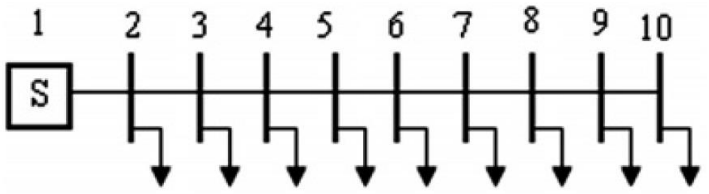

Figure 3.3: Single line diagram for the IEEE 10-bus radial distribution system

Table 3.3: IEEE 10-bus radial distribution system line and load data

Branch	Sending bus	Receiving bus	R (Ω)	X (Ω)	Load at Receiving Bus	
					P (kW)	Q (kVAr)
1	1	2	0.1233	0.4127	1840	460
2	2	3	0.0140	0.6057	980	340
3	3	4	0.7463	1.2050	1790	446
4	4	5	0.6984	0.6084	1598	1840
5	5	6	1.9831	1.7276	1610	600
6	6	7	0.9053	0.7886	780	110
7	7	8	2.0552	1.1640	1150	60
8	8	9	4.7953	2.7160	980	130
9	9	10	5.3434	3.0264	1640	200

B. The IEEE 33-bus radial distribution system

The system is made up of 33 buses and 32 branches with three laterals. It has a rated line voltage of 12.66 kV and the total active and reactive power loads are 3,715 kW and 2,300 kVAr respectively. Figure 3.4 gives the single-line diagram for the 33-bus test system whereas Table 3.4 gives the line and load data (Tamilselvan et al., 2018).

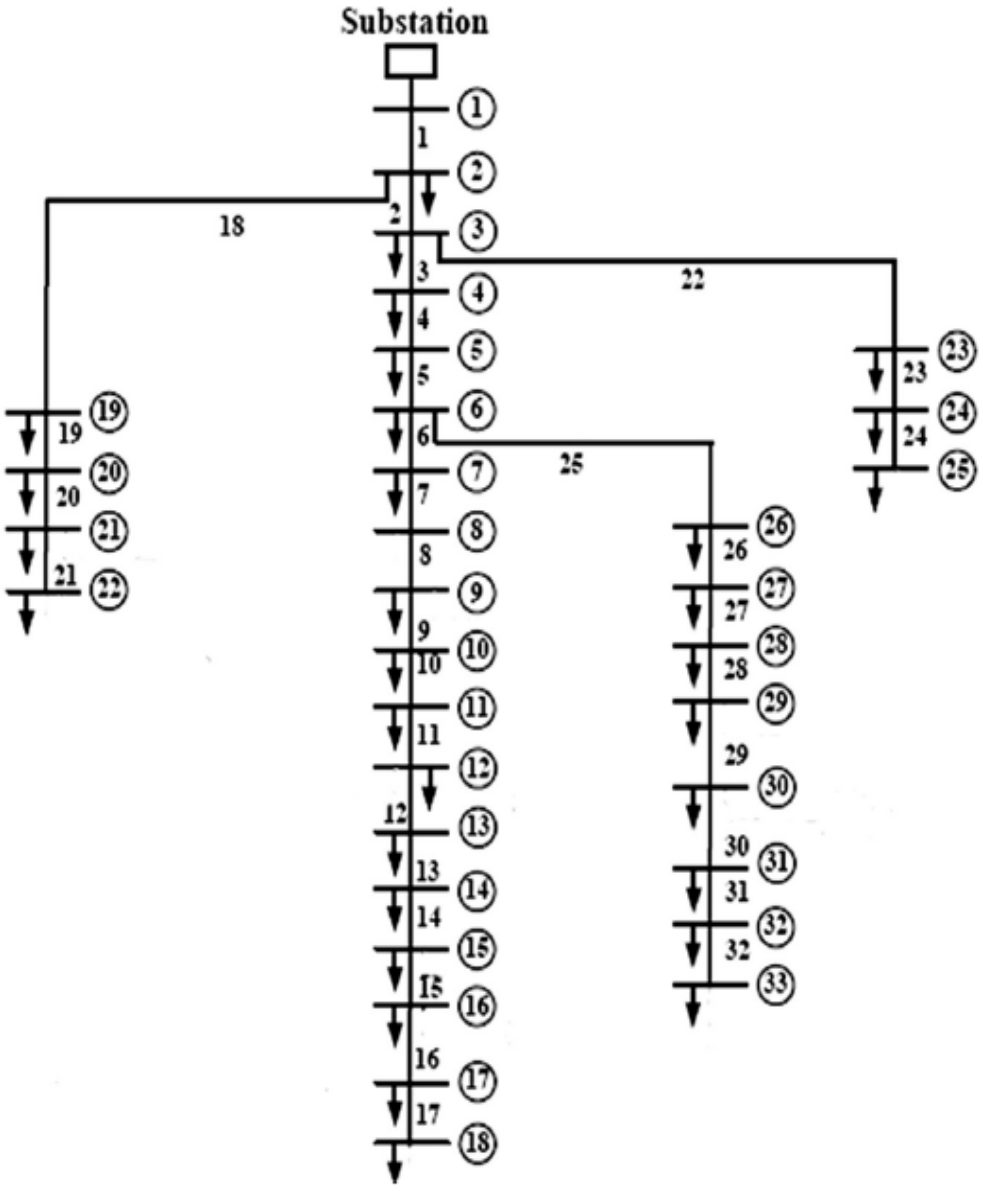

Figure 3.4: Single line diagram for the IEEE 33-bus radial distribution system

Table 3.4: IEEE 33-bus radial distribution system line and load data

Branch	Sending bus	Receiving bus	R (Ω)	X (Ω)	Load at Receiving Bus	
					P (kW)	Q (kVAr)
1	1	2	0.0922	0.0470	100	60
2	2	3	0.4930	0.2511	90	40
3	3	4	0.3660	0.1864	120	80
4	4	5	0.3811	0.1941	60	30
5	5	6	0.8190	0.7070	60	20
6	6	7	0.1872	0.6188	200	100
7	7	8	0.7114	0.2351	200	100
8	8	9	1.0300	0.7400	60	20
9	9	10	1.0440	0.7400	60	20
10	10	11	0.1966	0.0650	45	30
11	11	12	0.3744	0.1298	60	35
12	12	13	1.4680	1.1550	60	35
13	13	14	0.5416	0.7129	120	80
14	14	15	0.5910	0.5260	60	10
15	15	16	0.7463	0.5450	60	20
16	16	17	1.2890	1.7210	60	20
17	17	18	0.7320	0.5740	90	40
18	2	19	0.1640	0.1565	90	40
19	19	20	1.5042	1.3554	90	40
20	20	21	0.4095	0.4784	90	40
21	21	22	0.7089	0.9373	90	40
22	3	23	0.4512	0.3083	90	50
23	23	24	0.8980	0.7091	420	200
24	24	25	0.8960	0.7011	420	200
25	6	26	0.2030	0.1034	60	25
26	26	27	0.2842	0.1447	60	25
27	27	28	1.0590	0.9337	60	20
28	28	29	0.8042	0.7006	120	70
29	29	30	0.5075	0.2585	200	600
30	30	31	0.9744	0.9630	150	70
31	31	32	0.3105	0.3619	210	100
32	32	33	0.3410	0.5302	60	40

3.10. Validation of the Developed approach

To assess the accuracy of the developed approach, results obtained using the developed approach were compared with those obtained using the exhaustive search based approach, the exhaustive search and MVO based approach, and other results available in literature that were obtained using ABC, CrSA, CSA, DE, DFO, GA, GSA, GWO, ICrSA, MCA, MFO and PSO. For the exhaustive search based approach, the global optimum solution was found by searching through the exhaustive search space of buses and the exhaustive search space of shunt capacitor sizes. On the other hand, for the exhaustive search and MVO based approach, the global optimum bus(es) were identified by searching through the exhaustive search space of buses, while the optimum shunt capacitor size(s) were determined using MVO.

For the installation of shunt capacitors at a total of 1 up to 4 buses in the IEEE 10-bus radial distribution system, the developed approach, the exhaustive search based approach and the exhaustive search and MVO based approach were used to determine the optimum results. On the other hand, due to the vastness of the search space of buses and shunt capacitors sizes; for the installation of shunt capacitors at a total of 5 up to 9 buses in the IEEE 10-bus radial distribution system, only the developed approach and the exhaustive search and MVO based approach were used to determine the optimum results.

For the installation of shunt capacitors at a total of 1 up to 3 buses in the IEEE 33-bus radial distribution system, the developed approach, the exhaustive search based approach and the exhaustive search and MVO based approach were used to determine the optimum results. On the other hand, due to the vastness of the search space of buses and shunt capacitors sizes; for the installation of shunt capacitors at a total of 4 buses in the IEEE 33-bus radial distribution system, only the developed approach and the exhaustive search and MVO based approach were used to determine the optimum results.

Thereafter, the results obtained using the three approaches (for both test systems) were compared. The comparison was based on the obtained optimum bus number(s)

on which to install shunt capacitors, the associated shunt capacitor sizes, overall cost, power losses, voltage magnitude, search space dimension and computation time.

Lastly, the results obtained using the developed approach for both the IEEE 10- and 33-bus radial distribution systems were then compared with the results available in literature that were obtained using ABC, CrSA, CSA, DE, DFO, GA, GSA, GWO, ICrSA, MCA, MFO and PSO.

CHAPTER FOUR

RESULTS AND DISCUSSION

4.1. Highlights

This chapter present and discusses results of this research. The results have been obtained from tests that were carried out on the IEEE 10- and 33-bus radial distribution systems using the developed optimal shunt capacitors' placement and sizing approach that is based on MLSF, MVO and MATLAB matrix reduction methods. It must be emphasized that in this work the focus was on minimizing the overall cost of total real power losses, shunt capacitors' purchase, installation, and O&M. As such, the first parts of this chapter present results that include all the stated costs. However, towards the end, the presented results are only made up of the combined costs of total real power losses and shunt capacitors' purchase. This has been necessitated by the fact that the results from literature that have been used for comparison also disregarded the shunt capacitors installation, operation and maintenance costs.

4.2. IEEE 10-Bus Radial Distribution System

4.2.1. Base Case Load Flow Results

The load flow simulation was run on the system with no shunt capacitors installed and with loads as given in section 3.9. The system registered real and reactive power losses totaling 783.79 kW and 1036.66 kVAr respectively. These losses represent 6.34% and 24.76% of the system's total real and reactive power loads respectively. The minimum bus voltage for the system was 0.8375 p.u. at bus 10.

4.2.2. Results for Loss Sensitivity Factors and Modified Loss Sensitivity Factors

Table 4.1 gives values of the LSF for the IEEE 10-bus radial distribution system arranged in a descending order.

Table 4.1: LSF for the IEEE 10-bus radial distribution system

Order	LSF	Sending Bus (*p*)	Receiving Bus (*q*)	Sending Bus Voltage (V_p)	Receiving Bus Voltage (V_q)	Normalized Receiving Bus Voltage ($V_q/0.95$)
1	0.0119	5	6	0.9480	0.9172	0.9654
2	0.0118	3	4	0.9874	0.9634	1.0141
3	0.0096	4	5	0.9634	0.9480	0.9979
4	0.0092	8	9	0.8890	0.8587	0.9039
5	0.0061	9	10	0.8587	0.8375	0.8816
6	0.0048	7	8	0.9072	0.8890	0.9357
7	0.0027	6	7	0.9172	0.9072	0.9549
8	0.0024	1	2	1.0000	0.9929	1.0452
9	0.0002	2	3	0.9929	0.9874	1.0393

It can be noted from Table 4.1 that as per LSF approach, shunt capacitors can only be installed at receiving end buses 5, 6, 7, 8, 9, and 10 whose normalized voltage, (V_q/0.95), is less than 1.01 as presented in section 2.4. Out of the six candidate buses, for capacitor installation at a single bus, the highly ranked receiving end bus, i.e. bus number 6 is identified as the global optimum bus since it has the highest LSF whereas bus number 7, with the lowest LSF, is identified as the least optimum bus.

Table 4.2 gives values of the MLSF for the IEEE 10-bus system arranged in a descending order.

Table 4. 2: MLSF for the IEEE 10-bus radial distribution system

Order	MLSF	Sending Bus (*p*)	Receiving Bus (*q*)	Sending Bus Voltage (V_p)	Receiving Bus Voltage (V_q)	Normalized Receiving Bus Voltage ($V_q/0.95$)
1	17599.97	4	5	0.9634	0.9480	0.9979
2	7120.77	5	6	0.9480	0.9172	0.9655
3	5285.07	3	4	0.9874	0.9634	1.0141
4	1217.92	9	10	0.8587	0.8375	0.8816
5	1200.06	8	9	0.8890	0.8587	0.9039
6	1119.92	1	2	1.0000	0.9929	1.0452
7	294.01	6	7	0.9172	0.9072	0.9549
8	286.24	7	8	0.9072	0.8890	0.9358
9	84.09	2	3	0.9929	0.9874	1.0394

It can be noted from Table 4.2 that based on the MLSF values, bus number 5 is identified as the highly ranked receiving end bus since it has the largest MLSF whereas bus 3, with the lowest MLSF, is identified as the least ranked receiving end bus. This contrasts with the LSF approach (Table 4.1), in which bus number 6 was identified as the highly ranked bus.

In the search space reduction technique that has been developed as part of this study, consideration was only given to the highly ranked bus in the MLSF bus rank vector. This bus was taken to be the critical bus and as such it was used in reducing the search space of optimal buses for shunt capacitors placement. As discussed in Chapter 3, only the critical bus (for capacitor placement at a single bus) or bus combinations (for capacitor placement at a multiple buses) that included the highly ranked bus or the critical bus (based on the MLSF) were the ones that formed the final search space.

4.2.3. Results for the Compensated IEEE 10-Bus Radial Distribution System

The first simulation set up considered reactive power compensation through optimal shunt capacitors placement and sizing while assuming fixed system loading at full (100%) load. On the other hand, the second simulation set up considered load variations. For the second set up, the system was assumed to operate at three different load patterns, i.e. light (50%); medium (75%) and full (100%) load. The assumed yearly hours of operation for the respective load patterns were taken to be 2000, 5260 and 1500 (Das, 2008; El-Fergany & Abdelaziz, 2014b; Mahfoud et al., 2020).

A. Optimal placement and sizing of shunt capacitors for fixed system loading

Table 4.3 gives results of the overall costs, power losses and voltage magnitudes for the fixed system loading case. The results are then compared with those that were obtained using approaches based on the exhaustive search, and a combination of the exhaustive search and MVO.

Table 4.3: Comparison of costs, power losses and voltage magnitudes obtained using the exhaustive search based approach, exhaustive search and MVO based approach, and the developed approach at fixed loading of the IEEE 10-bus system

Method	No of buses with capacitors	Overall cost ($)	P_{loss} (kW)	Q_{loss} $(kVAr)$	V_{min} $(p.u.)$	V_{max} $(p.u.)$
-	0	131,676.72	783.79	1036.66	0.8375	1.0000
Exhaustive	1	145,307.56	858.77	1019.70	0.9011	1.0000
Exhaustive & MVO		145,307.56	858.77	1019.70	0.9011	1.0000
Developed		Voltage constraint violated				
Exhaustive	2	123,901.28	724.06	947.46	0.9001	1.0015
Exhaustive & MVO		123,901.28	724.06	947.46	0.9001	1.0015
Developed		123,901.28	724.06	947.46	0.9001	1.0015
Exhaustive	3	119,489.94	692.98	925.97	0.9003	1.0053
Exhaustive & MVO		119,489.94	692.98	925.97	0.9003	1.0053
Developed		119,489.94	692.98	925.97	0.9003	1.0053
Exhaustive	4	117,865.51	680.67	924.34	0.9000	1.0059
Exhaustive & MVO		117,865.51	680.67	924.34	0.9000	1.0059
Developed		117,865.51	680.67	924.34	0.9000	1.0059
Exhaustive & MVO	**5**	**117,837.56**	**676.87**	**936.54**	**0.9001**	**1.0073**
Developed		**117,837.56**	**676.87**	**936.54**	**0.9001**	**1.0073**
Exhaustive & MVO	6	118,164.60	675.70	935.12	0.9000	1.0073
Developed		118,164.60	675.70	935.12	0.9000	1.0073
Exhaustive & MVO	7	118,613.71	675.37	935.00	0.9003	1.0073
Developed		118,613.71	675.37	935.00	0.9003	1.0073
Exhaustive & MVO	8	119,124.77	675.39	931.67	0.9001	1.0070
Developed		119,124.77	675.39	931.67	0.9001	1.0070
Exhaustive & MVO	9	119,657.31	675.97	926.81	0.9000	1.0065
Developed		119,657.31	675.97	926.81	0.9000	1.0065

It can be noted from Table 4.3 that for all instances, except for capacitor placement at a single bus, the developed approach attained the same overall costs, power losses and voltage magnitudes as the approach based on a combination of the exhaustive search and MVO. It can also be noted from Table 4.3 that for the compensation of a total of 2 to 4 buses, i.e., options for which exhaustive searches for optimal buses and shunt capacitor sizes were carried out, the developed approach attained the same overall costs, power losses and voltage magnitudes as the approaches based on the

exhaustive search, and a combination of the exhaustive search and MVO. It can further be noted from Table 4.3 that the overall optimum total number of buses to be compensated is 5. This is indicated by the highlighted row in Table 4.3. Compensating the 5 buses reduced the yearly overall cost of running the system from $131,676.72, without compensation, to $117,837.56. This represents a 10.51% reduction in the overall cost. However, despite giving the best minimum overall cost, the optimal placement and sizing of shunt capacitors at 5 buses did not give the best minimum voltage level improvement. As shown in Table 4.3, the best minimum voltage level improvement was achieved when shunt capacitors were optimally placed and sized at a total of 3 or 7 optimal locations / buses.

Additionally, as shown in Table 4.3, the optimal placement and sizing of shunt capacitors at the identified 5 buses did not result in the least total real and reactive power losses. The least total real and reactive power losses were attained when reactive power compensation was provided to a total of 7 and 4 buses / locations respectively. Consequently, if consideration was to be given to the cost of total real power losses, then the provision of reactive power to 7 buses would have given the optimal overall cost. However, since the shunt capacitors' purchase, installation and O&M costs were also taken into consideration, the provision of reactive power to the 7 buses resulted in a non-optimal overall cost.

Table 4.4 gives the corresponding optimal capacitor locations (bus numbers) and the shunt capacitor sizes for the results given in Table 4.3. The results for the installation of shunt capacitors at a single bus that are given in Table 4.4 are only those obtained using approaches based on the exhaustive search, and a combination of the exhaustive search and MVO. For the compensation of a single bus, the lower voltage constraint was violated when the developed approach was employed. This was so because the installation of a capacitor at the highly ranked bus (i.e. bus number 5) did not improve the minimum voltage to the acceptable lower limit of 0.9 p.u. Further, for the compensation of a total of 2 to 4 buses, the results for optimal shunt capacitors' placement and sizing obtained using the developed approach were identical to those obtained using approaches based on the exhaustive search, and a combination of the exhaustive search and MVO. Lastly, for the compensation of a

total of 5 to 9 buses, the results for optimal shunt capacitors' placement and sizing that were obtained using the developed approach were identical to those obtained using the approach based on a combination of the exhaustive search and MVO.

Table 4.4: Optimal locations and capacitor sizes obtained using the developed approach, the exhaustive search, and the exhaustive search and MVO based approaches for various compensation options in the IEEE 10-bus system under fixed load condition

No of buses with capacitors	Optimal capacitor locations (bus numbers)	Optimal capacitor sizes (kVAr)
1	9	3300
2	5	4050
	7	3150
3	3	4050
	5	4050
	10	1050
4	3	4050
	5	3600
	7	1200
	10	600
5	**3**	**3900**
	4	**2400**
	5	**2100**
	6	**1200**
	10	**600**
6	3	4050
	4	2100
	5	2100
	6	1200
	9	450
	10	300
7	3	4050
	4	2100
	5	2100
	6	900
	7	450
	9	150
	10	450
8	3	4050
	4	1800
	5	2400
	6	450
	7	600
	8	150
	9	150
	10	450

No of buses with capacitors	Optimal capacitor locations (bus numbers)	Optimal capacitor sizes (kVAr)
9	2	150
	3	4050
	4	1200
	5	2400
	6	900
	7	450
	8	150
	9	150
	10	450

It can be noted from Table 4.4 that despite disregarding some bus combinations, the developed approach still managed to find the global optimal locations / bus numbers and shunt capacitor sizes for the different total number of buses to be compensated.

Table 4.5 gives comparative results of the average computation time and search space dimensions obtained using the approach based on a combination of the exhaustive search and MVO, and the developed approach for various compensation options in the IEEE 10-bus system under fixed load condition.

Table 4.5: Comparison of average computation time and search space dimensions obtained using an approach based on the exhaustive search and MVO, and the developed approach for various compensation options in the IEEE 10-bus system under full load condition

No of buses with capacitors	Exhaustive search and MVO		Developed Approach		Decrease in average computation time (%)
	Average computation time (s)	Search space dimension	Average computation time (s)	Search space dimension	
1	189.13	9×1	Voltage constraint violated		
2	834.42	36×2	164.76	8×2	80.25
3	1698.05	84×3	576.91	28×3	66.03
4	2,494.56	126×4	1,082.77	56×4	56.59
5	**2,543.01**	**126×5**	**1,471.91**	**70×5**	**42.12**
6	1,688.14	84×6	1,178.83	56×6	30.17
7	740.92	36×7	579.04	28×7	21.85
8	180.99	9×8	157.48	8×8	12.99
9	18.72	1×9	18.72	1×9	0

It can be noted from Table 4.5 that the developed approach helped in reducing the average computation time for instances where capacitors were to be installed at a total of 2 up to 8 buses. For the installation of shunt capacitors at two buses, the developed approach reduced the average computation time by 80.25% from 834.42

to 164.76 seconds. On the other hand, when shunt capacitors were to be installed at 8 buses, the developed approach reduced the average computation time by 12.99% from 180.99 to 157.48 seconds. The average computation time reduced in accordance with reductions in search space dimensions. As shown in Table 4.5, for the installation of shunt capacitors at 9 buses, the developed approach did not reduce both the search space and the average computation time. This was so because the total number of buses to be compensated were equal to the total number of buses available for reactive power compensation. As such this resulted in equal dimensions of the search space and equal average computation time for both the approach based on a combination of the exhaustive search and MVO, and the developed approach.

Table 4.6 gives the bus voltage magnitudes of the IEEE 10-bus radial distribution system at fixed load condition for the uncompensated (base) case and the optimally compensated case in which optimally sized shunt capacitors were optimally placed at 5 buses.

Table 4.6: IEEE 10-bus system voltage magnitudes for the uncompensated case and optimally compensated case under fixed load condition

Bus Number	Bus Voltages (p.u.)		% Change
	Uncompensated	Optimally compensated	
1	1.0000	1.0000	0
2	0.9929	1.0010	0.82
3	0.9874	1.0073	2.02
4	0.9634	0.9986	3.65
5	0.9480	0.9885	4.27
6	0.9172	0.9653	5.24
7	0.9072	0.9568	5.47
8	0.8890	0.9411	5.86
9	0.8587	0.9160	6.67
10	0.8375	0.9001	7.48

It can be seen from Table 4.6 that the installation of shunt capacitors results in an improvement of the bus voltage magnitudes for all the load (or P-Q) buses. In Table 4.6, it is shown that the greatest and least improvement in bus voltages occurs at buses 10 and 2 respectively. For bus 10 the voltage improves by 7.48% while for bus 2, the voltage improves by 0.82%. The voltage magnitude at bus 1 does not change because it was set to be a slack bus during simulations. Figure 4.1 illustrates the bus voltage magnitudes of the IEEE 10-bus radial distribution system for the

uncompensated (base) case and the overall optimally compensated case under the fixed load condition.

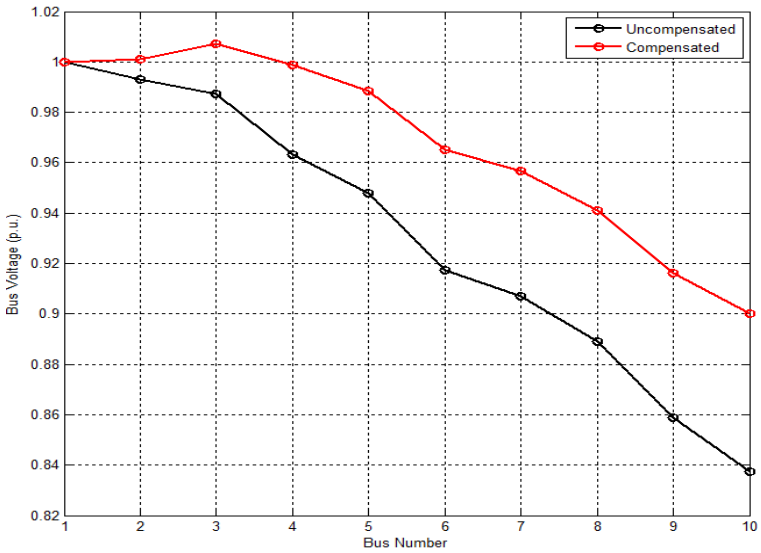

Figure 4.1: Comparison of IEEE 10-bus system voltage magnitudes with and without compensation at fixed load condition

Table 4.7 gives the branch currents of the IEEE 10-bus radial distribution system for the uncompensated (base) case and the optimally compensated case at fixed load condition.

Table 4.7: IEEE 10-bus system branch currents for the uncompensated case and optimally compensated case at fixed load

Branch	Sending Bus (p)	Receiving Bus (q)	Current flow $\|I_{p-q}\|$ Amps		Change in current flow (%)
			Uncompensated	Optimally compensated	
1	1	2	615.25	608.62	1.08
2	**2**	**3**	**532.94**	**544.08**	**-2.09**
3	3	4	487.30	450.37	7.58
4	4	5	404.73	359.44	11.19
5	5	6	309.71	288.50	6.85
6	6	7	229.73	214.87	6.47
7	7	8	191.98	179.50	6.50
8	8	9	135.83	126.60	6.79
9	9	10	85.77	81.54	4.93

It can be noted from Table 4.7 that the installation of shunt capacitors results in the reduction of currents flowing in branches 1, 3, 4, 5, 6, 7, 8 and 9. On the other hand,

in branch number 2 the current increased by 2.09%. The current in branch number 2 increased because the apparent power loading of branch number 2 increased more than the sending and receiving end bus voltages. Further, it can be noted that the total current flowing before the installation of shunt capacitors was about 615.25 A. However, the installation of shunt capacitors reduced this current by about 1.08% to 608.62 A.

Table 4.8 gives the branch power losses of the IEEE 10-bus radial distribution system for the uncompensated (base) case and the overall optimally compensated case at fixed load.

Table 4.8: IEEE 10-bus system power losses for the uncompensated case and optimally compensated case at fixed load

Branch	**Sending Bus (p)**	**Receiving Bus (q)**	**Branch power losses**				**Change in power losses (%)**	
			Uncompensated		**Optimally compensated**			
			P (kW)	**Q (kVAr)**	**P (kW)**	**Q (kVAr)**	ΔP_{loss}	ΔQ_{loss}
1	1	2	46.67	156.22	45.67	152.87	2.15	2.15
2	**2**	**3**	**3.98**	**172.03**	**4.14**	**179.30**	**-4.23**	**-4.23**
3	3	4	177.22	286.14	151.37	244.41	14.58	14.58
4	4	5	114.40	99.66	90.23	78.60	21.13	21.13
5	5	6	190.22	165.72	165.05	143.79	13.23	13.23
6	6	7	47.78	41.62	41.80	36.41	12.51	12.51
7	7	8	75.74	42.90	66.22	37.50	12.58	12.58
8	8	9	88.47	50.11	76.85	43.53	13.13	13.13
9	9	10	39.31	22.26	35.53	20.12	9.61	9.61
Total losses			783.79	1,036.66	676.86	936.53	13.64	9.66

It can be noted from Table 4.8 that the installation of shunt capacitors results in the reduction of real and reactive power losses in branches 1, 3, 4, 5, 6, 7, 8 and 9. The power losses in these branches reduced because of the corresponding reduction in branch currents. However, the power losses in branch number 2 increased due to a corresponding increase in current flow. It may also be noted from Table 4.8 that the percentage changes in the branches' real and reactive power losses are the same. This is so because when calculating both real and reactive power losses, the square of branch current (i.e. I^2) is a common variable while R and X are constants.

Figures 1 (a) and (b) in Appendix II give graphical illustrations of the branches real and reactive power losses (as tabulated in Table 4.8) before and after the optimal

installation of shunt capacitors while operating at fixed load.

It can be noted from Tables 4.7, 4.8 and Figure 1 (a) in Appendix II that despite not having the highest flow of current for both the uncompensated and the optimally compensated cases, the real power losses in branch 5 are the highest. The real power losses in branch 5 are higher than those in branches 1, 2, 3 and 4 because, as it can be seen from Table 3.3, this branch has the highest resistance as compared to the other four upstream branches. On the other hand, the real power losses in branch 5 are higher than those in branch 6 because branch 5 has both higher resistance and current flow than branch 6. Lastly, the real power losses in branch 5 are higher than those in branches 7, 8 and 9 because branch 5 is upstream and thus, the current flowing through this branch is higher than that in the downstream branches.

Similarly, it can also be noted from Tables 4.7, 4.8 and Figure 1 (b) in Appendix II that despite not having the highest flow of current for both the uncompensated and the optimally compensated cases, the reactive power losses in branch 3 are the highest. The reactive power losses in branch 3 are higher than those in branches 1 and 2 because, as it can be seen from Table 3.3, this branch has the highest reactance as compared to the other two upstream branches. On the other hand, the reactive power losses in branch 3 are higher than those in branches 4, 6 and 7 because branch 3 has both higher reactance and current flow than the three branches. Lastly, the reactive power losses in branch 3 are higher than those in branches 5, 8 and 9 because branch 3 is upstream and thus, the current flowing through this branch is higher than that in the downstream branches.

B. Optimal placement and sizing of shunt capacitors for variable system loading

Table 4.9 shows simulation results for a case where shunt capacitors were optimally placed and sized in the IEEE 10-bus radial distribution system while considering load variations. For this case, the system was assumed to operate at three different load patterns, i.e. light (50%), medium (75%), and full (100%) load. The assumed yearly hours of operation for the respective load patterns were taken to be 2000, 5260 and 1500 (Das, 2008; El-Fergany & Abdelaziz, 2014b; Mahfoud et al., 2020).

Table 4.9: Comparison of costs, power losses and voltage magnitudes obtained using approaches based on the exhaustive search, the exhaustive search and MVO, and the developed approach at variable loading of the IEEE 10-bus system

Method	No of buses with capacitors	Loading	Overall cost ($)	P_{loss} (kW)	Q_{loss} $(kVAr)$	V_{min} $(p.u.)$	V_{max} $(p.u.)$
-	0	Light (50%)	219,891.66	169.97	229.01	0.9254	1.0000
		Medium (75%)		408.60	545.83	0.8836	1.0000
		Full (100%)		783.79	1036.7	0.8375	1.0000
Exhaustive	1	Light (50%)	220,979.72	163.47	218.54	0.9339	1.0000
		Medium (75%)		389.86	513.82	0.9013	1.0000
		Full (100%)		858.77	1019.7	0.9011	1.0000
Exhaustive & MVO	1	Light (50%)	220,979.72	163.47	218.54	0.9339	1.0000
		Medium (75%)		389.86	513.82	0.9013	1.0000
		Full (100%)		858.77	1019.7	0.9011	1.0000
Developed Approach	1	Light (50%)	Voltage constraint violated				
		Medium (75%)					
		Full (100%)					
Exhaustive	2	Light (50%)	202,405.38	156.86	206.49	0.9400	1.0000
		Medium (75%)		367.96	481.03	0.9136	1.0000
		Full (100%)		727.07	923.75	0.9001	1.0000
Exhaustive & MVO	2	Light (50%)	202,405.38	156.86	206.49	0.9400	1.0000
		Medium (75%)		367.96	481.03	0.9136	1.0000
		Full (100%)		727.07	923.75	0.9001	1.0000
Developed Approach	2	Light (50%)	202,405.38	156.86	206.49	0.9400	1.0000
		Medium (75%)		367.96	481.03	0.9136	1.0000
		Full (100%)		727.07	923.75	0.9001	1.0000
Exhaustive	3	Light (50%)	199,476.59	155.24	207.38	0.9443	1.0009
		Medium (75%)		364.73	492.92	0.9173	1.0035
		Full (100%)		696.07	930.93	0.9007	1.0056
Exhaustive & MVO	3	Light (50%)	199,476.59	155.24	207.38	0.9443	1.0009
		Medium (75%)		364.73	492.92	0.9173	1.0035
		Full (100%)		696.07	930.93	0.9007	1.0056
Developed Approach	3	Light (50%)	199,476.59	155.24	207.38	0.9443	1.0009
		Medium (75%)		364.73	492.92	0.9173	1.0035
		Full (100%)		696.07	930.93	0.9007	1.0056
Exhaustive	**4**	**Light (50%)**	**198,134.94**	**155.74**	**212.09**	**0.9448**	**1.0024**
		Medium (75%)		**362.49**	**488.46**	**0.9197**	**1.0035**
		Full (100%)		**683.81**	**916.50**	**0.9001**	**1.0047**
Exhaustive & MVO	**4**	**Light (50%)**	**198,134.94**	**155.74**	**212.09**	**0.9448**	**1.0024**
		Medium (75%)		**362.49**	**488.46**	**0.9197**	**1.0035**
		Full (100%)		**683.81**	**916.50**	**0.9001**	**1.0047**
Developed Approach	**4**	**Light (50%)**	**198,134.94**	**155.74**	**212.09**	**0.9448**	**1.0024**
		Medium (75%)		**362.49**	**488.46**	**0.9179**	**1.0030**
		Full (100%)		**683.81**	**916.50**	**0.9001**	**1.0047**

Method	No of buses with capacitors	Loading	Overall cost ($)	P_{loss} (kW)	Q_{loss} $(kVAr)$	V_{min} $(p.u.)$	V_{max} $(p.u.)$
Exhaustive & MVO	5	Light (50%)	198,229.32	156.84	208.63	0.9398	1.0009
		Medium (75%)		362.11	488.31	0.9181	1.0030
		Full (100%)		677.13	936.16	0.9006	1.0073
Developed Approach	5	Light (50%)	198,229.32	156.84	208.63	0.9398	1.0009
		Medium (75%)		362.11	488.31	0.9181	1.0030
		Full (100%)		677.13	936.16	0.9006	1.0073
Exhaustive & MVO	6	Light (50%)	198,614.89	154.88	206.74	0.9470	1.0009
		Medium (75%)		362.06	491.15	0.9183	1.0035
		Full (100%)		679.88	921.91	0.9004	1.0057
Developed Approach	6	Light (50%)	198,614.89	154.88	206.74	0.9470	1.0009
		Medium (75%)		362.06	491.15	0.9183	1.0035
		Full (100%)		679.88	921.91	0.9004	1.0057
Exhaustive & MVO	7	Light (50%)	199,240.67	154.93	206.34	0.9464	1.0006
		Medium (75%)		362.11	489.90	0.9188	1.0032
		Full (100%)		679.58	921.57	0.9006	1.0052
Developed Approach	7	Light (50%)	199,240.67	154.93	206.34	0.9464	1.0006
		Medium (75%)		362.11	489.90	0.9188	1.0032
		Full (100%)		679.58	921.57	0.9006	1.0052
Exhaustive & MVO	8	Light (50%)	199,865.39	155.38	211.21	0.9457	1.0023
		Medium (75%)		362.16	488.30	0.9156	1.0030
		Full (100%)		678.40	939.53	0.9003	1.0075
Developed Approach	8	Light (50%)	199,865.39	155.38	211.21	0.9457	1.0023
		Medium (75%)		362.16	488.30	0.9156	1.0030
		Full (100%)		678.40	939.53	0.9003	1.0075
Exhaustive & MVO	9	Light (50%)	200,941.75	154.40	208.98	0.9447	1.0018
		Medium (75%)		362.41	491.81	0.9167	1.0035
		Full (100%)		684.68	931.60	0.9023	1.0063
Developed Approach	9	Light (50%)	200,941.75	154.40	208.98	0.9447	1.0018
		Medium (75%)		362.41	491.81	0.9167	1.0035
		Full (100%)		684.68	931.60	0.9023	1.0063

It can be noted from Table 4.9 that for all instances, except for capacitor placement at a single bus, the developed approach attained the same overall costs, power losses and voltage magnitudes as the exhaustive search and MVO based approach. It can also be noted from Table 4.9 that for the compensation of a total of 2 to 4 buses, i.e., options for which exhaustive searches for optimal buses and capacitor sizes were carried out, the developed approach attained the same overall costs, power losses and voltage magnitudes as the exhaustive search, and the exhaustive search and MVO based approaches. It can further be noted from Table 4.9 that the overall optimum total number of buses to be compensated is 4. This is given by the highlighted row in Table 4.9. Compensating the 4 buses reduces the yearly overall cost of running the system from $219,891.66, without compensation, to $198,134.94. This represents a 9.89% reduction in the overall cost.

Table 4.10 gives the corresponding optimal capacitor locations (bus numbers) and the shunt capacitor sizes for the results given in Table 4.9. The results for the installation of shunt capacitors at a single bus that are given in Table 4.10 are only those obtained using the exhaustive search, and the exhaustive search and MVO based approaches. This is so because when the developed approach was used to identify a single optimal bus on which to install optimally sized capacitors, the voltage constraint was violated. Further, for the compensation of a total of 2 to 4 buses, the results for optimal shunt capacitors' placement and sizing that were obtained using the developed approach were identical to those obtained using approaches based on the exhaustive search, and a combination of the exhaustive search and MVO. Lastly, for the compensation of a total of 5 to 9 buses, the results for optimal shunt capacitors' placement and sizing that were obtained using the developed approach were identical to those obtained using the approach based on a combination of the exhaustive search and MVO.

Table 4.10: Optimal locations and capacitor sizes obtained using the developed approach, the exhaustive search, and the exhaustive search and MVO based approaches for various compensation options in the IEEE 10-bus system with variable loading

Loading	No of buses with capacitors	Optimal capacitor locations (bus numbers)	Optimal capacitor sizes (kVAr)
Light (50%)	1	9	450
Medium (75%)		9	900
Full (100%)		9	3300
Light (50%)	2	5	1050
		9	450
Medium (75%)		5	3000
		9	600
Full (100%)		5	3750
		9	1950
Light (50%)	3	3	1350
		5	1800
		9	300
Medium (75%)		3	3450
		5	2400
		9	600
Full (100%)		3	4050
		5	3750
		9	1500

Loading	No of buses with capacitors	Optimal capacitor locations (bus numbers)	Optimal capacitor sizes (kVAr)
Light (50%)	**4**	**3**	**2100**
		5	**1950**
		10	**150**
Medium (75%)		**3**	**3150**
		5	**1800**
		6	**900**
		10	**300**
Full (100%)		**3**	**3900**
		5	**2400**
		6	**1800**
		10	**750**
Light (50%)	5	3	1350
		4	450
		5	1650
Medium (75%)		3	2850
		4	750
		5	1350
		6	900
		10	300
Full (100%)		3	4050
		4	2400
		5	1650
		6	1500
		10	600
Light (50%)	6	2	300
		3	1200
		4	450
		5	900
		6	450
		10	300
Medium (75%)		3	3150
		4	600
		5	1650
		6	750
		10	300
Full (100%)		2	150
		3	3600
		4	1200
		5	2550
		6	1200
		10	750
Light (50%)	7	3	1350
		4	300
		5	1050
		6	300
		10	300
Medium (75%)		3	2850
		4	900
		5	1350
		6	900
		10	300

Loading	No of buses with capacitors	Optimal capacitor locations (bus numbers)	Optimal capacitor sizes (kVAr)
Full (100%)	7	2	300
		3	2700
		4	1950
		5	2250
		6	750
		7	750
		10	600
Light (50%)		2	1050
		3	2100
		5	900
		6	450
		8	300
Medium (75%)	8	3	2850
		4	750
		5	1500
		6	750
		9	300
Full (100%)		2	300
		3	4050
		4	1800
		5	2100
		6	900
		7	450
		8	300
		9	600
Light (50%)		3	1800
		4	450
		5	1050
		6	150
		7	300
		9	150
Medium (75%)	9	3	2850
		4	1350
		5	1200
		6	750
		9	300
Full (100%)		2	2850
		3	1800
		4	1500
		5	1500
		6	1200
		7	600
		8	150
		9	450
		10	300

It can be noted from Table 4.10 that despite disregarding some bus combinations, the developed approach still managed to find the optimal locations / bus numbers and shunt capacitor sizes for the different total number of buses to be compensated.

Table 4.11 gives comparative results of the average computation time and search space dimensions obtained using an approach based on the exhaustive search and MVO, and the developed approach for various compensation options in the IEEE 10-bus system under variable load condition.

Table 4.11: Comparison of average computation time and search space dimensions obtained using an approach based on the exhaustive search and MVO, and the developed approach for various compensation options in the IEEE 10-bus system with variable load

No of buses with capacitors	Exhaustive Search and MVO		Developed Approach		Decrease in average computation time (%)
	Average computation time (s)	Search space dimension	Average computation time (s)	Search space dimension	
1	423.22	9×1	Voltage constraint violated		
2	1539.32	36×2	371.09	8×2	75.89
3	4047.29	84×3	1318.77	28×3	67.42
4	**5894.99**	**126×4**	**2827.09**	**56×4**	**52.04**
5	5565.13	126×5	3638.90	70×5	34.61
6	4186.44	84×6	2882.24	56×6	31.15
7	1882.84	36×7	1457.44	28×7	22.59
8	467.86	9×8	389.41	8×8	16.77
9	57.46	1×9	57.46	1×9	0

It can be noted from Table 4.11 that the developed approach helped in reducing the average computation time for instances where shunt capacitors were to be installed at a total of 2 up to 8 buses. For the installation of shunt capacitors at two buses, the developed approach reduced the average computation time by 75.89% from 1539.32 to 371.09 seconds. On the other hand, when shunt capacitors were to be installed at 8 buses, the developed approach reduced the average computation time by 16.77% from 467.86 to 389.41 seconds. The average computation time reduced in accordance with reductions in search space dimensions. As shown in Table 4.11, for the installation of shunt capacitors at 9 buses, the developed approach did not reduce both the search space and the average computation time. This was so because the total number of buses to be compensated were equal to the total number of buses available for reactive power compensation. As such this resulted in equal dimensions of the search space and equal average computation time for both the exhaustive search and MVO based approach and the developed approach.

Table 4.12 gives isolated results of the different parameters of the IEEE 10-bus radial distribution system for the uncompensated (base) case and the overall optimally compensated case. The overall optimally compensated case is the case in which optimally sized shunt capacitors were optimally installed at 4 buses. In computing the cost of energy loss per year, the power losses given in Table 4.12 were assumed to be constant for an hour whereas the average electrical energy cost was taken to be 0.06$ / kWh.

Table 4.12: Comparison of power losses, energy losses and costs of the IEEE 10-bus radial distribution system for the uncompensated case and the overall optimally compensated case under variable load conditions

Loading/Parameters	**Uncompensated**	**Optimally compensated**
Light (50%) load (2000 hours of operation annually)		
Real power losses (kW)	169.97	155.74
Real power losses reduction (kW)	-	14.23
Real power losses reduction (%)	-	8.37
Reactive power losses (kVAr)	229.01	212.09
Reactive power losses reduction (kVAr)	-	16.92
Reactive power losses reduction (%)	-	7.39
Annual energy losses (MWh)	339.94	311.48
Cost of energy losses/year ($)	20,396.40	18,688.80
Optimal buses and capacitor sizes (kVAr)	-	3 2100 5 1950 10 150
Total kVAr installed	-	4200
V_{min} (p.u.)	0.9254	0.9448
V_{max} (p.u.)	1.0000	1.0024
Medium (75%) load (5260 hours of operation annually)		
Real power losses (kW)	408.60	362.49
Real power losses reduction (kW)	-	46.11
Real power losses reduction (%)	-	11.28
Reactive power losses (kVAr)	545.83	488.46
Reactive power losses reduction (kVAr)	-	57.37
Reactive power losses reduction (%)	-	10.51
Annual energy losses (MWh)	2,149.24	1,906.70
Cost of energy losses/year ($)	128,954.16	114,402.00
Optimal buses and capacitor sizes (kVAr)	-	3 3150 5 1800 6 900 10 300
Total kVAr installed	-	6150
V_{min} (p.u.)	0.8836	0.9179
V_{max} (p.u.)	1.0000	1.0030

Loading/Parameters	Uncompensated	Optimally compensated
Full (100%) load (1500 hours of operation annually)		
Real power losses (kW)	783.79	683.81
Real power losses reduction (kW)	-	99.98
Real power losses reduction (%)	-	12.76
Reactive power losses (kVAr)	1036.66	916.50
Reactive power losses reduction (kVAr)	-	120.16
Reactive power losses reduction (%)	-	11.59
Annual energy losses (MWh)	1,175.69	1,025.72
Cost of energy loss/year ($)	70,541.10	61,542.90
Optimal buses and capacitor sizes (kVAr)	-	3 3900 5 2400 6 1800 10 750
Total kVAr installed	-	8850
V_{min} (p.u.)	0.8375	0.9001
V_{max} (p.u.)	1.0000	1.0047
Overall optimal buses and maximum capacitor sizes to be installed (kVAr)	-	3 3900 5 2400 6 1800 10 750
Total kVAr installed	-	8850
Annual energy losses (MWh)	3,664.86	3,243.89
Cost of energy loss/year ($)	219,891.66	194,633.54
Capacitors' purchase cost/year ($)	-	1,661.40
Capacitors' installation cost/year ($)	-	640.00
Capacitors' maintenance cost/year ($)	-	1,200.00
Total cost/year ($)	**219,891.66**	**198,134.94**
Net savings/year ($)		**21,756.72**

It can be observed from Table 4.12, which is derived from Tables 4.9 and 4.10, that despite the expenditure incurred in procuring the shunt capacitors, having them installed, operated and maintained, the yearly overall cost was still less than that of the total real power losses in the uncompensated system. Consequently, a yearly saving of $21,756.72 was made, and in 10 years, a total saving of $217,567.20 would be made.

Furthermore, it can be noted from Table 4.12 that for the overall optimally compensated case, buses 3, 5, 6 and 10 are the buses that require reactive power compensation while 3900, 2400, 1800 and 750 kVAr are the corresponding optimum shunt capacitor sizes to be installed at the identified buses. The results also show that for light (50%) loading the optimum total number of buses to be compensated are 3

whereas 4 buses need to be compensated for the medium (75%) and full (100%) loading conditions.

At light (50%) loading, buses 3, 5 and 10 are the specific buses that require reactive power compensation with 2100, 1950 and 150 kVAr being the corresponding optimum shunt capacitor sizes to be installed. On the other hand, at medium (75%) loading, buses 3, 5, 6 and 10 are the specific buses that require reactive power compensation while 3150, 1800, 900 and 300 kVAr are the corresponding optimum shunt capacitor sizes to be installed. The same buses require reactive power compensation of 3900, 2400, 1800 and 750 kVAr respectively, at full (100%) loading. Therefore, for the compensation to work satisfactorily under the varying load conditions, details of the required type and size of capacitor banks (fixed or switched) at each bus are as shown in Table 4.13.

Table 4.13: Type and sizes of shunt capacitors to be installed in the IEEE 10-bus radial distribution system under variable loading

Bus number	Load level and capacitor size (kVAr)			Type and size (kVAr)	
	Light (50%)	Medium (75%)	Full (100%)	Fixed	Switched
3	2100	3150	3900	2100	1050 750
5	1950	1800	2400	1800	150 450
6	-	900	1800	-	900 (2No)
10	150	300	750	150	150 450

It can be noted from Table 4.13 that bus 6 requires two switched capacitors and does not require any fixed shunt capacitors. On the other hand, buses 3, 5 and 10, each require one fixed and two switched shunt capacitors.

Parameters of the IEEE 10-bus radial distribution system under variable load conditions

Table 4.14 gives the bus voltage magnitudes of the IEEE 10-bus radial distribution system for the uncompensated (base) case and the optimally compensated case at light, medium and full load conditions.

Table 4.14: IEEE 10-bus system voltage magnitudes for the uncompensated case and optimally compensated case under light, medium and full load conditions

Bus Number	Light (50%) load			Medium (75%) load			Full (100%) load		
	Bus Voltages (p.u.)		% Change	Bus Voltages (p.u.)		% Change	Bus Voltages (p.u.)		% Change
	Uncompensated	Optimally compensated		Uncompensated	Optimally compensated		Uncompensated	Optimally compensated	
1	1.0000	1.0000	0	1.0000	1.0000	0	1.0000	1.0000	0
2	0.9967	1.0000	0.33	0.9949	0.9998	0.49	0.9929	0.9999	0.71
3	0.9942	1.0024	0.82	0.9910	1.0030	1.21	0.9874	1.0047	1.75
4	0.9830	0.9961	1.33	0.9736	0.9929	1.98	0.9634	0.9929	3.06
5	0.9758	0.9915	1.61	0.9625	0.9855	2.39	0.9480	0.9839	3.79
6	0.9616	0.9780	1.71	0.9403	0.9680	2.95	0.9172	0.9631	5.00
7	0.9570	0.9737	1.75	0.9332	0.9616	3.04	0.9072	0.9548	5.25
8	0.9487	0.9659	1.81	0.9202	0.9497	3.21	0.8890	0.9394	5.67
9	0.9350	0.9533	1.96	08986	0.9305	3.55	0.8587	0.9151	6.57
10	0.9254	0.9448	2.10	0.8836	0.9179	3.88	0.8375	0.9001	7.47

It can be seen from Table 4.14 that the installation of shunt capacitors under light, medium and full load conditions results in the improvement of bus voltage magnitudes for all the load (or P-Q) buses. From Table 4.14 it is shown that the greatest and least improvement in bus voltage magnitudes under light, medium and full load occurs at buses 10 and 2 respectively. Under light, medium and full load conditions, the voltage at bus 10 improves by 2.1, 3.88 and 7.47% respectively, while that for bus 2 improves by 0.33, 0.49 and 0.71% respectively. For all the three load levels, the voltage magnitude at bus 1 did not change because during simulations bus 1 was set to be a slack bus.

Figure 4.2 illustrates the bus voltages of the IEEE 10-bus radial distribution system for the uncompensated (base) case and the overall optimally compensated case at light, medium and full load conditions.

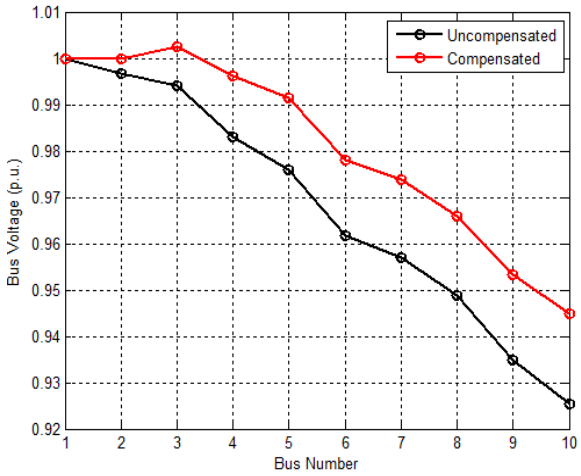

(a) Light (50%) load

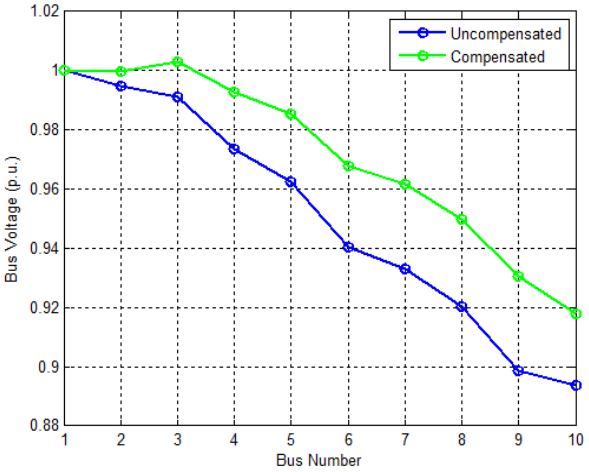

(b) Medium (75%) load

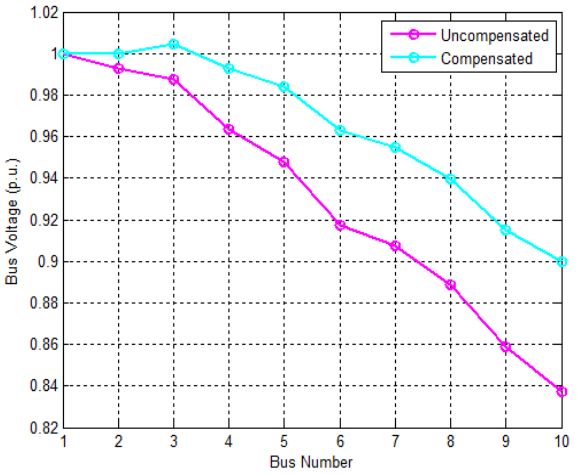

(c) Full (100) load

Figure 4.2: Comparison of IEEE 10-bus system voltages with and without compensation at light, medium and full load

Table 4.15 gives the branch currents of the IEEE 10-bus radial distribution system for the uncompensated (base) case and the overall optimally compensated case at light, medium and full load conditions.

It can be noted from Table 4.15 that under light load, the installation of shunt capacitors results in the reduction of currents flowing in branches (1 – 2), (3 – 4), (4 – 5), (5 – 6), (6 – 7), (7 – 8), (8 – 9) and (9 – 10). On the other hand, in branch (2 – 3) the current increased by 0.09%. The current in branch (2 – 3) increased because the apparent power loading of branch (2 – 3) increased more than the sending and receiving end bus voltages. Further, it can be noted that the total current flowing before the installation of shunt capacitors under light load was about 294.13 A. The installation of shunt capacitors reduced this current by about 2.19% to 287.69 A.

It may also be noted from Table 4.15 that the installation of shunt capacitors under medium and full load conditions results in the reduction of currents flowing in all the branches of the IEEE 10-bus radial system. For medium load, it can be noted that the total current flowing before the installation of shunt capacitors was about 450.53 A. The installation of shunt capacitors reduced the current by about 3.85% to 433.17 A. On the other hand, for the full load condition, it can be seen from Table 4.15 that the total current flowing before the installation of shunt capacitors was about 615.25 A. The installation of shunt capacitors reduced the current by about 4.04% to 590.40 A.

Table 4.16 gives the branch power losses of the IEEE 10-bus radial distribution system for the uncompensated (base) case and the overall optimally compensated case at light, medium and full load conditions.

It can be noted from Table 4.16 that under light load the installation of shunt capacitors results in the reduction of real and reactive power losses in branches (1 – 2), (3 – 4), (4 – 5), (5 – 6), (6 – 7), (7 – 8), (8 – 9) and (9 – 10). The power losses in these branches reduced because of the corresponding reduction in branch currents. However, the power losses in branch (2 – 3) increased due to a corresponding increase in current flow.

It may also be noted from Table 4.16 that the installation of shunt capacitors under medium and full load conditions results in the reduction of both real and reactive power losses in all the branches of the IEEE 10-bus radial distribution system. The branch power losses reduced because of the corresponding reduction in branch

Table 4.15: IEEE 10-bus system branch currents for the uncompensated case and optimally compensated case under light, medium and full load conditions

Branch (p–q)	Light (50%) load			Medium (75%) load			Full (100%) load		
	Current flow $\|I_{p-q}\|$ (Amps)		Change in current flow (%)	Current flow $\|I_{p-q}\|$ (Amps)		Change in current flow (%)	Current flow $\|I_{p-q}\|$ (Amps)		Change in current flow (%)
	Uncompensated	Optimally compensated		Uncompensated	Optimally compensated		Uncompensated	Optimally compensated	
1 – 2	294.13	287.69	2.19	450.53	433.17	3.85	615.25	590.40	4.04
2 – 3	**253.01**	**253.23**	**-0.09**	388.81	380.35	2.18	532.94	521.18	2.21
3 – 4	230.33	213.67	7.23	354.70	325.11	8.34	487.30	442.69	9.15
4 – 5	189.81	175.76	7.40	293.37	267.40	8.85	404.73	368.27	9.01
5 – 6	144.06	140.46	2.50	223.51	213.25	4.59	309.71	294.22	5.00
6 – 7	106.01	103.52	2.35	165.07	158.73	3.84	229.73	215.59	6.16
7 – 8	88.12	86.01	2.39	137.55	132.18	3.90	191.98	180.35	6.06
8 – 9	61.80	60.10	2.75	96.85	92.70	4.28	135.83	127.67	6.01
9 – 10	38.81	37.81	2.58	60.97	58.70	3.72	85.77	83.56	2.58

Table 4.16: IEEE 10-bus system power losses for the uncompensated case and optimally compensated case under light, medium and full load conditions

Branch ($p-q$)	Light (50%) load						Medium (75%) load						Full (75%) load					
	Power Losses				Change in power losses (%)		Power Losses				Change in power losses (%)		Power Losses				Change in power losses (%)	
	Uncompensated		Optimally compensated				Uncompensated		Optimally compensated				Uncompensated		Optimally compensated			
	P (kW)	Q (kVAr)	P (kW)	Q (kVAr)	ΔP_{loss}	ΔQ_{loss}	P (kW)	Q (kVAr)	P (kW)	Q (kVAr)	ΔP_{loss}	ΔQ_{loss}	P (kW)	Q (kVAr)	P (kW)	Q (kVAr)	ΔP_{loss}	ΔQ_{loss}
1 – 2	10.67	35.70	10.20	34.16	4.33	4.33	25.03	83.77	23.14	77.44	7.55	7.55	46.67	156.22	42.98	143.85	7.92	7.92
2 – 3	0.90	38.77	0.90	38.84	-0.18	-0.18	2.12	91.57	2.03	87.62	4.31	4.31	3.98	172.03	3.80	164.53	4.36	4.36
3 – 4	39.59	63.93	34.07	55.01	13.95	13.95	93.89	151.60	78.88	127.36	15.99	15.99	177.22	286.14	146.25	236.15	17.47	17.47
4 – 5	25.16	21.92	21.57	18.79	14.26	14.26	60.11	52.36	49.94	43.50	16.92	16.92	114.40	99.66	94.72	82.51	17.21	17.21
5 – 6	41.16	35.85	39.12	34.08	4.94	4.94	99.07	86.30	90.18	78.56	8.97	8.97	190.22	165.72	171.67	149.55	9.75	9.75
6 – 7	10.17	8.86	9.70	8.45	4.64	4.64	24.67	21.49	22.81	19.87	7.54	7.54	47.78	41.62	42.08	36.65	11.93	11.93
7 – 8	15.96	9.04	15.21	8.61	4.73	4.73	38.88	22.02	35.91	20.34	7.65	7.65	75.74	42.90	66.85	37.86	11.75	11.75
8 – 9	18.31	10.37	17.32	9.81	5.40	5.40	44.98	25.47	41.20	23.34	8.39	8.39	88.47	50.11	78.16	44.27	11.65	11.65
9 – 10	8.05	4.56	7.64	4.33	5.11	5.11	19.87	11.25	18.41	10.43	7.33	7.33	39.31	22.26	37.31	21.13	5.09	5.09
Total losses	169.97	229.00	155.73	212.08	8.37	7.39	408.62	545.83	362.5	488.46	11.28	10.51	783.79	1,036.7	683.82	916.50	12.76	11.59

currents. It may also be noted from Table 4.16 that for the light, medium and full load conditions, the percentage changes in the branches' real and reactive power losses are the same. This is so because when calculating both real and reactive power losses, the square of branch current (i.e. I^2) is a common variable while R and X are constants.

Figure 2 in Appendix II give graphical illustrations of the branches real and reactive power losses (as tabulated in Table 4.16) before and after the installation of shunt capacitors while operating at light (50%), medium (75%) and full (100%) load.

It can be noted from Tables 4.15, 4.16 and Figures 2 (a), (c), and (e) in Appendix II that despite not having the highest flow of current for both the uncompensated and the optimally compensated cases, the real power losses in branch (5 – 6) are the highest. The real power losses in branch (5 – 6) are higher than those in branches (1 – 2), (2 – 3), (3 – 4) and (4 – 5) because, as it can be seen from Table 3.3, this branch has the highest resistance as compared to the other four upstream branches. On the other hand, the real power losses in branch (5 – 6) are higher than those in branch (6 – 7) because branch (5 – 6) has both higher resistance and current flow than branch (6 – 7). Lastly, the real power losses in branch (5 – 6) are higher than those in branches (7 – 8), (8 – 9) and (9 – 10) because branch (5 – 6) is upstream and thus, the current flowing through this branch is higher than that in the downstream branches.

Similarly, it can also be noted from Tables 4.15, 4.16 and Figures 2 (b), (d), and (f) in Appendix II that despite not having the highest flow of current for both the uncompensated and the optimally compensated cases, the reactive power losses in branch number (3 – 4) are the highest. The reactive power losses in branch (3 – 4) are higher than those in branches (1 – 2) and (2 – 3) because, as it can be seen from Table 3.3, this branch has the highest reactance as compared to the other two upstream branches. On the other hand, the reactive power losses in branch (3 – 4) are higher than those in branches (4 – 5), (6 – 7) and (7 – 8) because branch (3 – 4) has both higher reactance and current flow than the three branches. Lastly, the reactive power losses in branch (3 – 4) are higher than those in branches (5 – 6), (8 – 9) and (9 – 10) because branch (3 – 4) is upstream and thus, the current flowing through this

branch is higher than that in the downstream branches.

4.3. IEEE 33-Bus Radial Distribution System

4.3.1. Base Case Load Flow Results

The load flow simulation was run on the system with no shunt capacitors installed and with loads as given in section 3.9. The system registered real and reactive power losses totaling 202.68 kW and 135.16 kVAr respectively. These losses represent 5.46% and 5.88% of the system's total real and reactive power loads respectively. The minimum bus voltage for the system was 0.9131 p.u. at bus 18.

4.3.2. Results for Loss Sensitivity Factors and Modified Loss Sensitivity Factors

Table 4.17 gives values of the LSF for the IEEE 33-bus radial distribution system arranged in a descending order.

Table 4.17: LSF for the IEEE 33-bus radial distribution system

Order	LSF	Sending Bus *(p)*	Receiving Bus *(q)*	Sending Bus Voltage (V_p)	Receiving Bus Voltage (V_q)	Normalized Receiving Bus Voltage $(V_q/0.95)$
1	0.0170	5	6	0.9681	0.9497	0.9996
2	0.0137	2	3	0.9970	0.9829	1.0347
3	0.0136	27	28	0.9452	0.9337	0.9829
4	0.0103	28	29	0.9337	0.9255	0.9742
5	0.0080	4	5	0.9755	0.9681	1.0190
6	0.0080	3	4	0.9829	0.9755	1.0268
7	0.0060	29	30	0.9255	0.9219	0.9705
8	0.0047	23	24	0.9794	0.9727	1.0239
9	0.0046	8	9	0.9413	0.9351	0.9843
10	0.0045	12	13	0.9269	0.9208	0.9692
11	0.0044	9	10	0.9351	0.9292	0.9782
12	0.0042	7	8	0.9462	0.9413	0.9909
13	0.0037	26	27	0.9477	0.9452	0.9949
14	0.0030	30	31	0.9219	0.9178	0.9661
15	0.0028	1	2	1.0000	0.9970	1.0495
16	0.0026	6	26	0.9497	0.9477	0.9976
17	0.0026	3	23	0.9829	0.9794	1.0309
18	0.0024	24	25	0.9727	0.9694	1.0204
19	0.0023	19	20	0.9965	0.9929	1.0452
20	0.0014	13	14	0.9208	0.9185	0.9668
21	0.0014	6	7	0.9497	0.9462	0.9960
22	0.0013	11	12	0.9284	0.9269	0.9757
23	0.0012	16	17	0.9157	0.9137	0.9618
24	0.0009	15	16	0.9171	0.9157	0.9639
25	0.0008	14	15	0.9185	0.9171	0.9653
26	0.0008	10	11	0.9292	0.9284	0.9772

Order	LSF	Sending Bus *(p)*	Receiving Bus *(q)*	Sending Bus Voltage *(V_p)*	Receiving Bus Voltage *(V_q)*	Normalized Receiving Bus Voltage *(V_q/0.95)*
27	0.0006	31	32	0.9178	0.9169	0.9651
28	0.0004	17	18	0.9137	0.9131	0.9611
29	0.0004	20	21	0.9929	0.9922	1.0444
30	0.0004	2	19	0.9970	0.9965	1.0490
31	0.0004	21	22	0.9922	0.9916	1.0438
32	0.0002	32	33	0.9169	0.9166	0.9648

It can be noted from Table 4.17 that as per LSF approach, shunt capacitors can only be installed at buses 6, 7, 8, 9, 10, 11, 12, 13, 14, 15, 16, 17, 18, 26, 27, 28, 29, 30, 31, 32, and 33, where (V_q/0.95) < 1.01 as presented in section 2.4. Out of the twenty-one candidate buses, for capacitor installation at a single bus, the highly ranked receiving end bus, i.e. bus number 6 is identified as the global optimum bus since it has the highest LSF whereas bus number 33, with the lowest LSF, is identified as the least optimum bus.

Table 4.18 gives values of the MLSF for the IEEE 33-bus system arranged in a descending order.

Table 4.18: MLSF for the IEEE 33-bus radial distribution system

Order	MLSF	Sending Bus *(p)*	Receiving Bus *(q)*	Sending Bus Voltage *(V_p)*	Receiving Bus Voltage *(V_q)*	Normalized Receiving Bus Voltage *(V_q/0.95)*
1	3610.13	29	30	0.9255	0.9219	0.9705
2	946.50	23	24	0.9794	0.9727	1.0239
3	717.62	28	29	0.9337	0.9255	0.9742
4	636.91	3	4	0.9829	0.9755	1.0268
5	546.54	2	3	0.9970	0.9829	1.0347
6	475.09	24	25	0.9727	0.9694	1.0204
7	418.03	7	8	0.9462	0.9413	0.9909
8	339.06	5	6	0.9681	0.9497	0.9996
9	272.37	27	28	0.9452	0.9337	0.9829
10	239.01	4	5	0.9755	0.9681	1.0190
11	212.13	30	31	0.9219	0.9178	0.9661
12	168.10	1	2	1.0000	0.9970	1.0495
13	155.95	12	13	0.9269	0.9208	0.9692
14	136.74	6	7	0.9497	0.9462	0.9960
15	130.92	3	23	0.9829	0.9794	1.0309
16	109.60	13	14	0.9208	0.9185	0.9668
17	93.51	26	27	0.9477	0.9452	0.9949
18	92.82	8	9	0.9413	0.9351	0.9843
19	91.43	19	20	0.9965	0.9929	1.0452

Order	MLSF	Sending Bus *(p)*	Receiving Bus *(q)*	Sending Bus Voltage *(V_p)*	Receiving Bus Voltage *(V_q)*	Normalized Receiving Bus Voltage *($V_q/0.95$)*
20	88.50	9	10	0.9351	0.9292	0.9782
21	65.62	6	26	0.9497	0.9477	0.9976
22	64.52	31	32	0.9178	0.9169	0.9651
23	46.34	11	12	0.9284	0.9269	0.9757
24	23.39	10	11	0.9292	0.9284	0.9772
25	23.16	16	17	0.9157	0.9137	0.9618
26	17.85	15	16	0.9171	0.9157	0.9639
27	17.52	17	18	0.9137	0.9131	0.9611
28	16.62	20	21	0.9929	0.9922	1.0444
29	15.82	2	19	0.9970	0.9965	1.0490
30	14.40	21	22	0.9922	0.9916	1.0438
31	8.10	32	33	0.9169	0.9166	0.9648
32	7.95	14	15	0.9185	0.9171	0.9653

It can be noted from Table 4.18 that based on the MLSF values, bus number 30 is identified as the highly ranked receiving end bus since it has the largest MLSF whereas bus 15, with the lowest MLSF, is identified as the least ranked receiving end bus. This contrasts with the LSF approach (Table 4.17), in which bus number 6 was identified as the highly ranked bus.

4.3.3. Results for the Compensated IEEE 33-Bus Radial Distribution System

The first simulation set up considered reactive power compensation through optimal shunt capacitors placement and sizing while assuming fixed system loading at full (100%) load. On the other hand, the second simulation set up considered load variations. For the second set up, the system was assumed to operate at three different load patterns, i.e. light (50%), medium (75%), and full (100%) load. The assumed yearly hours of operation for the respective load patterns were taken to be 2000, 5260 and 1500 (Das, 2008; El-Fergany & Abdelaziz, 2014b; Mahfoud et al., 2020).

A. Optimal placement and sizing of shunt capacitors for fixed system loading

Table 4.19 gives results of the overall costs, power losses and voltage magnitudes for the fixed system loading case. The results are then compared with those obtained using approaches based on the exhaustive search, and a combination of the exhaustive search and MVO. Due to the large number of bus combinations in the

IEEE 33-bus system, the performance evaluation of the developed approach in the provision of reactive power compensation was limited to a maximum of 4 buses.

Table 4.19: Comparison of costs, power losses and voltage magnitudes obtained using the exhaustive search based approach, exhaustive search and MVO based approach, and the developed approach at fixed loading of the IEEE 33-bus system

Method	No of buses with capacitors	Overall cost ($)	P_{loss} (kW)	Q_{loss} $(kVAr)$	V_{min} $(p.u.)$	V_{max} $(p.u.)$
-	0	34,050.24	202.68	135.16	0.9131	1.0000
Exhaustive	1	24,805.60	143.70	96.32	0.9251	1.0000
Exhaustive & MVO		24,805.60	143.70	96.32	0.9251	1.0000
Developed		24,805.60	143.70	96.32	0.9251	1.0000
Exhaustive	2	24,082.61	135.77	90.57	0.9357	1.0000
Exhaustive & MVO		24,082.61	135.77	90.57	0.9357	1.0000
Developed		24,082.61	135.77	90.57	0.9357	1.0000
Exhaustive	**3**	**24,080.79**	**132.68**	**88.63**	**0.9355**	**1.0000**
Exhaustive & MVO		**24,080.79**	**132.68**	**88.63**	**0.9355**	**1.0000**
Developed		**24,080.79**	**132.68**	**88.63**	**0.9355**	**1.0000**
Exhaustive & MVO	4	24,300.04	130.73	87.42	0.9411	1.0000
Developed		24,300.04	130.73	87.42	0.9411	1.0000

It can be noted from Table 4.19 that for all instances, the developed approach gave the same overall costs, power losses and voltage magnitudes as those obtained using the exhaustive search and MVO based approach. It can also be noted from Table 4.19 that for the compensation of a total of 1 to 3 buses, i.e., options for which exhaustive searches for optimal buses and shunt capacitor sizes were carried out, the developed approach gave the same overall costs, power losses and voltage magnitudes as those obtained using approaches based on the exhaustive search, and a combination of the exhaustive search and MVO. Furthermore, it can be noted from Table 4.19 that the overall optimum total number of buses to be compensated is 3. This is given by the highlighted row in Table 4.19. Compensating the 3 buses reduced the yearly overall cost of running the system from $34,050.24, without compensation, to $24,080.79. This represents a 29.28% reduction in the overall cost. However, despite giving the best minimum overall cost, the optimal placement and sizing of shunt capacitors at the 3 buses did not result in the best minimum voltage levels as well as the least total

real and reactive power losses. As shown in Table 4.19, the best minimum voltages as well as the least total real and reactive power losses were attained when shunt capacitors were optimally placed and sized at 4 buses. Consequently, if consideration was only given to the cost of total real power losses and/or voltage level improvement, then the provision of reactive power to 4 buses would have given the optimal overall cost. However, since the shunt capacitors' purchase, installation and O&M costs were also taken into consideration, the provision of reactive power to the 4 buses results in a non-optimal overall cost.

Table 4.20 gives the corresponding optimal capacitor locations (bus numbers) and the shunt capacitor sizes for the results given in Table 4.19. For all the given compensation options, the results of optimal capacitor location and size obtained using the developed approach were identical to those obtained using the approach based on a combination of the exhaustive search and MVO. For the compensation of a total of 1 to 3 buses, i.e., options for which exhaustive searches for optimum buses and shunt capacitor sizes were carried out, the results for optimal shunt capacitors' placement and sizing that were obtained using the developed approach were also identical to those obtained using the approach based on the exhaustive search.

Table 4.20: Optimal locations and capacitor sizes obtained using the developed approach, the exhaustive search, and the exhaustive search and MVO based approaches for various compensation options in the IEEE 33-bus system under fixed load condition

No of buses with capacitors	**Optimal capacitor locations (bus numbers)**	**Optimal capacitor sizes (kVAr)**
1	30	1200
2	12	450
	30	1050
3	12	450
	24	600
	30	900
4	7	450
	14	300
	24	450
	30	900

It can be noted from Table 4.20 that despite disregarding some bus combinations, the developed approach was still able to find the global optimum locations / bus numbers and shunt capacitor sizes for the different total number of buses to be compensated.

Table 4.21 gives comparative results of the average computation time and search space dimensions obtained using an approach based on a combination of the exhaustive search and MVO, and the developed approach for various compensation options in the IEEE 33-bus system under fixed load condition.

Table 4.21: Comparison of average computation time and search space dimensions obtained using an approach based on the exhaustive search and MVO, and the developed approach for various compensation options in the IEEE 33-bus system with fixed load

No of buses with capacitors	Exhaustive Search and MVO		Developed Approach		Decrease in average computation time (%)
	Average computation time (s)	Search space dimension	Average computation time (s)	Search space dimension	
1	1112.89	32×1	31.88	1×1	97.14
2	19491.19	496×2	969.98	31×2	95.02
3	**195264.68**	**4960×3**	**17667.35**	**465×3**	**90.95**
4	886495.57	35960×4	180555.06	4495×4	79.63

It can be noted from Table 4.21 that the developed approach helped in reducing the average computation time. For the installation of shunt capacitors at a single bus, the developed approach reduced the average computation time by 97.14% from 1112.89 to 31.88 seconds. On the other hand, when shunt capacitors were to be installed at 4 buses, the developed approach reduced the average computation time by 79.63% from 886495.57 to 180555.06 seconds. The average computation time was reduced in accordance with reductions in search space dimensions.

Table 4.22 gives the bus voltage magnitudes of the IEEE 33-bus radial distribution system for the uncompensated (base) case and the optimally compensated case in which optimally sized shunt capacitors were optimally installed at 3 buses.

Table 4.22: IEEE 33-bus system voltage magnitudes for the uncompensated case and the optimally compensated case under fixed load condition

Bus Number	Bus Voltages (p.u.)		% Change
	Uncompensated	Optimally compensated	
1	1.0000	1.0000	0
2	0.9970	0.9977	0.07
3	0.9829	0.9869	0.41
4	0.9755	0.9812	0.58
5	0.9681	0.9757	0.79
6	0.9497	0.9639	1.50
7	0.9462	0.9622	1.69
8	0.9413	0.9582	1.80
9	0.9351	0.9542	2.04
10	0.9292	0.9507	2.31
11	0.9284	0.9501	2.34
12	0.9269	0.9490	2.38
13	0.9208	0.9430	2.41
14	0.9185	0.9408	2.43
15	0.9171	0.9394	2.43
16	0.9157	0.9381	2.45
17	0.9137	0.9361	2.45
18	0.9131	0.9355	2.45
19	0.9965	0.9971	0.06
20	0.9929	0.9936	0.07
21	0.9922	0.9929	0.07
22	0.9916	0.9922	0.06
23	0.9794	0.9845	0.52
24	0.9727	0.9806	0.81
25	0.9694	0.9773	0.81
26	0.9477	0.9626	1.57
27	0.9452	0.9610	1.67
28	0.9337	0.9553	2.31
29	0.9255	0.9515	2.81
30	0.9219	0.9496	3.00
31	0.9178	0.9455	3.02
32	0.9169	0.9446	3.02
33	0.9166	0.9444	3.03

It can be seen from Table 4.22 that the installation of shunt capacitors results in an improvement of the bus voltage magnitudes for all the load (or P-Q) buses. In Table 4.22, it is shown that the greatest improvement in bus voltage occurs at bus 33. The voltage at bus 33 improves by 3.03%. On the other hand, the least improvement in bus voltages occurs at buses 19 and 22. For these buses the voltage improves by 0.06%. The voltage magnitude at bus 1 does not change because it was set to be a slack bus during the simulations. Figure 4.3 illustrates the bus voltage magnitudes of the IEEE 33-bus radial distribution system for the uncompensated (base) case and the overall optimally compensated case under fixed load condition.

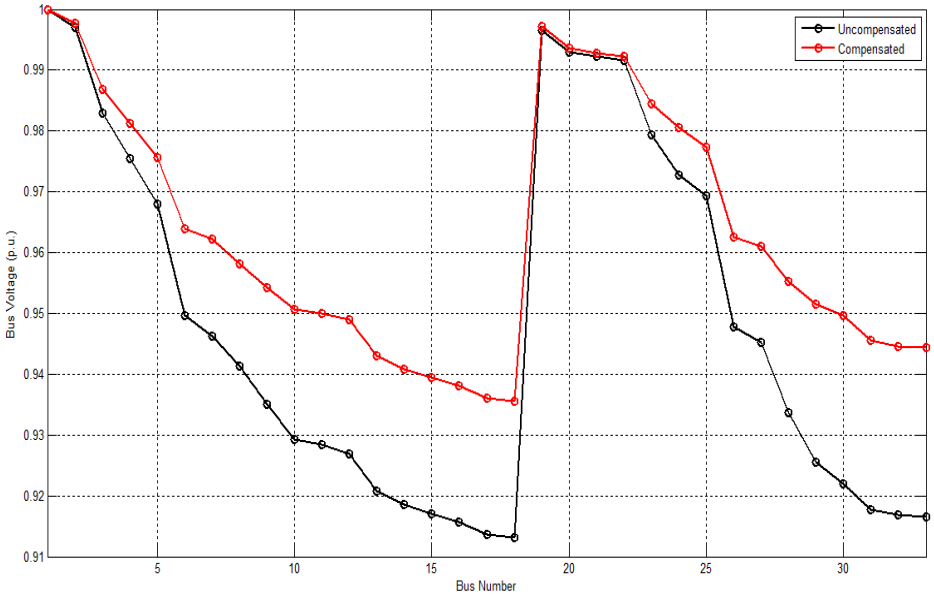

Figure 4.3: Comparison of IEEE 33-bus radial distribution system bus voltages with and without compensation at fixed load condition

Table 4.23 gives the branch currents of the IEEE 33-bus radial distribution system for the uncompensated (base) case and the optimally compensated case at fixed load condition.

Table 4.23: IEEE 33-bus system branch currents for the uncompensated case and optimally compensated case at fixed load

Branch	Sending Bus (p)	Receiving Bus (q)	Current flow $\|I_{p-q}\|$ Amps		Change in current flow (%)
			Uncompensated	Optimally compensated	
1	1	2	364.36	305.89	16.05
2	2	3	324.12	267.98	17.32
3	3	4	233.18	186.76	19.91
4	4	5	221.51	176.45	20.34
5	5	6	216.11	171.39	20.69
6	6	7	101.13	89.71	11.29
7	7	8	82.47	73.15	11.30
8	8	9	63.71	57.64	9.53
9	9	10	58.40	53.15	8.99
10	10	11	53.07	48.80	8.05
11	11	12	48.51	46.11	4.95
12	12	13	42.62	41.60	2.39
13	13	14	36.69	35.82	2.37
14	14	15	24.58	23.99	2.40
15	15	16	19.42	18.96	2.37
16	16	17	13.97	13.64	2.36
17	17	18	8.52	8.32	2.35

Branch	Sending Bus (p)	Receiving Bus (q)	Current flow $\|I_{p-q}\|$ Amps		Change in current flow (%)
			Uncompensated	Optimally compensated	
18	2	19	34.21	33.39	2.40
19	19	20	23.52	23.51	0.04
20	20	21	15.69	15.68	0.06
21	21	22	7.85	7.84	0.13
22	3	23	83.24	75.56	9.23
23	23	24	75.68	69.64	7.98
24	24	25	37.91	37.60	0.82
25	6	26	110.89	75.61	31.82
26	26	27	108.23	71.64	33.81
27	27	28	103.30	66.66	35.47
28	28	29	98.69	61.71	37.47
29	29	30	87.61	52.24	40.37
30	30	31	40.44	39.25	2.94
31	31	32	26.20	25.43	2.94
32	32	33	6.21	6.03	2.90

It can be noted from Table 4.23 that the installation of shunt capacitors results in the reduction of currents flowing in all the branches of the IEEE 33-bus radial distribution system. Further, it can also be noted from Table 4.23 that the total current flowing before the installation of shunt capacitors was about 364.36 A. However, the installation of shunt capacitors reduced the total current by about 16.05% to 305.89 A.

Table 4.24 gives the branch power losses of the IEEE 33-bus radial distribution system for the uncompensated (base) case and the overall optimally compensated case at fixed load.

Table 4.24: IEEE 33-bus system power losses for the uncompensated case and optimally compensated case at fixed load

Branch	Sending Bus (p)	Receiving Bus (q)	Power Losses				Change in power losses (%)	
			Uncompensated		Optimally compensated			
			P (W)	Q (VAr)	P (W)	Q (VAr)	ΔP_{loss}	ΔQ_{loss}
1	1	2	12,240.47	6,239.72	8,627.18	4,397.81	29.52	29.52
2	2	3	51,791.46	26,378.98	35,402.97	18,031.82	31.64	31.64
3	3	4	19,900.60	10,135.17	12,766.46	6,501.82	35.85	35.85
4	4	5	18,699.07	9,523.72	11,864.81	6,042.93	36.55	36.55
5	5	6	38,248.89	33,018.27	24,058.06	20,768.07	37.10	37.10
6	6	7	1,914.54	6,328.61	1,506.48	4,979.75	21.31	21.31
7	7	8	4,838.03	1,598.85	3,806.34	1,257.90	21.32	21.32
8	8	9	4,180.61	3,003.54	3,421.93	2,458.47	18.15	18.15
9	9	10	3,560.98	2,524.07	2,948.70	2,090.07	17.19	17.19

Branch	Sending Bus (p)	Receiving Bus (q)	Power Losses				Change in power losses (%)	
			Uncompensated		Optimally compensated			
			P (W)	Q (VAr)	P (W)	Q (VAr)	ΔP_{loss}	ΔQ_{loss}
10	10	11	553.71	183.07	468.13	154.77	15.46	15.46
11	11	12	881.15	305.49	795.98	275.96	9.67	9.67
12	12	13	2,666.30	2,097.80	2,540.84	1,999.10	4.71	4.71
13	13	14	729.18	959.81	694.82	914.59	4.71	4.71
14	14	15	356.98	317.72	340.12	302.71	4.72	4.72
15	15	16	281.47	205.55	268.16	195.83	4.73	4.73
16	16	17	251.64	335.98	239.72	320.06	4.74	4.74
17	17	18	53.14	41.67	50.62	39.69	4.74	4.74
18	2	19	160.95	153.59	160.75	153.40	0.13	0.13
19	19	20	832.18	749.86	831.12	748.91	0.13	0.13
20	20	21	100.76	117.71	100.63	117.56	0.13	0.13
21	21	22	43.63	57.69	43.58	57.62	0.13	0.13
22	3	23	3,181.63	2,173.97	2,603.96	1,779.26	18.16	18.16
23	23	24	5,143.68	4,061.67	4,354.47	3,438.48	15.34	15.34
24	24	25	1,287.45	1,007.40	1,266.59	991.08	1.62	1.62
25	6	26	2,600.90	1,324.79	1,193.09	607.71	54.13	54.13
26	26	27	3,328.99	1,694.95	1,458.57	742.63	56.19	56.19
27	27	28	11,300.86	9,963.75	4,705.21	4,148.49	58.36	58.36
28	28	29	7,833.35	6,824.23	3,062.13	2,667.66	60.91	60.91
29	29	30	3,895.67	1,984.30	1,384.73	705.33	64.45	64.45
30	30	31	1,593.64	1,574.99	1,501.39	1,483.82	5.79	5.79
31	31	32	213.20	248.49	200.85	234.09	5.79	5.79
32	32	33	13.17	20.48	12.41	19.29	5.80	5.80
Total losses			202,678.28	135,155.89	132,680.80	88,626.68	34.53	34.43

It can be noted from Table 4.24 that the installation of shunt capacitors results in the reduction of real and reactive power losses in all the branches of the IEEE 33-bus radial distribution system. The branch power losses reduced because of the corresponding reduction in branch currents. It may also be noted from Table 4.24 that the percentage changes in the branches' real and reactive power losses are the same. This is so because when calculating both real and reactive power losses, the square of branch current (i.e., I^2) is a common variable while R and X are constants.

Figures 1 (a) and (b) in Appendix III give graphical illustrations of the branches real and reactive power losses (as tabulated in Table 4.24) before and after the installation of shunt capacitors while operating at fixed load.

It can be noted from Tables 4.23, 4.24 and Figure 1 (a) in Appendix III that despite not having the highest flow of current for both the uncompensated and the optimally compensated cases, the real power losses in branch number 2 are the highest. The real power losses in branch number 2 are higher than those in branch number 1

because, as it can be seen from Table 3.4, branch number 2 has the highest resistance than branch number 1. On the other hand, the real power losses in branch number 2 are higher than those in branches 3, 4, 6, 10, 11, 18, 20, 22, 25, 26, 31 and 32 because branch number 2 has both higher resistance and current flow than the twelve branches. Lastly, the real power losses in branch number 2 are higher than those in branches 5, 7, 8, 9, 12, 13, 14, 15, 16, 17, 19, 21, 23, 24, 27, 28, 29 and 30 because branch number 2 is upstream and thus, the current flowing through this branch is higher than that in the downstream branches.

Similarly, it can also be noted from Tables 4.23, 4.24 and Figure 1 (b) in Appendix III that despite not having the highest flow of current for both the uncompensated and the optimally compensated cases, the reactive power losses in branch number 5 are the highest. The reactive power losses in branch number 5 are higher than those in branches 1, 2, 3 and 4 because, as it can be seen from Table 3.4, this branch has the highest reactance as compared to the other four upstream branches. On the other hand, the reactive power losses in branch number 5 are higher than those in branches 6, 7, 10, 11, 14, 15, 17, 18, 20, 22, 24, 25, 26, 28, 29, 31 and 32 because branch number 5 has both higher reactance and current flow than the seventeen branches. Lastly, the reactive power losses in branch 5 are higher than those in branches 8, 9, 12, 13, 16, 19, 21, 23, 27 and 30 because branch 5 is upstream and thus, the current flowing through this branch is higher than that in the downstream branches.

B. Optimal placement and sizing of shunt capacitors for variable system loading

Table 4.25 shows simulation results for a case where shunt capacitors were optimally placed and sized in the IEEE 33-bus radial distribution system while considering load variations. For this case, the system was assumed to operate at three different load patterns, i.e. light (50%), medium (75%) and full (100%) load. The assumed yearly hours of operation for the respective load patterns were taken to be 2000, 5260 and 1500 (Das, 2008; El-Fergany & Abdelaziz, 2014b; Mahfoud et al., 2020).

Table 4.25: Comparison of costs, power losses and voltage magnitudes obtained using approaches based on the exhaustive search, the exhaustive search and MVO, and the developed approach at variable loading of the IEEE 33-bus system

Method	No of buses with capacitors	Loading	Overall cost ($)	P_{loss} (kW)	Q_{loss} $(kVAr)$	V_{min} $(p.u.)$	V_{max} $(p.u.)$
-	0	Light (50%)	58,526.70	47.07	31.35	0.9583	1.0000
		Medium (75%)		109.75	73.15	0.9362	1.0000
		Full (100%)		202.68	135.16	0.9131	1.0000
Exhaustive	1	Light (50%)	42,488.72	34.02	22.79	0.9638	1.0000
		Medium (75%)		78.61	52.67	0.9448	1.0000
		Full (100%)		143.70	96.32	0.9251	1.0000
Exhaustive & MVO	1	Light (50%)	42,488.72	34.02	22.79	0.9638	1.0000
		Medium (75%)		78.61	52.67	0.9448	1.0000
		Full (100%)		143.70	96.32	0.9251	1.0000
Developed Approach	1	Light (50%)	42,488.72	34.02	22.79	0.9638	1.0000
		Medium (75%)		78.61	52.67	0.9448	1.0000
		Full (100%)		143.70	96.32	0.9251	1.0000
Exhaustive	2	Light (50%)	40,960.18	32.50	21.72	0.9688	1.0000
		Medium (75%)		74.63	49.73	0.9535	1.0000
		Full (100%)		135.93	90.68	0.9391	1.0000
Exhaustive & MVO	2	Light (50%)	40,960.18	32.50	21.72	0.9688	1.0000
		Medium (75%)		74.63	49.73	0.9535	1.0000
		Full (100%)		135.93	90.68	0.9391	1.0000
Developed Approach	2	Light (50%)	40,960.18	32.50	21.72	0.9688	1.0000
		Medium (75%)		74.63	49.73	0.9535	1.0000
		Full (100%)		135.93	90.68	0.9391	1.0000
Exhaustive	**3**	**Light (50%)**	**40,469.48**	**31.81**	**21.21**	**0.9707**	**1.0000**
		Medium (75%)		**72.64**	**48.54**	**0.9521**	**1.0000**
		Full (100%)		**132.83**	**88.65**	**0.9352**	**1.0000**
Exhaustive & MVO	**3**	**Light (50%)**	**40,469.48**	**31.81**	**21.21**	**0.9707**	**1.0000**
		Medium (75%)		**72.64**	**48.54**	**0.9521**	**1.0000**
		Full (100%)		**132.83**	**88.65**	**0.9352**	**1.0000**
Developed Approach	**3**	**Light (50%)**	**40,469.48**	**31.81**	**21.21**	**0.9707**	**1.0000**
		Medium (75%)		**72.64**	**48.54**	**0.9521**	**1.0000**
		Full (100%)		**132.83**	**88.65**	**0.9352**	**1.0000**
Exhaustive & MVO	4	Light (50%)	40,698.41	31.31	20.93	0.9693	1.0000
		Medium (75%)		72.27	48.27	0.9555	1.0000
		Full (100%)		131.06	87.63	0.9378	1.0000
Developed Approach	4	Light (50%)	40,698.41	31.31	20.93	0.9693	1.0000
		Medium (75%)		72.27	48.27	0.9555	1.0000
		Full (100%)		131.06	87.63	0.9378	1.0000

It can be noted from Table 4.25 that for all instances, the developed approach attained the same overall costs, power losses and voltage magnitudes as those obtained using the exhaustive search and MVO based approach. It can also be noted

from Table 4.25 that for the compensation of a total of 1 to 3 buses, i.e., options for which exhaustive searches for optimum buses and shunt capacitor sizes were carried out, the developed approach attained the same overall costs, power losses and voltage magnitudes as those obtained using approaches based on the exhaustive search, and a combination of the exhaustive search and MVO. Furthermore, it can also be noted from Table 4.25 that the overall optimum total number of buses to be compensated is 3. This is given by the highlighted row in Table 4.25. Compensating the 3 buses reduced the yearly overall cost of running the system from $58,526.70, without compensation, to $40,469.48. This represents a 30.85% reduction in the yearly overall cost.

Table 4.26 gives the corresponding optimal capacitor locations (bus numbers) and the shunt capacitor sizes for the results given in Table 4.25. For all the given compensation options, the results of optimal capacitor location and size obtained using the developed approach are identical to those obtained using the exhaustive search and MVO based method. For the compensation of a total of 1 to 3 buses, i.e., options for which exhaustive searches for optimum buses and shunt capacitor sizes were carried out, the results for optimal shunt capacitors' placement and sizing that were obtained using the developed approach were also identical to those obtained using the exhaustive search based approach.

Table 4.26: Optimal locations and capacitor sizes obtained using the developed approach, the exhaustive search, and the exhaustive search and MVO based approaches for various compensation options in the IEEE 33-bus system with variable loading

Loading	No of buses with capacitors	Optimal capacitor locations (bus numbers)	Optimal capacitor sizes (kVAr)
Light (50%)		30	600
Medium (75%)	1	30	900
Full (100%)		30	1200
Light (50%)		13	150
		30	600
Medium (75%)	2	13	300
		30	750
Full (100%)		13	450
		30	1050
		12	**300**
Light (50%)		**24**	**300**
		30	**450**
		12	**300**
Medium (75%)	**3**	**24**	**450**
		30	**750**
		12	**450**
Full (100%)		**24**	**450**
		30	**900**
		13	150
Light (50%)		24	150
		26	300
		30	450
		13	300
Medium (75%)	4	24	300
		26	300
		30	600
		13	450
Full (100%)		24	300
		26	450
		30	900

It can be noted from Table 4.26 that despite disregarding some bus combinations, the developed approach was still able to find the global optimal locations / bus numbers and shunt capacitor sizes for the different total number of buses to be compensated.

Table 4.27 gives comparative results of the average computation time and search space dimensions obtained using the exhaustive search and MVO, and the developed approach for various compensation options in the IEEE 33-bus system under variable load conditions.

Table 4.27: Comparison of average computation time and search space dimensions obtained using an approach based on the exhaustive search and MVO, and the developed approach for various compensation options in the IEEE 33-bus system with variable load

No of buses with capacitors	Exhaustive Search and MVO		Developed Approach		Decrease in average computation time (%)
	Average computation time (s)	Search space dimension	Average computation time (s)	Search space dimension	
1	2133.82	32×1	71.70	1×1	96.64
2	31894.48	496×2	2140.10	31×2	93.29
3	**330540.90**	**4960×3**	**29801.90**	**465×3**	**90.98**
4	2398452.08	35960×4	416261.17	4495×4	82.64

It can be noted from Table 4.27 that the developed approach helped in reducing the average computation time. For the installation of shunt capacitors at a single bus, the developed approach reduced the average computation time by 96.64% from 2133.82 to 71.70 seconds. On the other hand, when shunt capacitors were to be installed at 4 buses, the developed approach reduced the average computation time by 82.64% from 2398452.08 to 416261.17 seconds. The average computation time reduced in accordance with reductions in search space dimensions.

Table 4.28 gives isolated results of the different parameters of the IEEE 33-bus radial distribution system for the uncompensated (base) case and the overall optimally compensated case. The overall optimally compensated case is the case in which optimally sized shunt capacitors were optimally installed at 3 buses. In computing the cost of energy losses per year, the power losses given in Table 4.28 were assumed to be constant for an hour whereas the average electrical energy cost was taken to be 0.06$/kWh.

Table 4.28: Comparison of power losses, energy losses and costs of the IEEE 33-bus radial distribution system for the uncompensated case and the overall optimally compensated case under variable load conditions

Loading/Parameters	Uncompensated	Optimally compensated	
Light (50%) load (2000 hours of operation annually)			
Real power losses (kW)	47.07	31.81	
Real power losses reduction (kW)	-	15.26	
Real power losses reduction (%)	-	32.42	
Reactive power losses (kVAr)	31.35	21.21	
Reactive power losses reduction (kVAr)	-	10.14	
Reactive power losses reduction (%)	-	32.35	
Annual energy losses (MWh)	94.14	63.62	
Cost of energy losses/year ($)	5,648.40	3,817.20	
		12	300
Optimal buses and capacitor sizes (kVAr)	-	24	300
		30	450
Total kVAr installed	-	1050	
V_{min} (p.u.)	0.9583	0.9707	
V_{max} (p.u.)	1.0000	1.0000	
Medium (75%) load (5260 hours of operation annually)			
Real power losses (kW)	109.75	72.64	
Real power losses reduction (kW)	-	37.11	
Real power losses reduction (%)	-	33.81	
Reactive power losses (kVAr)	73.15	48.54	
Reactive power losses reduction (kVAr)	-	24.61	
Reactive power losses reduction (%)	-	33.64	
Annual energy losses (MWh)	577.29	382.09	
Cost of energy losses/year ($)	34,637.40	22,925.40	
		12	300
Optimal buses and capacitor sizes (kVAr)	-	24	450
		30	750
Total kVAr installed	-	1500	
V_{min} (p.u.)	0.9362	0.9521	
V_{max} (p.u.)	1.0000	1.0000	
Full (100%) load (1500 hours of operation annually)			
Real power losses (kW)	202.68	132.83	
Real power losses reduction (kW)	-	69.85	
Real power losses reduction (%)	-	34.46	
Reactive power losses (kVAr)	135.16	88.65	
Reactive power losses reduction (kVAr)	-	46.51	
Reactive power losses reduction (%)	-	34.41	
Annual energy losses (MWh)	3,040.20	1,992.45	
Cost of energy losses/year ($)	18,241.20	11,954.70	
		12	450
Optimal buses and capacitor sizes (kVAr)	-	24	450
		30	900
Total kVAr installed	-	1800	
V_{min} (p.u.)	0.9131	0.9352	
V_{max} (p.u.)	1.0000	1.0000	

Loading/Parameters	Uncompensated	Optimally compensated	
Overall optimal buses and maximum capacitor sizes to be installed (kVAr)	-	12 24 30	450 450 900
Total kVAr installed	-	1800	
Annual energy losses (MWh)	975.47	644.97	
Cost of energy loss/year ($)	58,527.95	38,698.08	
Capacitors' purchase cost/year ($)	-	392.40	
Capacitors' installation cost/year ($)	-	480.00	
Capacitors' operation and maintenance cost/year ($)	-	900.00	
Total cost/year ($)	58,526.70	40,469.48	
Net savings/year ($)		18,057.22	

It can be observed from Table 4.28 (which is derived from Tables 4.25 and 4.26), that despite the expenditure incurred in procuring the shunt capacitors, having them installed, operated and maintained, the yearly overall cost of running the system is still less than that of the total real power losses in the uncompensated system. Consequently, there is a saving of $18,057.22 per year and in 10 years, a total saving of $180,572.20 would be made.

Furthermore, it can be noted from Table 4.28 that for the overall optimally compensated case, buses 12, 24, and 30 are the buses that require reactive power compensation whereas 450, 450, and 900 are the corresponding optimum shunt capacitor sizes to be installed at the identified buses. The results also show that for all the loading patterns, the total number of buses to be compensated are 3.

At light (50%) loading, buses 12, 24, and 30 are the specific buses that require reactive power compensation with 300, 300 and 450 kVAr being the corresponding optimum shunt capacitor sizes to be installed. The same buses require reactive power compensation of 300, 450, and 750 respectively, at medium (75%) loading. Lastly, at full (100%) loading, buses 12, 24, and 30 require reactive power compensation of 450, 450, and 900 kVAr respectively. Therefore, for the compensation to work satisfactorily under the varying load conditions, the details of the type and size of capacitor banks required at each bus is as shown in Table 4.29.

Table 4.29: Type and sizes of shunt capacitors to be installed in the 33-bus radial distribution system

Bus number	Load level and capacitor size (kVAr)			Type and size (kVAr)	
	Light (50%)	Medium (75%)	Full (100%)	Fixed	Switched
12	300	300	450	300	150
24	300	450	450	300	150
30	450	750	900	450	150 300

From Table 4.29, it can be noted that buses 12 and 24 require one fixed and one switched shunt capacitors. On the other hand, bus 30 require one fixed and two switched shunt capacitors.

Parameters of the IEEE 33-bus radial distribution system under variable load conditions

Table 4.30 gives the bus voltage magnitudes of the IEEE 33-bus radial distribution system for the uncompensated (base) case and the overall optimally compensated case at light, medium and full load conditions.

Table 4.30: IEEE 33-bus system voltage magnitudes for the uncompensated case and optimally compensated case under light, medium and full load conditions

Bus Number	Light (50%) load			Medium (75%) load			Full (100%) load		
	Bus Voltages (p.u.)		% Change	Bus Voltages (p.u.)		% Change	Bus Voltages (p.u.)		% Change
	Uncompensated	Optimally compensated		Uncompensated	Optimally compensated		Uncompensated	Optimally compensated	
1	1.0000	1.0000	0	1.0000	1.0000	0	1.0000	1.0000	0
2	0.9986	0.9989	0.03	0.9978	0.9983	0.05	0.9970	0.9976	0.06
3	0.9917	0.9938	0.21	0.9874	0.9904	0.30	0.9829	0.9866	0.38
4	0.9881	0.9911	0.30	0.9819	0.9862	0.44	0.9755	0.9809	0.55
5	0.9846	0.9885	0.40	0.9765	0.9822	0.58	0.9681	0.9754	0.74
6	0.9757	0.9831	0.76	0.9630	0.9736	1.10	0.9497	0.9636	1.46
7	0.9741	0.9826	0.87	0.9604	0.9723	1.24	0.9462	0.9620	1.67
8	0.9718	0.9808	0.93	0.9568	0.9693	1.30	0.9413	0.9579	1.76
9	0.9688	0.9792	1.07	0.9522	0.9662	1.47	0.9351	0.9539	2.01
10	0.9660	0.9779	1.23	0.9480	0.9634	1.62	0.9292	0.9504	2.28
11	0.9656	0.9776	1.24	0.9474	0.9629	1.64	0.9284	0.9498	2.31
12	0.9648	0.9771	1.27	0.9463	0.9621	1.67	0.9269	0.9487	2.35
13	0.9619	0.9743	1.29	0.9418	0.9577	1.69	0.9208	0.9427	2.38
14	0.9608	0.9732	1.29	0.9401	0.9560	1.69	0.9185	0.9405	2.40
15	0.9602	0.9725	1.28	0.9391	0.9550	1.69	0.9171	0.9391	2.40
16	0.9595	0.9719	1.29	0.9381	0.9540	1.69	0.9157	0.9378	2.41
17	0.9585	0.9709	1.29	0.9366	0.9526	1.71	0.9137	0.9358	2.42
18	0.9583	0.9706	1.28	0.9362	0.9521	1.70	0.9131	0.9352	2.42
19	0.9983	0.9986	0.03	0.9974	0.9979	0.05	0.9965	0.9971	0.06
20	0.9965	0.9968	0.03	0.9947	0.9952	0.05	0.9929	0.9935	0.06
21	0.9962	0.9965	0.03	0.9942	0.9947	0.05	0.9922	0.9928	0.06
22	0.9958	0.9962	0.04	0.9937	0.9942	0.05	0.9916	0.9922	0.06
23	0.9900	0.9926	0.26	0.9847	0.9886	0.40	0.9794	0.9840	0.47
24	0.9867	0.9906	0.40	0.9798	0.9857	0.60	0.9727	0.9794	0.69
25	0.9850	0.9890	0.41	0.9773	0.9832	0.60	0.9694	0.9760	0.68
26	0.9748	0.9825	0.79	0.9615	0.9728	1.18	0.9477	0.9623	1.54

Bus Number	Light (50%) load			Medium (75%) load			Full (100%) load		
	Bus Voltages (p.u.)		% Change	Bus Voltages (p.u.)		% Change	Bus Voltages (p.u.)		% Change
	Uncompensated	Optimally compensated		Uncompensated	Optimally compensated		Uncompensated	Optimally compensated	
27	0.9736	0.9817	0.83	0.9597	0.9716	1.24	0.9452	0.9607	1.64
28	0.9681	0.9790	1.13	0.9513	0.9679	1.74	0.9337	0.9550	2.28
29	0.9642	0.9771	1.34	0.9453	0.9654	2.13	0.9255	0.9512	2.78
30	0.9625	0.9762	1.42	0.9426	0.9641	2.28	0.9219	0.9493	2.97
31	0.9605	0.9742	1.43	0.9396	0.9611	2.29	0.9178	0.9452	2.99
32	0.9601	0.9738	1.43	0.9389	0.9605	2.30	0.9169	0.9443	2.99
33	0.9599	0.9737	1.44	0.9387	0.9603	2.30	0.9166	0.9441	3.00

It can be seen from Table 4.30 that the installation of shunt capacitors under light, medium and full load conditions results in the improvement of bus voltage magnitudes for all the load (or P-Q) buses. From Table 4.30 it is shown that the greatest improvement in bus voltage magnitudes under light and full load conditions occurs at bus 33. For the light and full load conditions, the voltage at bus 33 improves by 1.44 and 3% respectively. Additionally, Table 4.30 also shows that the greatest improvement in bus voltage magnitudes under medium load occurs at buses 32 and 33. For these buses, the voltage improves by 2.3%.

On the other hand, Table 4.30 shows that the least improvement in bus voltage magnitudes under light load occurs at buses 2, 19, 20 and 21. For these buses the voltage improves by 0.03%. It can also be noted from Table 4.30 that the least improvement in bus voltage magnitudes under medium and full load conditions occurs at buses 2, 19, 20, 21 and 22. Under medium load, the voltage at buses 2, 19, 20, 21 and 22 improves by 0.05% while under full load the voltage at buses 2, 19, 20, 21 and 22 improves by 0.06%. Figure 4.4 illustrates the bus voltage magnitudes of the IEEE 33-bus radial system for the uncompensated (base) case and the overall optimally compensated case at light, medium and full load.

Table 4.31 gives the branch currents of the IEEE 33-bus radial distribution system for the uncompensated (base) case and the overall optimally compensated case at light, medium and full load conditions.

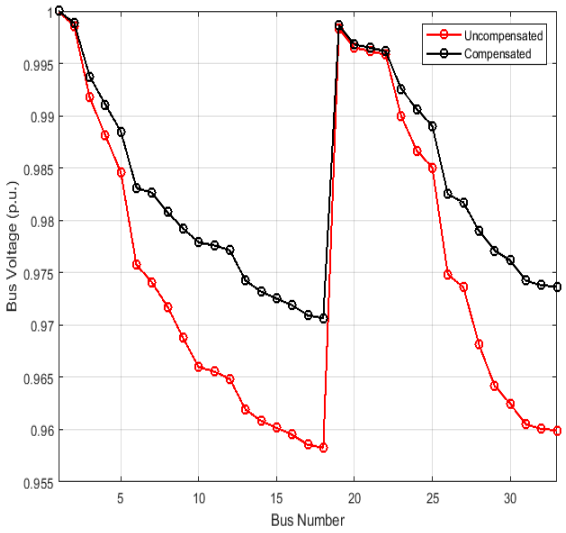

(a) Light (50%) load

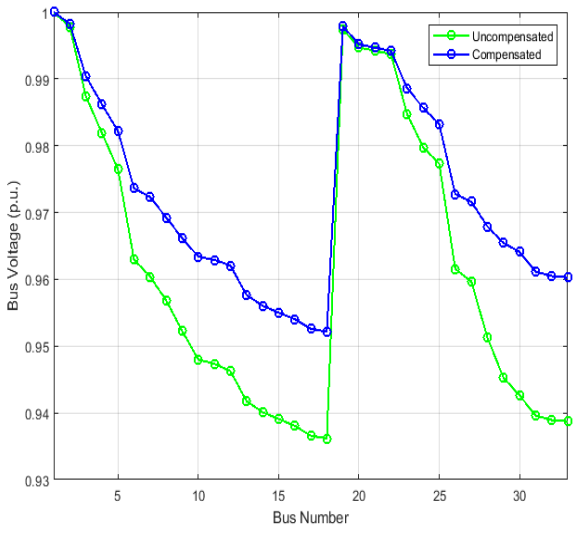

(b) Medium (75%) load

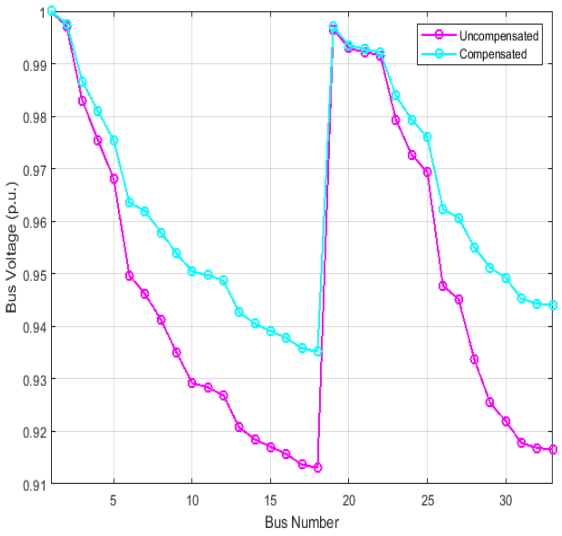

(c) Full (100%) load

Figure 4.4: Comparison of IEEE 33-bus radial distribution system voltages with and without compensation at light, medium and full load

Table 4.31: IEEE 33-bus system branch currents for the uncompensated case and optimally compensated case under light, medium and full load conditions

Branch (p–q)	Light (50%) load			Medium (75%) load			Full (100%) load		
	Current flow $\|I_{p-q}\|$ (Amps)		Change in current flow (%)	Current flow $\|I_{p-q}\|$ (Amps)		Change in current flow (%)	Current flow $\|I_{p-q}\|$ (Amps)		Change in current flow (%)
	Uncompensated	Optimally compensated		Uncompensated	Optimally compensated		Uncompensated	Optimally compensated	
1 – 2	177.03	149.54	15.53	269.26	226.85	15.75	364.36	307.47	15.61
2 – 3	156.97	131.03	16.52	239.12	198.66	16.92	324.12	269.00	17.01
3 – 4	112.14	90.46	19.34	171.41	137.84	19.58	233.18	186.82	19.88
4 – 5	106.38	85.57	19.56	162.71	130.26	19.95	221.51	176.50	20.32
5 – 6	103.72	83.16	19.82	158.70	126.54	20.27	216.11	171.44	20.67
6 – 7	48.64	43.66	10.24	74.35	66.56	10.47	101.13	89.74	11.27
7 – 8	39.58	36.26	8.39	60.56	54.00	10.82	82.47	73.17	11.27
8 – 9	30.49	29.74	2.47	46.72	42.08	9.92	63.71	57.66	9.50
9 – 10	27.93	27.88	0.21	42.81	38.62	9.79	58.40	53.16	8.97
10 – 11	**25.37**	**26.13**	**-3.01**	38.89	35.24	9.38	53.07	48.81	8.02
11 – 12	**23.18**	**25.25**	**-8.96**	35.54	33.04	7.03	48.51	46.12	4.93
12 – 13	20.35	20.09	1.27	31.21	30.69	1.67	42.62	41.62	2.35
13 – 14	17.51	17.29	1.27	26.86	26.42	1.67	36.69	35.83	2.35
14 – 15	11.72	11.57	1.27	17.99	17.69	1.68	24.58	24.00	2.36
15 – 16	9.26	9.14	1.28	14.21	13.97	1.68	19.42	18.96	2.36
16 – 17	6.66	6.57	1.28	10.22	10.05	1.68	13.97	13.64	2.37
17 – 18	4.06	4.01	1.28	6.23	6.13	1.68	8.52	8.32	2.37
2 – 19	16.27	16.06	1.28	25.00	24.58	1.68	34.21	33.40	2.37
19 – 20	11.71	11.71	0.03	17.61	17.60	0.05	23.52	23.51	0.06
20 – 21	7.81	7.81	0.03	11.74	11.73	0.05	15.69	15.68	0.06
21 – 22	3.91	3.90	0.03	5.87	5.87	0.05	7.85	7.84	0.06
3 – 23	41.20	37.49	9.02	62.11	56.45	9.12	83.24	74.67	10.29
23 – 24	37.27	34.44	7.59	56.33	51.94	7.78	75.68	67.97	10.20
24 – 25	18.65	18.58	0.40	28.20	28.03	0.60	37.91	37.65	0.69
6 – 26	53.73	37.06	31.03	81.83	56.09	31.45	110.89	75.71	31.73

Branch (p–q)	Light (50%) load			Medium (75%) load			Full (100%) load		
	Current flow $\|I_{p-q}\|$ (Amps)		Change in current flow (%)	Current flow $\|I_{p-q}\|$ (Amps)		Change in current flow (%)	Current flow $\|I_{p-q}\|$ (Amps)		Change in current flow (%)
	Uncompensated	Optimally compensated		Uncompensated	Optimally compensated		Uncompensated	Optimally compensated	
26 – 27	51.83	34.82	32.81	79.38	53.09	33.12	108.23	71.66	33.79
27 – 28	49.44	32.39	34.48	75.75	49.60	34.52	103.30	66.68	35.45
29 – 30	41.90	25.37	39.45	64.22	39.90	37.88	87.61	52.25	40.36
30 – 31	19.31	19.04	1.41	29.62	28.96	2.24	40.44	39.27	2.91
31 – 32	12.51	12.34	1.41	19.19	18.76	2.24	26.20	25.44	2.91
32 – 33	2.97	2.93	1.41	4.55	4.45	2.25	6.21	6.03	2.91

It can be noted from Table 4.31 that the installation of shunt capacitors under light load results in the reduction of currents flowing in branches (1 – 2), (2 – 3), (3 – 4), (4 – 5), (5 – 6), (6 – 7), (7 – 8), (8 – 9), (9 – 10), (12 – 13), (13 – 14), (14 – 15), (15 – 16), (16 – 17), (17 – 18), (2 – 19), (19 – 20), (20 – 21), (21 – 22), (3 – 23), (23 – 24), (24 – 25), (6 – 26), (26 – 27), (27 – 28), (28 – 29), (29 – 30), (30 – 31), (31 – 32) and (32 – 33). On the other hand, the current in branches (10 – 11) and (11 – 12) increased by 3.01 and 8.96% respectively. Further, it can be noted that the total current flowing before the installation of shunt capacitors under light load was about 177.03 A. The installation of shunt capacitors reduced this current by about 15.53% to 149.54 A.

Table 4.31 also shows that the installation of shunt capacitors under medium and full load conditions results in the reduction of currents flowing in all the branches of the IEEE 33-bus radial system. Table 4.31 shows that the total current flowing before the installation of shunt capacitors under medium load was about 269.26 A and the installation of shunt capacitors reduced this current by about 15.75 % to 226.85 A. On the other hand, it can also be noted from Table 4.31 that the total current flowing before the installation of shunt capacitors under full load was about 364.36 A and the installation of shunt capacitors reduced the current by about 15.61% to 307.47 A.

Table 4.32 gives the branch power losses of the IEEE 33-bus radial distribution system for the uncompensated (base) case and the overall optimally compensated case at light, medium and full load conditions.

Table 4.32: IEEE 33-bus system power losses for the uncompensated case and optimally compensated case under light, medium and full load conditions

Branch ($p-q$)	Light (50%) load						Medium (75%) load						Full (100 %) load					
	Power Losses				Change in power losses (%)		Power Losses				Change in power losses (%)		Power Losses				Change in power losses (%)	
	Uncompensated		Optimally compensated				Uncompensated		Optimally compensated				Uncompensated		Optimally compensated			
	P (kW)	Q (kVAr)	P (kW)	Q (kVAr)	ΔP_{loss}	ΔQ_{loss}	P (kW)	Q (kVAr)	P (kW)	Q (kVAr)	ΔP_{loss}	ΔQ_{loss}	P (kW)	Q (kVAr)	P (kW)	Q (kVAr)	ΔP_{loss}	ΔQ_{loss}
1 – 2	2.8895	1.4730	2.0618	1.0510	28.64	28.64	6.6846	3.4076	4.7448	2.4187	29.02	29.02	12.240	6.2397	8.7165	4.4433	28.79	28.79
2 – 3	12.147	6.1868	8.4644	4.3112	30.32	30.32	28.1897	14.3579	19.457	9.9101	30.98	30.98	51.792	26.379	35.674	18.170	31.12	31.12
3 – 4	4.6027	2.3441	2.9947	1.5252	34.94	34.94	10.7537	5.4767	6.9543	3.5418	35.33	35.33	19.901	10.135	12.774	6.5058	35.81	35.81
4 – 5	4.3128	2.1966	2.7904	1.4212	35.30	35.30	10.0900	5.1390	6.4661	3.2933	35.92	35.92	18.699	9.5237	11.872	6.0467	36.51	36.51
5 – 6	8.8112	7.6063	5.6641	4.8895	35.72	35.72	20.6262	17.8056	13.113	11.320	36.43	36.43	38.249	33.018	24.073	20.781	37.06	37.06
6 – 7	0.4429	1.4642	0.3569	1.1796	19.43	19.43	1.0347	3.4204	0.8294	2.7416	19.85	19.85	1.9145	6.3286	1.5074	4.9828	21.26	21.26
7 – 8	1.1144	0.3683	0.9353	0.3091	16.07	16.07	2.6088	0.8621	2.0746	0.6856	20.48	20.48	4.8380	1.5988	3.8087	1.2587	21.28	21.28
8 – 9	0.9578	0.6881	0.9110	0.6545	4.88	4.88	2.2480	1.6151	1.8240	1.3104	18.86	18.86	4.1806	3.0035	3.4241	2.4600	18.10	18.10
9 – 10	0.8146	0.5774	0.8112	0.5750	0.41	0.41	1.9133	1.3562	1.5571	1.1037	18.61	18.61	3.5610	2.5241	2.9505	2.0914	17.14	17.14
10 – 11	**0.1265**	**0.0418**	**0.1342**	**0.0444**	**-6.10**	**-6.10**	0.2973	0.0983	0.2442	0.0807	17.87	17.87	0.5537	0.1831	0.4684	0.1549	15.40	15.40
11 – 12	**0.2011**	**0.0697**	**0.2388**	**0.0828**	**-18.73**	**-18.73**	0.4729	0.1639	0.4087	0.1417	13.57	13.57	0.8812	0.3055	0.7965	0.2761	9.61	9.61
12 – 13	0.6077	0.4781	0.5923	0.4660	2.53	2.53	1.4298	1.1250	1.3825	1.0877	3.31	3.31	2.6663	2.0978	2.5425	2.0004	4.64	4.64
13 – 14	0.1661	0.2186	0.1619	0.2131	2.53	2.53	0.3909	0.5145	0.3779	0.4974	3.32	3.32	0.7292	0.9598	0.6953	0.9152	4.65	4.65
14 – 15	0.0812	0.0723	0.0791	0.0704	2.53	2.53	0.1912	0.1702	0.1849	0.1645	3.32	3.32	0.3570	0.3177	0.3403	0.3029	4.66	4.66
15 – 16	0.0640	0.0467	0.0623	0.0455	2.53	2.53	0.1507	0.1101	0.1457	0.1064	3.33	3.33	0.2815	0.2056	0.2683	0.1960	4.67	4.67
16 – 17	0.0571	0.0763	0.0557	0.0743	2.54	2.54	0.1347	0.1798	0.1302	0.1738	3.33	3.33	0.2516	0.3360	0.2399	0.3203	4.68	4.68
17 – 18	0.0121	0.0095	0.0118	0.0092	2.54	2.54	0.0284	0.0223	0.0275	0.0216	3.33	3.33	0.0531	0.0417	0.0507	0.0397	4.68	4.68
2 – 19	0.0400	0.0381	0.0399	0.0381	0.06	0.06	0.0902	0.0861	0.0901	0.0860	0.09	0.09	0.1610	0.1536	0.1608	0.1534	0.12	0.12
19 – 20	0.2064	0.1860	0.2063	0.1859	0.06	0.06	0.4662	0.4201	0.4658	0.4197	0.09	0.09	0.8322	0.7499	0.8312	0.7490	0.12	0.12
20 – 21	0.0250	0.0292	0.0250	0.0292	0.06	0.06	0.0564	0.0659	0.0564	0.0659	0.09	0.09	0.1008	0.1177	0.1006	0.1176	0.12	0.12
21 – 22	0.0108	0.0143	0.0108	0.0143	0.06	0.06	0.0244	0.0323	0.0244	0.0323	0.09	0.09	0.0436	0.0577	0.0436	0.0576	0.12	0.12
3 – 23	0.7723	0.5277	0.6371	0.4353	17.50	17.50	1.7630	1.2047	1.4488	0.9900	17.82	17.82	3.1816	2.1740	2.5443	1.7385	20.03	20.03
23 – 24	1.2475	0.9851	1.0654	0.8413	14.60	14.60	2.8490	2.2497	2.4228	1.9131	14.96	14.96	5.1437	4.0617	4.1483	3.2757	19.35	19.35
24 – 25	0.3117	0.2439	0.3092	0.2419	0.80	0.80	0.7125	0.5575	0.7039	0.5508	1.20	1.20	1.2875	1.0074	1.2699	0.9936	1.37	1.37
6 – 26	0.5972	0.3042	0.2821	0.1437	52.76	52.76	1.4002	0.7132	0.6514	0.3318	53.48	53.48	2.6009	1.3248	1.1938	0.6081	54.10	54.10
26 – 27	0.7635	0.3887	0.3447	0.1755	54.85	54.85	1.7910	0.9119	0.8011	0.4079	55.27	55.27	3.3290	1.6950	1.4595	0.7431	56.16	56.16
27 – 28	2.5885	2.2823	1.1111	0.9796	57.08	57.08	6.0761	5.3572	2.6050	2.2968	57.13	57.13	11.300	9.9638	4.7081	4.1511	58.34	58.34

Branch ($p-q$)	Light (50%) load						Medium (75%) load						Full (100 %) load					
	Power Losses				Change in power losses (%)		Power Losses				Change in power losses (%)		Power Losses				Change in power losses (%)	
	Uncompensated		Optimally compensated				Uncompensated		Optimally compensated				Uncompensated		Optimally compensated			
	P (kW)	Q (kVAr)	P (kW)	Q (kVAr)	ΔP_{loss}	ΔQ_{loss}	P (kW)	Q (kVAr)	P (kW)	Q (kVAr)	ΔP_{loss}	ΔQ_{loss}	P (kW)	Q (kVAr)	P (kW)	Q (kVAr)	ΔP_{loss}	ΔQ_{loss}
28 – 29	1.7932	1.5622	0.7228	0.6297	59.69	59.69	4.2104	3.6680	1.7110	1.4906	59.36	59.36	7.8334	6.8242	3.0640	2.6693	60.88	60.88
29 – 30	0.8912	0.4539	0.3268	0.1664	63.33	63.33	2.0931	1.0662	0.8078	0.4114	61.41	61.41	3.8957	1.9843	1.3856	0.7058	64.43	64.43
30 – 31	0.3635	0.3592	0.3533	0.3492	2.80	2.80	0.8550	0.8449	0.8170	0.8075	4.44	4.44	1.5936	1.5750	1.5023	1.4847	5.73	5.73
31 – 32	0.0486	0.0567	0.0472	0.0551	2.80	2.80	0.1143	0.1333	0.1093	0.1274	4.44	4.44	0.2132	0.2485	0.2010	0.2342	5.73	5.73
32 – 33	0.0030	0.0047	0.0029	0.0045	2.80	2.80	0.0071	0.0110	0.0067	0.0105	4.44	4.44	0.0132	0.0205	0.0124	0.0193	5.74	5.74
Total losses	47.07	31.35	31.81	21.21	32.42	32.35	109.75	73.15	72.64	48.54	33.81	33.64	202.68	135.16	132.83	88.65	34.46	34.41

It can be noted from Table 4.32 that the installation of shunt capacitors under light load results in the reduction of real and reactive power losses in branches (1 – 2), (2 – 3), (3 – 4), (4 – 5), (5 – 6), (6 – 7), (7 – 8), (8 – 9), (9 – 10), (12 – 13), (13 – 14), (14 – 15), (15 – 16), (16 – 17), (17 – 18), (2 – 19), (19 – 20), (20 – 21), (21 – 22), (3 – 23), (23 – 24), (24 – 25), (6 – 26), (26 – 27), (27 – 28), (28 – 29), (29 – 30), (30 – 31), (31 – 32) and (32 – 33). The power losses in these branches reduced because of the corresponding reduction in branch currents. However, the power losses in branches (10 – 11) and (11 – 12) increased due to a corresponding increase in current flow.

Additionally, Table 4.32 shows that the installation of shunt capacitors under medium and full load conditions results in the reduction of both real and reactive power losses in all the branches of the IEEE 33-bus radial distribution system. The branch power losses reduced because of the corresponding reduction in branch currents. Lastly, it may also be noted from Table 4.32 that the percentage changes in the branches' real and reactive power losses are the same. This is so because when calculating both real and reactive power losses, the square of branch current (i.e. $I2$) is a common variable while R and X are constants.

Figure 2 in Appendix III give graphical illustrations of the branches real and reactive power losses (as tabulated in Table 4.32) before and after the installation of shunt capacitors while operating at light, medium and full load conditions.

It can be noted from Tables 4.31, 4.32 and Figure 2 (a), (c) and (e) in Appendix III that despite not having the highest flow of current for both the uncompensated and the optimally compensated cases, the real power losses in branch (2 – 3) are the highest. The real power losses in branch (2 – 3) are higher than those in branch (1 – 2) because, as shown in Table 3.4, branch (2 – 3) has the highest resistance than branch (1 – 2). On the other hand, the real power losses in branch (2 – 3) are higher than those in branches (3 – 4), (4 – 5), (6 – 7), (10 – 11), (11 – 12), (2 – 19), (20 – 21), (3 – 23), (6 – 26), (26 – 27), (31 – 32) and (32 – 33) because branch (2 – 3) has both higher resistance and current flow than the twelve branches. Lastly, the real power losses in branch (2 – 3) are higher than those in branches (5 – 6), (7 – 8), (8 –

9), (9 – 10), (12 – 13), (13 – 14), (14 – 15), (15 – 16), (16 – 17), (17 – 18), (19 – 20), (21 – 22), (23 – 24), (24 – 25), (27 – 28), (28 – 29), (29 – 30) and (30 – 31) because branch (2 – 3) is upstream and thus, the current flowing through this branch is higher than that in the downstream branches.

Similarly, it can be noted from Tables 4.31, 4.32 and Figure 2 (b), (d). and (f) in Appendix III that despite not having the highest flow of current for both the uncompensated and the optimally compensated cases, the reactive power losses in branch (5 – 6) are the highest. The reactive power losses in branch (5 – 6) are higher than those in branches (1 – 2), (2 – 3), (3 – 4) and (4 – 5) because, as shown in Table 3.4, this branch has the highest reactance as compared to the other four upstream branches. On the other hand, the reactive power losses in branch (5 – 6) are higher than those in branches (6 – 7), (7 – 8), (10 – 11), (11 – 12), (14 – 15), (15 – 16), (17 – 18), (2 – 19), (20 – 21), (3 – 23), (24 – 25), (6 – 26), (26 – 27), (28 – 29), (29 – 30), (31 – 32) and (32 – 33) because branch (5 – 6) has both higher reactance and current flow than the seventeen branches. Lastly, the reactive power losses in branch (5 – 6) are higher than those in branches (8 – 9), (9 – 10), (12 – 13), (13 – 14), (16 – 17), (19 – 20), (21 – 22), (23 – 24), (27 – 28) and (30 – 31) because branch (5 – 6) is upstream and thus, the current flowing through this branch is higher than that in the downstream branches.

4.4. Comparison of the Developed approach against Other Approaches

This section compares the performance of the developed optimal shunt capacitors' placement and sizing approach against other results available in literature that were obtained using ABC, CrSA, CSA, DE, DFO, GA, GSA, GWO, ICrSA, MCA, MFO and PSO. Tests were carried out on the same test systems that have been used in the preceding sections.

4.4.1. IEEE 10-Bus Radial Distribution System

Table 4.33 gives results of the total cost, power losses and voltage magnitudes that were obtained using the developed approach when optimally sized shunt capacitors were to be installed at four buses of the IEEE 10-bus radial distribution system. The results are then compared with those obtained using DE, ABC and, the exhaustive

search and MVO based approach. For the compensated case, the dashes are given because the respective studies did not report on values of the indicated parameters.

It can be noted from Table 4.33 that the developed approach and the exhaustive search and MVO based approach attained the same overall cost, total power losses and voltage magnitudes. The results for the overall cost and total power losses are better than the ones found by optimal shunt capacitor placement and sizing approaches based on DE (Diaz et al., 2018) and ABC (Diaz et al., 2018) optimization algorithms.

For the approaches based on DE and ABC, the search space was firstly reduced using LSF as is discussed under Section 2.4. Since after calculating the LSF only 6 buses (i.e. buses 5, 6, 7, 8, 9 and 10) qualify as candidates for the installation of shunt capacitors, therefore, for capacitor placement at four buses, the search space is given as a (15×4) vector.

It can also be noted from the best results given in Table 4.33 that buses 3, 5, 7 and 10 give the global optimum bus combination when shunt capacitors are to be installed at four buses. However, when LSF are used, bus number 3 is discarded because its normalized voltage level is greater than 1.01. Consequently, this results in having DE and ABC attaining sub-optimal results. On the other hand, under the exhaustive search and MVO based approach, a search for the global optimum bus combination was carried out in an unreduced search space where the 9 buses (i.e. buses 2 to 10) of the IEEE 10-bus test system were considered candidates for the installation of shunt capacitors. Hence, for the installation of shunt capacitors at four buses, the search space is given as a (126×4) vector. However, when the developed approach was used, the search was carried out in a reduced search space made up of a (56×4) vector.

It can further be noted from Table 4.33 that because in the developed approach the search for the global optimum bus combination was carried out in a reduced search space (i.e. a search space with a size of (56×4) instead of the original size of (126×4)), the developed approach attained the best overall cost and total real power losses with a relatively shorter average computation time than that which was taken

Table 4.33: Comparison of costs, power losses, voltage magnitudes and search space dimensions for the IEEE 10-bus radial distribution system for compensation of four buses

Parameters	Uncompensated	Compensated					
		Differential Evolution (DE) (Diaz et al., 2018)		Artificial Bee Colony (ABC) Algorithm (Diaz et al., 2018)		Exhaustive Search and Multi-Verse Optimizer	Developed Approach
Year of publication		2018		2018		**2023**	**2023**
Total cost/year ($)	131,676.72	118,793.97		118,329.19		**116,025.51**	**116,025.51**
Net savings/year ($)	-	12,882.75		13,347.53		**15,651.21**	**15,651.21**
Cost reduction/year (%)	-	9.78		10.14		**11.89**	**11.89**
Real power losses (kW)	783.79	700.24		697.18		**680.67**	**680.67**
Real power losses reduction (%)	-	10.66		11.05		**13.16**	**13.16**
Reactive power loss (kVAr)	1036.66	-		-		**924.34**	**924.34**
Reactive power losses reduction (%)	-	-		-		**10.83**	**10.83**
Optimal buses and capacitor sizes in kVAr	-	5	4050	5	4050	**3 4050**	**3 4050**
		6	900	6	1200	**5 3600**	**5 3600**
		9	600	8	600	**7 1200**	**7 1200**
		10	600	10	600	**10 600**	**10 600**
Total kVAr	-	6150		6450		**9450**	**9450**
V_{min} (p.u.)	0.8375	0.9005		0.9001		**0.9000**	**0.9000**
V_{max} (p.u.)	1.0000	1.0000		1.0000		**1.0059**	**1.0059**
Search space dimension	-	(15×4)		(15×4)		**(126×4)**	**(56×4)**
Average computation time (s)	-	-		-		**2,494.56**	**1,082.77**
Decrease in average computation time (%)	-	-		-		**-**	**56.59**

by the exhaustive search and MVO based approach. Application of the developed approach reduced the average computation time that was taken when the exhaustive search and MVO based approach was used by 56.59 % from 2,494.56 to 1,082.77 seconds.

Table 4.34 gives results of the total cost, power losses and voltage magnitudes that were obtained using the developed approach when optimally sized shunt capacitors were to be installed at five buses of the IEEE 10-bus radial distribution system. The results are then compared with those obtained using GSA, ICrSA, PSO and, the exhaustive search and MVO based approach. For the compensated case, the dashes are given because the respective studies did not report on values of the indicated parameters.

It can be noted from Table 4.34 that the developed approach and the exhaustive search and MVO based approach attained the same overall cost, total power losses and voltage magnitudes. The results for the overall cost and total power losses are better than the ones found by optimal shunt capacitor placement and sizing approaches based on GSA (Diaz et al., 2018), ICrSA (Diaz et al., 2018), and PSO (Askarzadeh, 2016).

For the approaches based on GSA and ICrSA, the search space was firstly reduced using LSF as is discussed under Section 2.4. Since after calculating the LSF only 6 buses (i.e. buses 5, 6, 7, 8, 9 and 10) qualify as candidates for the installation of shunt capacitors, therefore, for capacitor placement at five buses, the search space is given as a (6×5) vector. It can also be noted from the best results given in Table 4.34 that buses 3, 4, 5, 6 and 10 give the global optimum bus combination when shunt capacitors are to be installed at five buses. However, when LSF are used, buses 3 and 4 are discarded because their respective normalized voltage levels are greater than 1.01. Consequently, this results in having GSA and ICrSA attaining sub-optimal results. For the PSO based approach, its failure to attain the global optimum results may be attributed to parameter settings as well as the algorithm's limited exploration and exploitation capabilities. Under the PSO based approach, and the exhaustive search and MVO based approach, a search for the global optimum buses was carried

Table 4.34: Comparison of costs, power losses, voltage magnitudes and search space dimensions for the IEEE 10-bus radial distribution system for compensation of five buses

Parameters	Uncompensated	Compensated									
		Gravitational Search Algorithm (GSA) (Diaz et al., 2018)		**Improved Crow Search Algorithm (ICrSA) (Diaz et al., 2018)**		**Particle Swarm Optimization (PSO) (Askarzadeh, 2016)**		**Exhaustive Search and Multi-Verse Optimizer**		**Developed Approach**	
Year of publication		2018		2018		2016		**2023**		**2023**	
Total cost/year ($)	131,676.72	118,798.11		118,245.48		115,593.40		**115,537.56**		**115,537.56**	
Net savings/year ($)	-	12,878.61		13,431.24		16,083.32		**16,139.16**		**16,139.16**	
Cost reduction/year (%)	-	9.78		10.20		12.21		**12.26**		**12.26**	
Real power losses (kW)	783.79	699.67		696.76		677.02		**676.87**		**676.87**	
Real power losses reduction (%)	-	10.73		11.10		13.62		**13.64**		**13.64**	
Reactive power loss (kVAr)	1036.66	-		-		-		**936.54**		**936.54**	
Reactive power losses reduction (%)	-	-		-		-		**9.66**		**9.66**	
Optimal buses and capacitor sizes in kVAr	-	5	3150	5	3900	2	4050	**3**	**3900**	**3**	**3900**
		6	1650	6	1200	3	1800	**4**	**2400**	**4**	**2400**
		7	150	8	450	4	2100	**5**	**2100**	**5**	**2100**
		9	600	9	150	5	1500	**6**	**1200**	**6**	**1200**
		10	450	10	600	10	600	**10**	**600**	**10**	**600**
Total kVAr	-	6000		6300		10050		**10200**		**10200**	
V_{min} (p.u.)	0.8375	0.9002		0.9000		0.9004		**0.9001**		**0.9001**	
V_{max} (p.u.)	1.0000	1.0000		1.0000		1.0009		**1.0073**		**1.0073**	
Search space dimension	-	(6×5)		(6×5)		(126×5)		**(126×5)**		**(70×5)**	
Approximate computation time (s)	-	-		-		-		**2,543.01**		**1,471.91**	
Decrease in average computation time (%)	-	-		-		-		**-**		**42.12**	

out in an unreduced search space where the 9 buses (i.e. buses 2 to 10) of the IEEE 10-bus test system were considered candidates for the installation of shunt capacitors. Hence, for the installation of shunt capacitors at five buses, the search space is given as a (126×5) vector. However, when the developed approach was used, the search was carried out in a reduced search space made up of a (70×5) vector.

It can also be noted from Table 4.34 that because in the developed approach the search for the global optimum bus combination was carried out in a reduced search space (i.e. a search space with a size of (70×5) instead of the original size of (126×5)), the developed approach attained the best overall cost and total real power losses with a relatively shorter average computation time than that which was taken by the exhaustive search and MVO based approach. Application of the developed approach reduced the average computation time that was taken when the exhaustive search and MVO based approach was used by 42.12 % from 2,543.01 to 1,471.91 seconds.

Table 4.35 gives results of the total cost, power losses and voltage magnitudes that were obtained using the developed approach when optimally sized shunt capacitors were to be installed at six buses of the IEEE 10-bus radial distribution system. The results are then compared with those obtained using GA, MCA, CrSA, ICrSA and, the exhaustive search and MVO based approach. For the compensated case, the dashes are given because the respective studies did not report on values of the indicated parameters.

It can be noted from Table 4.35 that the developed approach and the exhaustive search and MVO based approach attained the same overall cost, total power losses and voltage magnitudes. The results for the overall cost and total power losses are better than the ones found by optimal shunt capacitor placement and sizing approaches based on GA (Askarzadeh, 2016), MCA (Haldar & Chakravorty, 2015), CrSA (Askarzadeh, 2016), and ICrSA (Diaz et al., 2018).

For the GA, MCA, CrSA, ICrSA and exhaustive search and MVO based approaches, the search for the optimal bus combination was carried out in an unreduced search space where the 9 buses (i.e. buses 2 to 10) of the IEEE 10- bus test system were

Table 4.35: Comparison of costs, power losses, voltage magnitudes and search space dimensions for the IEEE 10-bus radial distribution system for compensation of six buses

Parameters	**Uncompensated**	**Compensated**					
		Genetic Algorithm (GA) (Askarzadeh, 2016)	**Modified Cultural Algorithm (MCA) (Haldar & Chakravorty, 2015)**	**Crow Search Algorithm (CrSA) (Askarzadeh, 2016)**	**Improved Crow Search Algorithm (ICrSA) (Diaz et al., 2018)**	**Exhaustive Search and MVO**	**Developed Approach**
Year of publication		2015	2013	2016	2018	**2023**	**2023**
Total cost/year ($)	131,676.72	115,819.90	115,756.27	115,521.11	115,414.14	**115,404.12**	**115,404.12**
Net savings/year ($)	-	15,856.74	15,920.37	16,155.53	16,262.58	**16,272.52**	**16,272.52**
Cost reduction/year (%)	-	12.04	12.09	12.27	12.35	**12.36**	**12.36**
Real power losses (kW)	783.79	683.33	677.54	676.22	675.78	**675.70**	**675.70**
Real power losses reduction (%)	-	12.82	13.56	13.72	13.78	**13.79**	**13.79**
Reactive power loss (kVAr)	1036.66	-	-	-	-	**935.12**	**935.12**
Reactive power losses reduction (%)	-	-	-	-	-	**9.79**	**9.79**
Optimal buses and capacitor sizes in kVAr	-	2 1050 3 3450 4 600 5 3000 6 1650 9 750	3 3300 4 2850 5 1950 6 1200 8 300 10 450	3 4050 4 2100 5 1950 6 900 7 450 10 600	3 4050 4 2400 5 1650 6 1200 8 450 10 450	**3 4050 4 2100 5 2100 6 1200 9 450 10 300**	**3 4050 4 2100 5 2100 6 1200 9 450 10 300**
Total kVAr	-	10500	10050	10050	10200	**10200**	**10200**
V_{min} (p.u.)	0.8375	0.9003	0.9003	0.9003	0.9000	**0.9000**	**0.9000**
V_{max} (p.u.)	1.0000	1.0007	1.0070	1.0007	1.0070	**1.0073**	**1.0073**
Search space dimension	-	(84×6)	(84×6)	(84×6)	(84×6)	**(84×6)**	**(56×6)**
Average computation time (s)	-	-	-	-	-	**1,688.14**	**1,178.83**
Decrease in average computation time (%)	-	-	-	-	-	-	**30.17**

considered candidates for the installation of shunt capacitors. Hence, for the installation of shunt capacitors at six buses, the search space is given as an (84×6) vector.

It can further be noted from the best results given in Table 4.35 that buses 3, 4, 5, 6, 9 and 10 gives the global optimum bus combination when shunt capacitors are to be installed at six buses. As it is shown in Table 4.35, the GA, MCA, CrSA and ICrSA based approaches fail to identify the global optimum bus combination and as a consequence they return sub-optimal results. The failure of the GA, MCA, CrSA and ICrSA based approaches to attain the global optimum results may be attributed to parameter settings as well as the respective algorithms' limited exploration and exploitation capabilities.

It can also be noted from Table 4.35 that because in the developed approach the search for the global optimum bus combination was carried out in a reduced search space (i.e. a search space with a size of (56×6) instead of the original size of (84×6)), the developed approach attained the best overall cost and total real power losses with a relatively shorter average computation time than that which was taken by the exhaustive search and MVO based approach. Application of the developed approach reduced the average computation time that was taken when the exhaustive search and MVO based approach was used by 30.17 % from 1,688.14 to 1,178.83 seconds.

4.4.2. IEEE 33-Bus Radial Distribution System

Table 4.36 gives results of the total cost, power losses and voltage magnitudes that were obtained using the developed approach when optimally sized shunt capacitors were to be installed at three buses of the IEEE 33-bus radial distribution system. The results are then compared with those obtained using MFO, GWO, PSO, CSA and, the exhaustive search and MVO based approach. For the compensated case, the dashes are given because the respective studies did not report on values of the indicated parameters. .

Table 4.36: Comparison of costs, power losses, voltage magnitudes and search space dimensions for the compensation of three buses of the IEEE 33-bus radial distribution system for compensation of three buses

Parameters	**Uncompensated**	**Compensated**						
		Moth-Flame Optimizer (MFO) (Diab & Rezk, 2018)	**Grey Wolf Optimizer (GWO) (Diab & Rezk, 2018)**	**Dragon-Fly Optimizer (DFO) (Diab & Rezk, 2018)**	**Particle Swarm Optimizer (PSO) (Idris & Zaid, 2016)**	**Cuckoo Search Algorithm (CSA) (Idris & Zaid, 2016)**	**Exhaustive Search and MVO**	**Developed Approach**
Year of publication		2018	2018	2018	2016	2016	**2023**	**2023**
Total cost/year ($)	34,049.95	22,908.00	22,908.00	22,908.00	22,805.23	22,787.00	**22,700.79**	**22,700.79**
Net savings/year ($)	-	11,141.95	11,141.95	11,141.95	11,262.95	11,262.95	**11,349.16**	**11,349.16**
Cost reduction/year ($)	-	32.72	32.72	32.72	33.02	33.08	**33.33**	**33.33**
Real power losses (kW)	202.68	134.07	134.07	134.07	133.12	133.09	**132.68**	**132.68**
Real power losses reduction (%)	-	33.85	33.85	33.85	34.32	34.34	**34.54**	**34.54**
Reactive power losses (kVAr)	135.16	-	-	-	-	-	**88.63**	**88.63**
Reactive power losses reduction (%)	-	-	-	-	-	-	**34.43**	**34.43**
Optimal buses and capacitor sizes in kVAr	-	8 450 13 300 30 900	8 450 13 300 30 900	8 450 13 300 30 900	14 300 24 600 30 1200	10 600 24 600 30 900	**12 450** **24 600** **30 900**	**12 450** **24 600** **30 900**
Total kVAr	-	1650	1650	1650	2100	2100	**1950**	**1950**
V_{min} (p.u.)	0.9131	0.9400	0.9400	0.9400		-	**0.9355**	**0.9355**
V_{max} (p.u.)	1.0000	-	-	-		-	**1.0000**	**1.0000**
Search space dimension	-	(56×3)	(56×3)	(56×3)	(4960×3)	(4960×3)	**(4960×3)**	**(465×3)**
Average computation time (s)	-	-	-	-	-	-	**195,264.68**	**17,667.35**
Decrease in average computation time (%)	-	-	-	-	-	-	-	**90.95**

It can be noted from Table 4.36 that the developed approach and the exhaustive search and MVO based approach attained the same overall cost, total power losses and voltage magnitudes. The results for the overall cost and power losses are better than the ones that were found by optimal shunt capacitor placement and sizing approaches based on MFO, GWO, DFO (Diab & Rezk, 2018), PSO algorithm (Idris & Zaid, 2016) and CSA (Idris & Zaid, 2016).

For the approaches based on MFO, GWO and DFO, the search space was firstly reduced using LSF as is discussed under Section 2.4. After calculating the LSF, only the top 8 buses (i.e. buses 6, 28, 29, 30, 9, 13, 10 and 8) were selected from the list of buses that qualify as candidates for the installation of shunt capacitors. Hence, for capacitor placement at three buses, the search space is given as a (56×3) vector.

It can also be noted from the best results given in Table 4.36 that buses 12, 24 and 30 give the global optimum bus combination when shunt capacitors are to be installed at three buses. However, when LSF are used, bus number 24 is discarded because its normalized voltage level is greater than 1.01. Furthermore, when only the top 8 buses are selected, bus number 12 is also discarded. Consequently, this resulted in having MFO, GWO and DFO based approaches attaining sub-optimal results. For the PSO and CSA based approaches, their failure to attain the global optimum results may be attributed to parameter settings as well as the respective algorithms' limited exploration and exploitation capabilities.

Under the PSO based approach, the CSA based approach and the exhaustive search and MVO based approach, a search for the global optimum buses was carried out in an unreduced search space where the 32 buses (i.e. buses 2 to 33) of the IEEE 33-bus test system were considered as candidates for the installation of shunt capacitors. Hence, for the installation of shunt capacitors at three buses, the search space is given as a vector whose dimension is (4960×3). However, when the developed approach was used, the search was carried out in a reduced search space with a dimension of (465×3).

It may also be noted from Table 4.36 that because in the developed approach the search for the optimum bus combination was carried out in a reduced search space

(i.e. a search space with a size of (465×5) instead of the original size of (4960×3)), the developed approach attained the best overall cost and total real power losses with a relatively shorter average computation time than that which was taken by the exhaustive search and MVO based approach. Application of the developed approach reduced the average computation time that was taken when the exhaustive search and MVO search-based approach was used by 90.95 % from 195,264.68 to 17,667.35 seconds.

Table 4.37 gives results of total costs, power losses and voltage magnitudes that were obtained using the developed approach when optimally sized shunt capacitors were to be installed at four buses of the IEEE 33-bus radial distribution system. The results are then compared with those obtained using PSO, CrSA and, the exhaustive search and MVO based approach. For the compensated case, the dashes are given because the respective studies did not report on values of the indicated parameters.

Table 4.37: Comparison of costs, power losses, voltage magnitudes and search space dimensions for the compensation of four buses of the IEEE 33-bus radial distribution system for compensation of four buses

Parameters	**Uncompensated**	**Compensated**							
		Particle Swarm Optimization (PSO) (Askarzadeh , 2016)		**Crow Search Algorithm (CrSA) (Askarzadeh , 2016)**		**Exhaustive Search and MVO**		**Developed Approach**	
Year of publication		2016		2016		**2023**		**2023**	
Total cost/year ($)	34,050.24	22,861.93		22,573.54		**22,460.04**		**22,460.04**	
Net savings/year ($)	-	11,188.31		11,476.70		**11,590.20**		**11,590.20**	
Cost reduction/year (%)	-	32.86		33.71		**34.04**		**34.04**	
Real power losses (kW)	202.68	132.4847		131.5359		**130.73**		**130.73**	
Real power losses reduction (%)	-	34.63		35.10		**35.50**		**35.50**	
Reactive power losses (kVAr)	135.16	-		-		**87.42**		**87.42**	
Reactive power losses reduction (%)	-	-		-		**35.32**		**35.32**	
Optimal buses and capacitor sizes in kVAr	-	2 7 15 29	900 450 300 450	11 24 30 33	600 450 600 300	**7** **14** **24** **30**	**450** **300** **450** **900**	**7** **14** **24** **30**	**450** **300** **450** **900**

Parameters	**Uncompensated**	**Compensated**			
		Particle Swarm Optimization (PSO) (Askarzadeh , 2016)	**Crow Search Algorithm (CrSA) (Askarzadeh , 2016)**	**Exhaustive Search and MVO**	**Developed Approach**
Total kVAr	-	2100	1950	**2100**	**2100**
V_{min} (p.u.)	0.9131	-	-	**0.9411**	**0.9411**
V_{max} (p.u.)	1.0000	-	-	**1.0000**	**1.0000**
Search space dimension	-	(35960×4)	(35960×4)	**(35960×4)**	**(4495×4)**
Average computation time (s)	-	-	-	**886,495.57**	**180,555.06**
Decrease in average computation time (%)	-	-	-	-	**79.63**

It can be noted from Table 4.37 that the developed approach and the exhaustive search and MVO based approach attained the same overall cost, total power losses and voltage magnitudes. The results for the overall cost and total power losses are better than the ones that were found by optimal shunt capacitor placement and sizing approaches that were based on PSO and CrSA (Askarzadeh, 2016).

For the PSO, CrSA and exhaustive search and MVO based approaches given in Table 4.37, the search for the optimal bus combination was carried out in an unreduced search space where the 32 buses (i.e. buses 2 to 33) of the IEEE 33-bus test system were considered candidates for the installation of shunt capacitors. Hence, for the installation of shunt capacitors at four buses, the search space is given as a (35960×4) vector.

It can further be noted from the best results given in Table 4.37 that buses 7, 14, 24 and 30 give the global optimum bus combination when shunt capacitors are to be installed at four buses. As it is shown in Table 4.37, the PSO and CrSA based approaches failed to identify the global optimum bus combination hence returning sub-optimal results. For the PSO and CrSA based approaches, their failure to attain the global optimum results may be attributed to parameter settings as well as the respective algorithms' limited exploration and exploitation capabilities.

It can also be noted from Table 4.37 that because in the developed approach the search for the optimum bus combination was carried out in a reduced search space (i.e. a search space with a size of (4495×4) instead of the original size of (35960×4)), the developed approach attained the best overall cost and total real power losses with a relatively shorter average computation time than that which was taken by the exhaustive search and MVO based approach. Application of the developed approach reduced the average computation time that was taken when the exhaustive search and MVO based approach was used by 79.63 % from 886,495.57 to 180,555.06 seconds.

CHAPTER FIVE

CONCLUSIONS AND RECOMMENDATIONS

5.1. Conclusions

In this thesis a new optimal shunt capacitors' placement and sizing algorithm for minimizing the overall cost of total real power losses, shunt capacitors' purchase, installation, and O&M in radial distribution systems has been developed, evaluated and validated. The developed approach is based on the MLSF, MVO and MATLAB matrix reduction methods i.e. MATLAB's *any* and *ismember* commands. In the developed approach, the MLSF and MATLAB's matrix reduction techniques have been used to reduce the search space of optimal buses that require the provision of reactive power through the installation of shunt capacitors. Thereafter, MVO was used to identify the optimal buses on which to install shunt capacitors as well as the corresponding optimum shunt capacitor sizes. The reduction in the search space of optimal buses also results in the consequential reduction in the computation time.

The performance of the developed approach was evaluated by using it to solve the optimal shunt capacitors placement and sizing problem in the IEEE 10- and 33-bus radial distribution systems. Simulations were carried out on the IEEE 10- and 33-bus radial distribution systems with shunt capacitors installed at 1 up to 9 and at 1 up to 4 buses respectively. Firstly, the simulations were carried out while assuming fixed system loading. For this case the two test systems were assumed to operate at full (100%) load. The simulation results for this case show that for the IEEE 10-bus radial distribution system, 5 is the overall optimum total number of buses to be compensated whereas for the IEEE 33-bus radial distribution system, 3 is the overall optimum total number of buses to be compensated, when the considered maximum total number of buses to be compensated is 4. Compensating a total of five buses of the IEEE 10-bus test system reduces the yearly overall cost of running the system from $131,676.72, without compensation, to $117,837.56. This represents a 10.51% reduction in the overall cost. On the other hand, compensating a total of three buses of the IEEE 33-bus test system reduces the yearly overall cost of running the system

from $34,050.24, without compensation, to $24,080.79. This represents a 29.28% reduction in the overall cost. Secondly, the simulations were carried out while assuming variable system loading. For this case the systems were assumed to operate at light (50%), medium (75%) and full (100%) load. Under variable load, the simulation results show that for the IEEE 10-bus radial distribution system, 4 is the overall optimum total number of buses to be compensated whereas for the IEEE 33-bus radial distribution system, 3 is the overall optimum total number of buses to be compensated, when the considered maximum total number of buses to be compensated is 4. Compensating a total of four buses of the IEEE 10-bus test system reduces the yearly overall cost of running the system from $219,891.66, without compensation, to $198,134.94. This represents a 9.89% reduction in the overall cost. On the other hand, compensating a total of three buses of the IEEE 33-bus test system reduces the yearly overall cost of running the system from $58,526.70, without compensation, to $40,469.48. This represents a 30.85% reduction in the yearly overall cost.

Further, to ensure that the developed approach was able to reduce the search space (of optimal buses that require the provision of reactive power through the installation of shunt capacitors) without any compromises in solutions accuracy, the results that were obtained using the developed approach were validated by comparing them with the ones that were obtained using the exhaustive search, and the exhaustive search and MVO based approaches. For the installation of shunt capacitors at a total of 2 up to 4 buses in the IEEE 10-bus test system, under both fixed and variable system loading, the developed approach attained the same results as the exhaustive search, and the exhaustive search and MVO based approaches. For the installation of shunt capacitors at a total of 5 up to 9 buses, the results obtained using the developed approach were in agreement with those obtained using the exhaustive search and MVO based approach – an approach against which the performance of the developed approach was compared.

In the IEEE 10-bus radial distribution system, the developed approach only failed to obtain the same results as the exhaustive search, and the exhaustive search and MVO based approach when shunt capacitors were to be installed at a single bus. This was

so because the lower voltage constraint was not satisfied. However, when the voltage constraint was relaxed the results obtained by the three approaches, i.e. the developed approach, the exhaustive search, and the exhaustive search and MVO based approach, were in agreement. On the other hand, for both cases of fixed and variable system loading in the IEEE 33-bus radial distribution system, the use of the developed approach yielded the same results as the exhaustive search, and the exhaustive search and MVO based approach when shunt capacitors were to be installed at a total of 1 up to 3 buses. For the installation of shunt capacitors at a total of 4 buses in the IEEE 33-bus radial distribution system, the results obtained using the developed algorithm were in agreement with those obtained using the exhaustive search and MVO based approach – an approach against which the performance of the developed approach was compared. Therefore, despite disregarding some bus combinations, the developed approach was still able to attain the global optimum results for different total number of buses to be compensated (except for the installation of capacitors at a single bus in the IEEE 10- bus radial distribution system). Additionally, since the search space was reduced, after disregarding some bus combinations, the developed approach attained the global optimum results within relatively shorter computation times than the exhaustive search, and the exhaustive search and MVO based approaches. For the IEEE 10-bus system, the decrease in the average computation time ranged between 80.25% and 12.00% for the compensation of two and eight buses, respectively. The corresponding decrement in computation time for the IEEE 33-bus system ranged between 97.14% and 79.63% for the compensation of one and four buses, respectively. The decrements in computation time were registered for both fixed and variable loading.

Finally, the results that were obtained using the developed approach were compared with the ones obtained using approaches based on ABC, CrSA, CSA, DE, DFO, GA, GSA, GWO, ICrSA, MCA, MFO and PSO algorithm. As indicated in Tables 4.33 up to 4.37, the comparison only considered the overall cost of total real power losses and shunt capacitors' purchase. The results presented in Tables 4.33 up to 4.37 also give the annual percentage net savings and real power losses reduction (%). Comparison of the results show that the performance of the developed approach is

better than other optimal shunt capacitors' placement and sizing algorithms that are based on ABC, CrSA, CSA, DE, DFO, GA, GSA, GWO, ICrSA, MCA, MFO and PSO algorithm. The developed algorithm attained the least overall cost of total real power losses and shunt capacitors' purchase than the other algorithms.

Based on the performance of the developed algorithm in relation to other available algorithms against which its performance has been compared, it can conclusively be stated that:

- By discarding buses with higher voltages and only installing shunt capacitors at buses with lower voltage levels (as is the case under the LSF approach), shunt capacitors' placement and sizing algorithms result in the attainment of sub-optimal results.
- It is possible to reduce the search space of potential candidate buses for shunt capacitors placement and still have the global optimum bus or bus combination in the reduced search space.
- The developed algorithm stands out as a potentially reliable tool for power system planners to adopt and use when solving the radial distribution systems' optimal shunt capacitors placement and sizing problem for either minimization of the overall cost of total real power losses and shunt capacitors' purchase or minimization of the overall cost of total real power losses, shunt capacitors' purchase, installation, and O&M. This is so because, unlike available optimal shunt capacitors' placement and sizing algorithms, the developed algorithm exactly matches the accuracy of the exhaustive search algorithm.

5.2. Recommendations for further studies

Firstly, this work employed an exhaustive approach when determining the optimum total number of buses to be compensated for the case of the IEEE 10-bus radial distribution system. However, due to the high number of buses within the IEEE 33-bus radial distribution system; for this system a check for the optimum total number of buses to be compensated was limited to four buses only. It is thus recommended that researchers consider developing efficient and accurate approaches for

determining the optimum total number of buses to be compensated within a given network.

Secondly, the optimal shunt capacitors' placement and sizing algorithm that has been presented in this thesis was specifically developed for radial distribution systems. However, there exists other network topologies apart from the radial one, e.g., ring main, interconnected, and parallel feeders' distribution systems, consequently, it is recommended that the developed approach be tried on the remaining topologies with necessary modifications being made to the algorithm.

Thirdly, in this study the branch power flows were not constrained. Therefore, it was permissible for the branch power flows in the optimally compensated system to be greater than the branch power flows in the uncompensated system. Consequently, this led to increased power losses in certain branches. As part of future works, researchers need to investigate the impact of the branch power flow constraint on cost optimality.

REFERENCES

Abdelaziz, A.Y., Ali, E.S. & Abd-Elazim, S.M. (2016a). Optimal sizing and locations of capacitors in radial distribution systems via Flower Pollination Optimization Algorithm and Power Loss Index. *International Journal of Engineering Science and Technology, 19(1),* 610-618.

Abdelaziz, A.Y., Ali, E.S. & Abd-Elazim, S.M. (2016b). Flower Pollination Algorithm and Loss Sensitivity Factors for optimal sizing and placement of capacitors in radial distribution systems. *International Journal of Electrical Power and Energy Systems, 78(2016),* 207-214.

Abdelaziz, A.Y., Ali, E.S. & Abd-Elazim, S.M. (2016c). Flower Pollination Algorithm for Optimal Capacitor Placement and Sizing in Distribution Systems. *Electric Power Components and Systems, 44(5),* 544-555.

Abou El-Ela, A.A., El - Sahiemy, R.A., Kinawy, A.M., & Mouwafi, M.T. (2016). Optimal capacitor placement in distribution systems for power loss reduction and voltage profile improvement. *IET Generation, Transmission & Distribution, 10(5),* 1209-1221.

Anilkumar, R., Devriese, G., & Srivastava, A.K. (2017). Voltage and reactive power control to maximize the energy savings in power distribution system with wind energy. *IEEE Transactions on* Industry *Applications, 54(1),* 656-664.

Arcanjo, D.N., Luiz, J., Pereira, R., Oliveira, E.J., Peres, W., Da Oliveira, L.W. & Da Silva, I.C. (2012). *Cuckoo Search Optimization technique applied to capacitor placement on distribution system problem.* Proceedings of the 2012 10th IEEE/IAS International Conference on Industry Applications (INDUSCON) (pp. 1-6). Fortaleza, Brazil.

Askarzadeh, A. (2016). Capacitor placement in distribution systems for power loss reduction and voltage improvement: A new methodology. *IET Generation, Transmission and* Distribution, *10(14),* 1-8.

Baghzouz, Y. (1991). Effects of nonlinear loads on optimal capacitor placement in radial feeders. *IEEE Transactions on Power Delivery, 6(1),* 245-251.

Bentouati, B., Chettih, S., Jangir, P., & Trivedi, I.N. (2016). A solution to the optimal power flow using Multi-Verse Optimizer. *Journal of Electrical Systems, 12(4),* 716-733.

Bigdeli, K., Hare, W. & Tesfamariam, S. (2012). Configuration optimization of dampers for adjacent buildings under seismic excitations. *Journal of Engineering Optimization*, 1-19.

Bilal, M., Shahzad, M., Arif, M., Barkat, U., Hisham, S.B., & Ali, S.S.A. (2021). Annual cost and loss minimization in a radial distribution network by capacitor allocation using PSO. *Applied Sciences, 11: 11840,* 1-18.

Bird, J. (2003). *Electric Circuit Theory and Technology* (2nd Ed.). Oxford, UK: Newnes Publication.

Chege, S.N., Murage, D.K. & Kihato, P.K. (2018). *Distribution Generation and capacitor placement in distribution systems.* Proceedings of the Sustainable Research and Innovation conference (pp. 63-69). Juja, Kenya.

Chopra, N., & Sharma, J. (2016). *Multi-objective optimum load dispatch using Multi-Verse Optimization*. Proceedings of the 2016 IEEE 1st International Conference on Power Electronics, Intelligent Control and Energy Systems (ICPEICES-2016) (pp. 1-5). Delhi, India.

Das, D. (2008). Optimal placement of capacitors in radial distribution system using a Fuzzy-GA method. *International Journal of Electrical Power and Energy Systems*, *30*(6-7), 361–367.

Devabalaji, K.R., Yuvaraj, T. & Ravi, K. (2018). An efficient method for solving the optimal sitting and sizing problem of capacitor banks based on Cuckoo Search Algorithm. *Ain* Shams *Engineering Journal, 9(4),* 589-597.

Diab, A.A.Z. & Rezk, H. (2018). Optimal sizing and placement of capacitors in radial distribution systems based on Grey Wolf, Dragonfly and Moth–Flame

optimization algorithms. *Iranian Journal of Science and Technology – Transactions of Electrical Engineering, 43(1).*

Diaz, P., Perez - Cisneros, M., Cuevas, E., Avalos, O., Galvez, J., Honojosa, S. & Zaldivar, D. (2018). An improved crow search algorithm applied to energy problems. *Energies, 11(3),* 571.

Dixit, M., Kundu, P. & Jariwala, H.R. (2016). *Optimal allocation and sizing of shunt Capacitor in distribution system for power loss minimization.* Proceedings of the 2016 IEEE Students' Conference on Electrical, Electronics and Computer Science (SCEECS) (pp. 1-6). Bhopal, India.

El – Fergany, A. A. & Abdelaziz, A. Y. (2014a). Capacitor allocation in radial distribution networks using Cuckoo Search Algorithm. *IET Generation, Transmission and Distribution, 8(2),* 223-232.

El – Fergany, A. A. & Abdelaziz, A.Y. (2014b). Artificial Bee Colony Algorithm to allocate fixed and switched static shunt capacitors in radial distribution networks. *Electric Power Components and Systems, 42(5),* 427-438.

Elsheikh, A., Helmy, Y., Abouelseoud, Y. & Elsherif, A. (2014). Optimal capacitor placement and sizing in radial electric power systems. *Alexandria Engineering Journal, 53(4),* 809-816.

EN 50160 Standard (2010). *Voltage characteristics of electricity supplied by public electricity networks.* European Committee for Electrotechnical Standardization (CENELEC).

Essallah, S., Bouallegue, A., & Kheldher, A. (2017). A comparative performance study of different indices for optimal DG placement in distribution systems. *2017 International Conference on Green Energy Conversion Systems (GECS),* 1-6.

EuropeAid. (2016). Grid loss reduction. *Sustainable Engineering Handbook.*

Fathy, A., & Rezk, H. (2017). Multi-Verse Optimizer for identifying the optimal

parameters of PEMFC model. *Energy*, *143(C)*, 634-644.

George, T., Youssef, A.R., Ebeed, M., & Kamel, S. (2018). *Ant Lion Optimization technique for optimal capacitor placement based on total cost and power loss minimization*. Proceedings of the 2018 International Conference on Innovative Trends in Computer Engineering (ITCE 2018), (pp. 350-356), Aswan, Egypt.

Ghosh, S., & Sinha, S. (2017). *Business Mathematics and Statics.* New Delhi, India: Oxford University Press.

Gill,P. (2008). *Electric Power Equipment Maintenance and Testing*. Boca Raton, FL, USA: CRC Press.

Gnanasekaran, N., Chandramohan, S., Sathish Kumar, P. & Mohamed Imran, A. (2016). Optimal placement of capacitors in radial distribution system using Shark Smell Optimization algorithm. *Ain Shams Engineering Journal*, *7(2),* 907-916.

Gonen, T. (2014). *Electric Power Distribution Engineering* (3rd ed.). Florida, USA: CRC Press.

Guha, D., Roy, P.K., & Banerjee, S. (2017). Multi - Verse Optimization: A novel method for solution of Load Frequency Control problem in power system. *IET Generation, Transmission and Distribution, The Institution of Engineering and Technology Journals*, *11(14),* 3601-3611.

Haldar, V., & Chakravorty, N. (2015). Power loss minimization by optimal capacitor placement in radial distribution system using Modified Cultural Algorithm. *International Transactions on Electrical Energy Systems, 25(1),* 54-71.

Hitzeroth, H.V. (1995). Optimal capacitor placement to minimize harmonics in power systems and software tools. *Masters thesis*. University of Cape Town.

Hung, D.Q., Mithulananthan, N., & Bansal, R. (2010). Analytical expressions for DG allocation in primary distribution networks. *IEEE Transactions on Energy Conversion, 25(3),* 814-820.

Idris R.M., & Zaid, N.M. (2016). *Optimal shunt capacitor placement in radial distribution system*. Proceedings of the 2016 IEEE International Conference on Power and Energy (PECon), (pp. 18-22). Melaka, Malaysia.

Jangjoo, M.A. & Seifi, A.R. (2014). Optimal voltage control and loss reduction in microgrid by active and reactive power generation. *Journal of Intelligent and Fuzzy Systems, 27(4),* 1649-1658.

Kavaliauskas, D. & Sakalauskas, L. (2019). Study of convergence in metaheuristics algorithms. *Baltic Journal of Modern Computing, 7(3),* 436-443.

Kothari, D.P., & Nagrath, I.J. (2003). *Modern power system analysis* (3rd ed.). New Delhi, India: McGraw Hill.

Kumar, A., & Suhag, S. (2017a). Multi-Verse optimized fuzzy-PID controller with a derivative filter for Load Frequency Control of multisource hydrothermal power system. *Turkish Journal of Electrical Engineering & Computer Sciences, 25(5),* 4187-4199.

Kumar, A., & Suhag, S. (2017b). Effect of TCPS, SMES, and DFIG on load frequency control of a multi-area multi-source power system using Multi-Verse optimized fuzzy-PID controller with derivative filter. *Journal of Vibration and Control, 24(24),* 5922-5937.

Kumar, P. H. & Rudramoorthy, M. (2021). Distribution network reconfiguration considering DGs using a hybrid CS-GWO algorithm for power loss minimization and voltage profile enhancement. *Indonesian Journal of Electrical Engineering and Informatics (IJEEI), 9(4),* 880-906.

Magadum, R.B., & Kulkarni, D.B. (2019). "Optimal placement of capacitor to enhance the efficiency of the distribution network," *International Journal of Innovative Technology and Exploring Engineering (IJITEE), 8(9),* 2877-2881.

Mahfoud, R.J., Alkayem, N.F., Sun, Y., Alhelou, H.H., Siano, P., & Parente, M. (2020). "Improved Hybridization of Evolutionary Algorithms with a Sensitivity-Based Decision-Making Technique for the Optimal Planning of Shunt

Capacitors in Radial Distribution Systems," *Applied Sciences, 10(4): 1384*, 1-26.

Messac, A. (2015). *Optimization in practice with MatLab for engineering students and professionals*. New York, USA: Cambridge University Press.

Mirjalili, S., Mirjalili, S.M., & Hatamlou, A. (2016). "Multi-Verse Optimizer: A nature inspired algorithm for global optimization," *Neural Computing and Applications, 27(2),* 495-513.

Mtonga, T.P.M., Kaberere, K.K., & G.K. Irungu, G.K. (2020). *Performance analysis of six search algorithms in minimizing the cost of real power losses and shunt capacitors purchase through optimal shunt capacitors sizing*. Proceedings of the 2020 Sustainable Research and Innovation (SRI) Conference, (pp. 130-143), JKUAT Main Campus, Kenya.

Murthy, K.V.S.R., Raju, M.R., & Rao G.G.(2010). *Comparison of Index Vector & Fuzzy-PSO methods with respect to optimal capacitor placement in agricultural distribution system*. Proceedings of the 16th National Power Systems Conference (pp. 728-733). Hyderabad, Telengana, India.

Natarajan, R. (2005). *Power System Capacitors.* Florida, USA: CRC Press.

Nesmachnow, S. (2014). An overview of metaheuristics: accurate and efficient Methods for optimization. *International Journal of Metaheuristics, 3(4),* 320-347.

Piotrowski, A., Napiorkowski, J.J. & Piotrowska, A.E. (2020). Population size in Particle Swarm Optimization. *Journal of Swarm and Evolutionary Computation, 58(2020),* 1-18.

Prakash, K. & Sydulu, M. (2007). Particle Swarm Optimization based capacitor placement on radial distribution systems. *2007 IEEE Power Engineering Society General Meeting*, 1-5.

Prakash, K. & Sydulu, M. (2012). Optimal capacitor placement in radial distribution systems using Differential Evolution. *Journal of Electrical Engineering, 12(2),*

pp. 144-149.

Priyanto, Y.T.K., & Robith, M. (2017). Economic dispatch and losses minimization using Multi-Verse Optimizer on 159kV Mahakam transmission system. *International Journal of Engineering Research & Technology (IJERT), 6(1),* 489-494.

Rao, R.S., Narasimham, S.V.L., & Ramalingaraju, M. (2011). Optimal capacitor placement in radial distribution system using Plant Growth Simulation Algorithm. *International Journal of Electrical Power and Energy Systems, 33(5),* 1133-1139.

Robbins, A. & Miller, W .C. (2000). *Circuit Analysis: Theory and Practice* (2nd Ed.). Delmar Publications.

Sattianadan, D. (2014). Comprehensive analysis for optimal placement of distributed generation in power systems. PhD. Thesis, Department of Electrical and Electronics Engineering, SRM University, Chennai, India. Retrieved on September 18, 2018, from http://hdl.handle.net/10603/50970

Sedighizadeh, M., & Bakhtiary, R. (2015). Optimal multi-objective reconfiguration and capacitor placement of distribution systems with the Hybrid Big Bang-Big Crunch algorithm in the fuzzy framework. *Ain Shams Engineering Journal, 2016(7),* 113-129.

Seifi, H., & Sepasian, M.S. (2011). *Electric power system planning– Issues, algorithms and solutions* (5th ed.). Berlin, Germany: Springer-Verlag.

Shetty, V.J. & Ankaliki, S.G. (2016). Fuzzy logic based optimal capacitor placement and Loss reduction in radial power system. *International Journal of Current Engineering Technology, 6(4),* 1139-1143.

Singh, H., Mehta, S., & Prashar, S. (2016). Economic load dispatch using Multi-Verse Optimization. *International Journal of Engineering & Research (IJOER),* 2(6), 43-51.

Sukraj, K., Yuvaraj, T. & Hariharan, R. (2018). Optimal allocation of shunt capacitor

in the radial distribution network using Bio Inspired Bat Algorithm. *International Journal of Pure and Applied Mathematics, 119(12),* 15901-15917.

Sulaiman, M.H., Mustaffa, Z., Mohamed, M.R., & Aliman, O. (2016). An application of Multi-Verse Optimizer for optimal reactive power dispatch problems. *International Journal of Simulation Systems, Science & Technology (IJSSST), 17(41),* 1-5.

Tamilselvan, V., Jayabarathi, T., Raghunathan, T. & Yang, X. (2018). Optimal capacitor placement in radial distribution systems using flower pollination algorithm. *Alexandria Engineering Journal (AEJ), 57(4),* 1-12.

Tolba, M.A., Tulsky, V.N., Vanin, A.S., & Diab, A.A.Z. (2017). *Comprehensive analysis of optimal allocation of capacitor banks in various distribution networks using different hybrid optimization algorithms.* Proceedings of the 2017 IEEE International Conference on Environment and Electrical Engineering and 2017 IEEE Industrial and Commercial Power Systems Europe (EEEIC/I&CPS Europe). Milan, Italy, 2017.

Trivedi, I.N., Parmar, S.A., Jangir, P., Bhoye, M., Jangir, N., & Kumar, A. (2016). *Voltage stability enhancement and voltage deviation minimization using Multi-Verse Optimizer algorithm*. Proceedings of the 2016 International Conference on Circuit, Power and Computing Technologies (ICCPCT) (pp. 1-5).

Tutorials Point (I) Pvt. Ltd. (2014). *MATLAB Numerical Computing.* Tutorials Point (I) Pvt. Ltd. [Available]: https://www.tutorialspoint.com/matlab/matlab_tutorial.pdf

Weedy, B.M., Cory, B.J., Jenkins, N., Ekanayake, J.B., & Strbac, G. (2012). *Electric Power* (5th ed.). West Sussex, United Kingdom: John Wiley & Sons Ltd.

WEG Electric Corporations (2012), "Power Factor Correction Capacitors," 6655 Sugarloaf Parkway, Duluth, GA 30097. [Available]: www.weg.net

Wood, F., & Horner, D. (2010). *Business Accounting Basics*. Essex, England: Pearson Education.

Yang, XS. (2012). Nature - inspired metaheuristic algorithms: success and new

challenges. Journal of Computer Engineering and Information Technology, 1(1), 1-3.

Youssef, A.R., Kamel, S., Ebeed, M., & Yu, J. (2018). Optimal capacitor allocation in radial distribution networks using a combined optimization approach. *Electric Power Components and Systems, 0(0),* 1-19.

Zhao, H., Han, X., & Guo, S. (2016). DGM (1,1) model optimized by MVO (Multi-Verse Optimizer) for annual peak load forecasting. *The Natural Computing Applications Forum, 30(6),* 1811-1825.

Zimmerman, R.D., Murillo - Sanchez, C.E., & Thomas, R.J. (2011). MATPOWER: Steady-State Operations, Planning and Analysis Tools for Power Systems Research and Education. *IEEE Transactions on Power Systems, 26(1),* 12-19.

APPENDICES

Appendix I: List of Publications

This appendix highlights the publications based on this research.

1. Journal Publication

Mtonga, T.P.M., Kaberere, K.K., and Irungu, G.K. (2021). Optimal Shunt Capacitors' Placement and Sizing in Radial Distribution Systems using Multi – Verse Optimizer. *IEEE Canadian Journal of Electrical and Computer Engineering, 44(1),* 10-21.

2. Conference Proceedings

1. Mtonga, T.P.M., Kaberere, K.K., and Irungu, G.K. (2019). *A comparative analysis of shunt capacitors placement techniques for real power losses and shunt capacitors' cost reduction*. Presented at the 14th JKUAT Scientific, Technological and Industrialization Conference and Exhibitions, Juja, Kenya.

2. Mtonga, T.P.M., Kaberere, K.K., and Irungu, G.K. (2020). *Performance analysis of six search algorithms in minimizing the cost of real power losses and shunt capacitors purchase through optimal shunt capacitors sizing*. Proceedings of the Sustainable Research and Innovation Conference (pp. 130-143). Juja, Kenya.

3. Mtonga, T.P.M., Kaberere, K.K., and Irungu, G.K. (2020). *A novel partial search based technique for optimal shunt capacitors placement and sizing in radial distribution systems*. Proceedings of the Sustainable Research and Innovation Conference (pp. 182-189). Juja, Kenya.

Appendix II: Graphical Illustrations of the Real and Reactive Power Losses of the IEEE 10-Bus Radial Distribution System

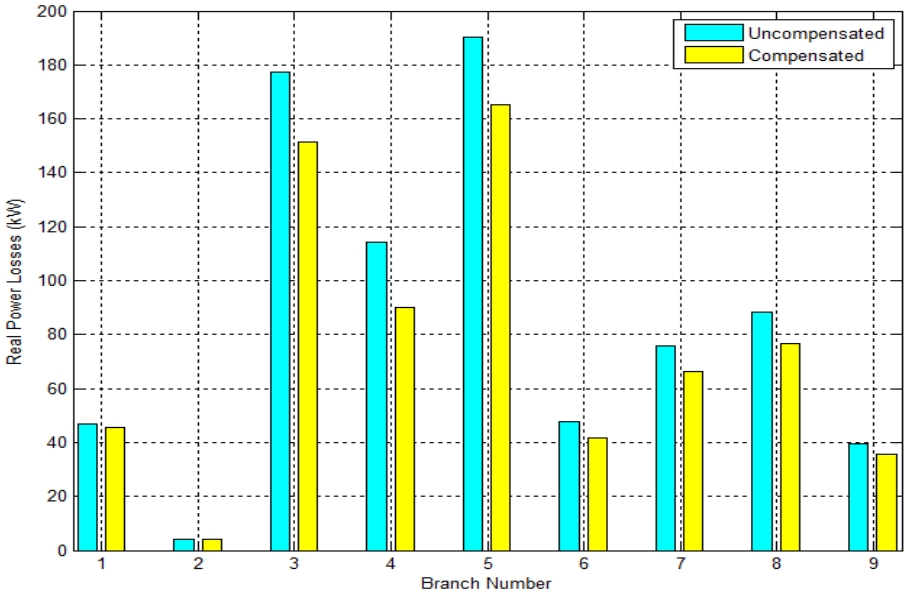

(a) Real power losses

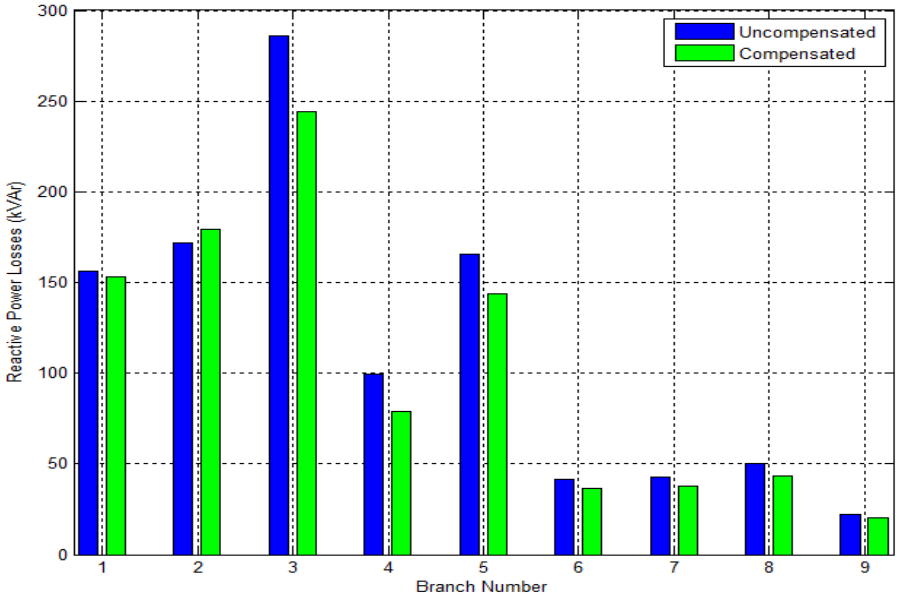

(b) Reactive power losses

Figure 1: Comparison of branch power losses for the IEEE 10-bus system for the uncompensated and optimally compensated cases at fixed load

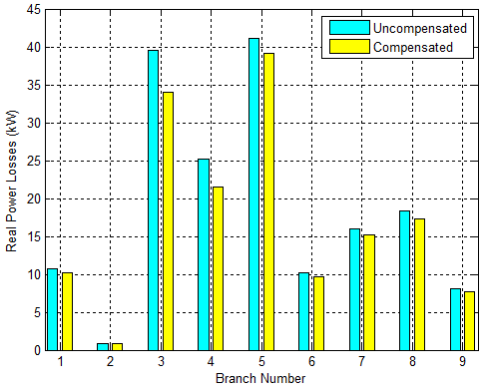

(a) Real power losses at light (50%) load

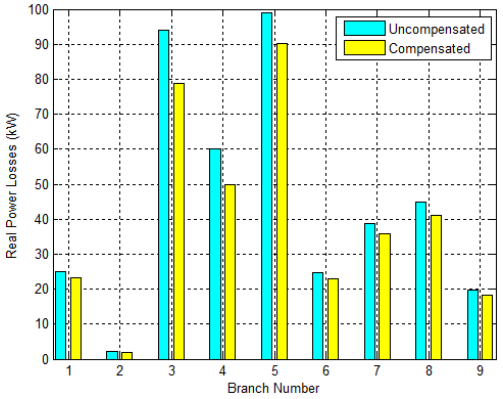

(c) Real power losses at medium (75%) load

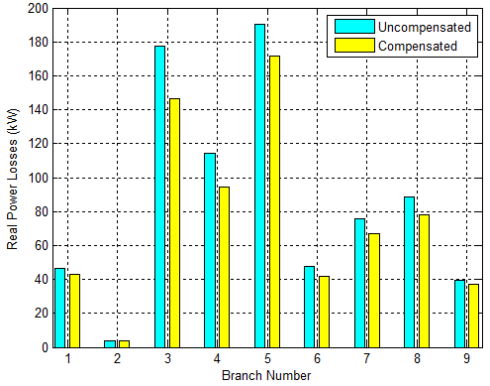

(e) Real power losses at full (100%) load

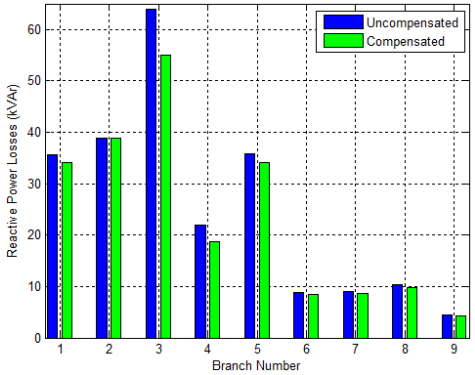

(b) Reactive power losses at light (50%) load

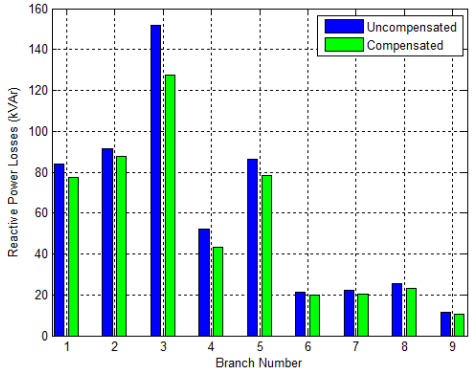

(d) Reactive power losses at medium (75%) load

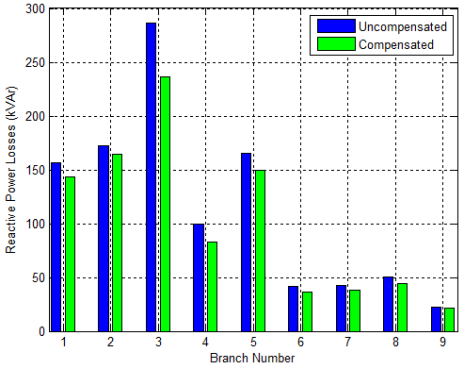

(f) Reactive power losses at full (100%) load

Figure 2: Comparison of branch power losses for the IEEE 10-bus radial distribution system at light, medium and full load

Appendix III: Graphical Illustrations of the Real and Reactive Power Losses of the IEEE 33-Bus Radial Distribution System

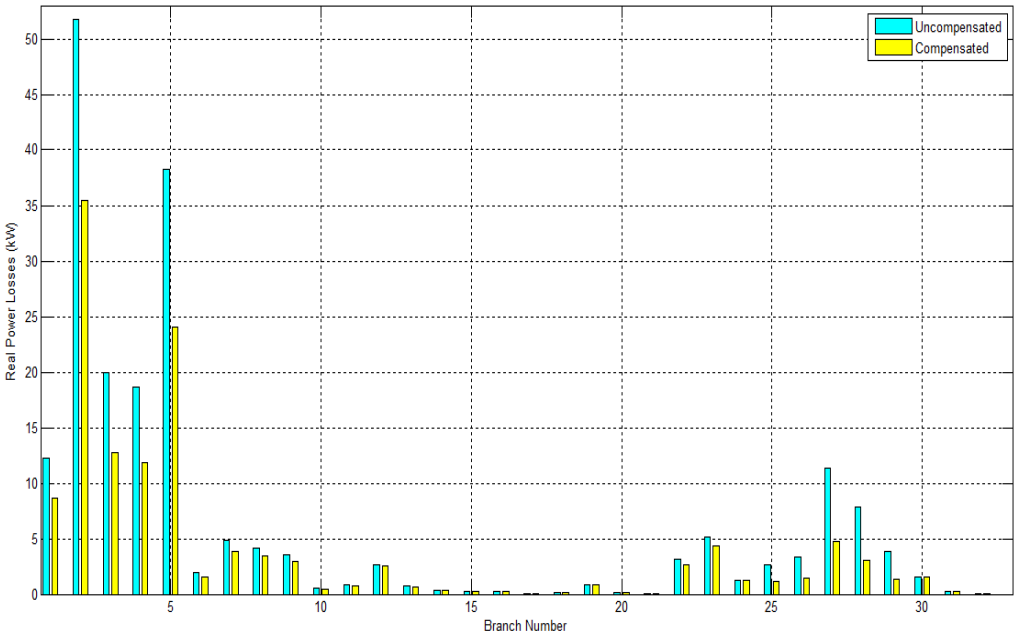

(a) Real power losses

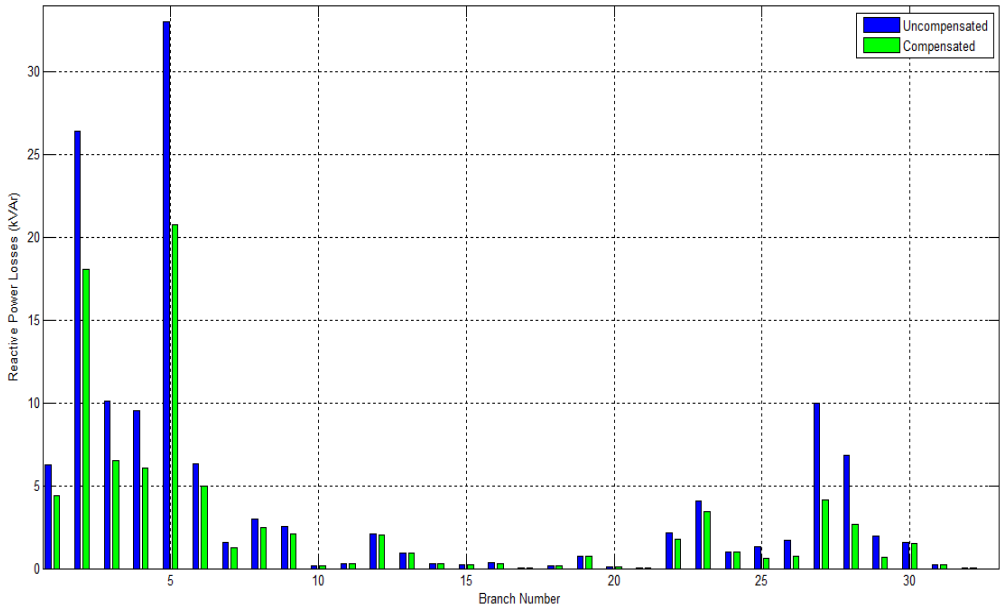

(b) Reactive power losses

Figure 1: Comparison of branch power losses for the IEEE 33-bus system for the uncompensated and optimally compensated cases at fixed load

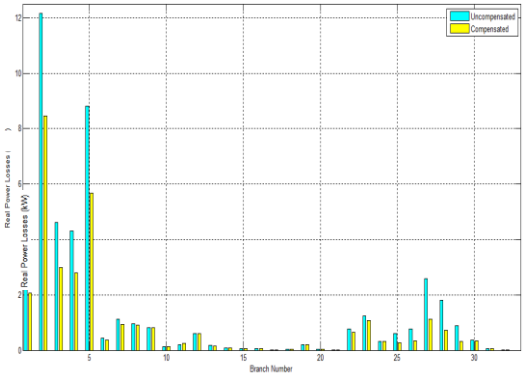

(a) Real power losses at light (50%) load

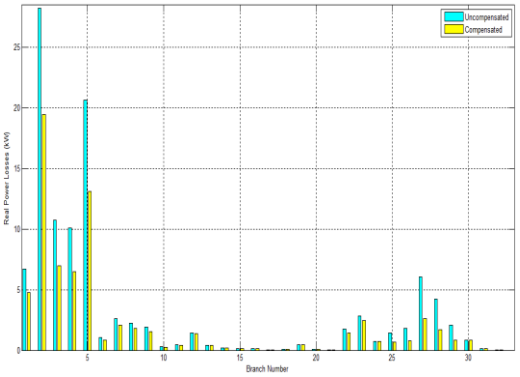

(c) Real power losses at medium (75%) load

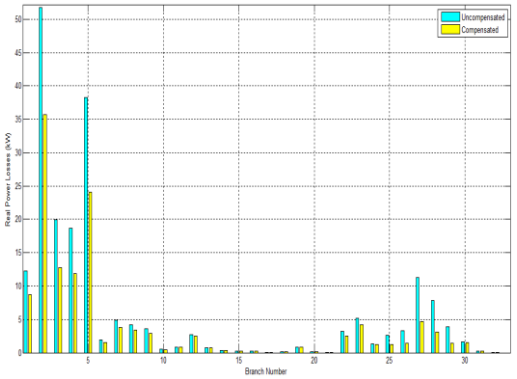

(e) Real power losses at full (100%) load

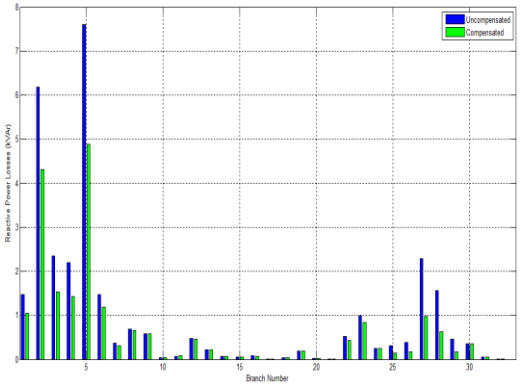

(b) Reactive power losses at light (50%) load

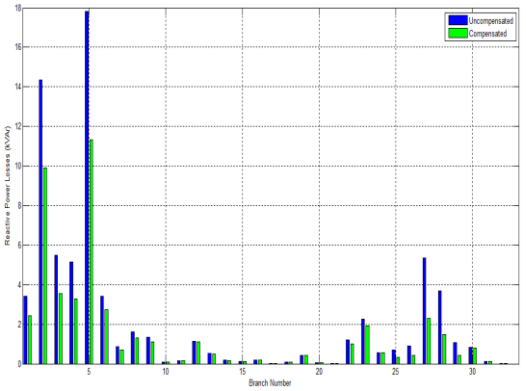

(d) Reactive power losses at medium (75%) load

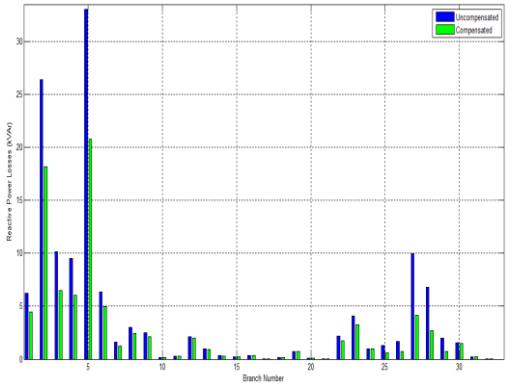

(f) Reactive power losses at full (100%) load

Figure 2: Comparison of branch power losses for the IEEE 33-bus radial distribution system at light, medium and full load